UNIVERSIDADE DO ALGARVE

Departamento de Ciências Biomédicas e Medicina

Gluconeogenesis and amino acids metabolism in ovarian clear cell carcinoma

Filipa Lopes Coelho

Dissertação

Mestrado em Ciências Biomédicas

Trabalho efetuado sob orientação de:

Profª. Doutora Jacinta Serpa (orientação externa)

Prof. Doutor Álvaro Tavares (orientação interna)

2013

UNIVERSIDADE DO ALGARVE

Departamento de Ciências Biomédicas e Medicina

Gluconeogenesis and amino acids metabolism in ovarian clear cell carcinoma

Filipa Lopes Coelho

Dissertação

Mestrado em Ciências Biomédicas

Trabalho efetuado sob orientação de:

Profª. Doutora Jacinta Serpa (orientação externa)

UIPM (IPO Lisboa)/CEDOC – Faculdade de Ciência Médicas da Universidade Nova de Lisboa

Prof. Doutor Álvaro Tavares (orientação interna)

CBME – Universidade do Algarve

2013

Título do trabalho: “Gluconeogenesis and amino acids metabolism in ovarian clear cell carcinoma”

Declaro ser a autora deste trabalho, que é original e inédito. Autores e trabalhos consultados estão devidamente citados no texto e constam da listagem de referências incluída.

Copyright Filipa Lopes Coelho

A Universidade do Algarve tem o direito, perpétuo e sem limites geográficos, de arquivar e publicitar este trabalho através de exemplares impressos reproduzidos em papel ou de forma digital, ou por qualquer outro meio conhecido ou que venha a ser inventado, de o divulgar através de repositórios científicos e de admitir a sua cópia e distribuição com objetivos educacionais ou de investigação, não comerciais, desde que seja dado crédito ao autor e editor.

Agradecimentos

Gostaria de dar o meu especial agradecimento à Doutora Jacinta Serpa, minha orientadora, que tornou possível este trabalho e me ajudou a superar e ultrapassar todos os obstáculos com que me deparei, ao longo deste ano. Obrigada por toda a disponibilidade, ajuda e conhecimentos transmitidos. Agradeço ainda toda a paciência, confiança, incentivo ao pensamento crítico e autonomia. Um sincero muito obrigada!

O meu agradecimento ao Doutor Álvaro Tavares pela disponibilidade de aceitar co-orientar a minha tese.

Gostaria de agradecer ao Doutor Luís Gafeira por me ter apresentado o enorme mundo do NMR e por toda a simpatia e disponibilidade.

Agradeço a todas as minhas colegas do grupo. À Fernanda por toda a simpatia e alegria que sempre transmitiu. Um especial agradecimento à Lídia e à Sofia por todos os ensinamentos e palavras de incentivo.

Um obrigada a todos os meus colegas do UIPM, que direta ou indiretamente tornaram este trabalho possível.

Agradeço aos meus amigos, que apesar de alguns deles estarem longe ouviram incondicionalmente os meus desabafos e as minhas irritações.

E por último, mas não menos importantes, agradeço à minha família por me ter dado um apoio incondicional, aturado as minhas frustrações e irritações e por todas as palavras de incentivo e força. Um especial obrigada aos meus pais e à minha irmã, sem eles não teria sido possível!

Obrigado a todos os que estiveram presentes nesta fase da minha vida que, aliás, foi das mais estimulantes nesta minha breve vida, no mundo da “ciência”.

Resumo

O cancro é considerado como um dos maiores problemas de saúde pública (Siegel et al., 2013). De acordo com a OMS (Organização Mundial de Saúde) o cancro é caracterizado como sendo um crescimento anormal de células, podendo desenvolver-se em qualquer parte do corpo e alastrar-se para outros órgãos (metástases). Sabe-se ainda que as metástases são maioritariamente responsáveis pela morbilidade e mortalidade em doentes com cancro (Seyfried and Shelton, 2010). Biologicamente, as células normais podem sofrer transformação maligna, sendo em parte esta transformação influenciada pelo microambiente envolvente, onde o tumor e as células circundantes estabelecem uma rede funcional (Hanahan and Weinberg, 2011; Serpa and Dias, 2011).

O carcinoma do ovário, é uma grande causa de mortalidade em mulheres, constitui cerca de 90% de todas neoplasias malignas do ovário, sendo 3-10% dos casos classificados como carcinoma de células claras (OCCC). Cerca de 57-81% de OCCC são diagnosticados nos estádios I/II, apresentando-se usualmente como uma massa pélvica. Doentes com CCC apresentam um comportamento clínico distinto e com pior prognóstico do que outras neoplasias de ovário (Feeley et al., 2001, Bjorkholm et al., 1982; Sorbe et al., 1982; Hogberg et al.,1993). Um dos motivos que contribuem para o mau prognóstico em CCC está relacionado com a baixa resposta à quimioterapia convencional baseada em cis-platina (Goff et al., 1996). Este tipo histológico de carcinoma do ovário deve o nome de células claras a algumas alterações morfológicas devidas à acumulação de glicogénio, cuja síntese é regulada pelo HNF1β (hepatocyte nuclear factor 1β), o gene central na tumorigénese do CCC (Anglesio et al., 2011).

Atualmente sabe-se que as células tumorais poderão apresentar perfis metabólicos distintos das células normais (Fuchs and Bode, 2005). Em 1956, Otto Warburg estabeleceu o primeiro elo de ligação entre o metabolismo e o cancro através das observações em que as células tumorais, mesmo na presença de oxigénio, apresentam um aumento da taxa da glicólise, tendo lactato como produto final (Warburg, 1956). Este fenómeno, conhecido como efeito de Warburg, coloca a hipótese das células tumorais apresentarem defeitos na mitocôndria, responsável pela anulação do ciclo TCA (ou ciclo de Krebs) e consequentemente aumento da taxa de glicólise (Vander Heiden et al., 2009), suportando a proliferação celular. Em vários tipos de cancro, existe uma associação entre o desregulação e aumento da proliferação /sobrevivência celular com um aumento da glicólise aeróbica (Wise and Thompson, 2010), onde as fontes de carbono, NADPH e ATP provêm da glucose (Dang, 2012).

A glucose e a glutamina são os principais substratos a serem utilizados como fontes de ATP e carbono, essenciais à síntese de macromoléculas e ao suporte da proliferação celular. A

glucose é responsável pela produção de ribose (fundamental para a síntese de ácidos nucleicos) e ATP, através da via das pentoses-fosfato (PPP). A glutamina, o aminoácido mais abundante na corrente sanguínea, é considerado um substrato bioenergético e dador de nitrogénio, sendo que este aminoácido se revela essencial para a produção de biomassa e energia (Dang, 2012).

A neoglucogénese é responsável por cerca de 35-50% da produção total de glucose, sendo uma via que requer ATP e NADPH para a conversão de piruvato, lactato e aminoácidos (como alanina e glutamina) em glucose *de novo*. Nos tecidos normais, a neoglucogénese é ativada por modificações pós-translacionais ou pela ativação alostérica de enzimas chave limitantes, responsáveis pelos eventos moleculares desta via. Geralmente, e de acordo com os requisitos metabólicos, os órgãos adaptam a importação, armazenamento, produção e libertação de glucose (Oh et al., 2013; Telang et al., 2012).

A conversão de piruvato em glucose é considerada como o maior passo da neoglucogénese, sendo catalisado por várias enzimas citoplasmáticas e mitocôndriais. Parte dos passos da neoglucogénese são catalisadas, no sentido inverso, por enzimas glicolíticas (Quintas et al., 2008a).

A nível molecular, o piruvato é transportado diretamente do citoplasma para a mitocôndria ou, tendo a alanina como percursor, a conversão para piruvato ocorre na mitocôndria por transaminação. O piruvato promove a formação de oxoloacetato (OAA) por ação da piruvato carboxilase (PC). O transportador carnitina permite o influxo de acetil-CoA na mitocôndria, que servirá como um activador essencial de PC. OAA é então reduzido a malato e transportado para o citoplasma via transportador malato-α-cetoglutarato. No citoplasma, o malato é oxidado a OAA e posteriormente a fosfoenolpiruvato (PEP), através de fosfoenolpiruvato carboxicinase citosólica (PCK1). Caso o OAA seja convertido diretamente no citoplasma, a conversão a PEP é catalisada por fosfoenolpiruvato carboxicinase mitocondrial (PCK2). A conversão de fructose-1,6-bifosfato (F1,6BP) em fructose-6-fosfato (F6P) pela fructose-1,6-bifosfatase (FBP1) é outra reação irreversível na neoglucogénese (Quintas et al., 2008b). Posteriormente, glucose-6-fosfatase (G6Pase) é então responsável pela desfosforilação de F6P em glucose *de novo* (Weickert and Pfeiffer, 2006). Por sua vez, a função da enzima 6-fosfofructo-2-cinase/ fructose-2,6-bifosfatase (PFKFB1) está associada à estimulação da glicólise e inibição da neoglucogénese, através da modulação da sua atividade cinase.

A glutamina pode ser considerada tão importante como a glucose a nível da produção de energia, estando provado que restrições de glutamina ou inibição de enzimas glutaminoliticas diminuem a proliferação celular, tanto *in vitro* como *in vivo* (Reynolds et al., 2013).

Os passos fundamentais da glutaminólise são a hidrólise de glutamina a glutamato, por ação da glutaminase (GA), e a subsequente conversão na mitocôndria do glutamato em α-cetoglutarato (α-KG). α-KG pode integrar o ciclo TCA e fornecer os intermediários metabólicos, como NADH (Piao et al., 2013). Porém, um metabolismo oxidativo incompleto pode conduzir à produção de lactato como produto final. O glutamato pode ainda ser convertido em piruvato pela transaminase glutamato-piruvato (GPT) e ser usado como substrato para a neoglucogénese (Matés et al., 2013).

O glutatião (GSH) é um tripeptido γ-glutamil-cisteinil-glicina, sendo considerado o antioxidante mais importante do organismo. GSH, um tiol antioxidante intracelular, atua como tampão redox contra o stress oxidativo. Alterações moleculares no sistema GSH em alguns tumores pode ser responsável por um aumento da proliferação celular, bem como da resistência a drogas (Traverso et al., 2013).

A cisteína, um aminoácido utilizado na síntese de GSH, é obtido através da dieta ou da transulfuração de outros amino acidos. A transulfuração desempenha um papel importante na homeostase de cisteína, sendo mediada em parte pela cis-tationa-gama-ligase (CTH) e 3-sulfotransferase de mercaptopiruvato (MPST). CTH é uma enzima citoplasmática e a última enzima-chave na via de transulfaração, catalisando a conversão de cistationina (derivada da metionina) em cisteína, amónia, 2-oxobutirato e é ainda responsável pela produção de H_2S (Wang and Hegele, 2003). A CTH tem ainda a capacidade de degradar cisteína, o que conduz à produção de lactato (Steegborn, 1999). Por sua vez, MPST é uma enzima envolvida da degradação da cisteína, catalisando a transferência de ião enxofre do 3-mercaptopiruvato em cianina ou outro tiol (Jurkowska et al., 2011).

Com base no trabalho científico que vem sendo dedicado na área do metabolismo tumoral nesta tese foram definidos dois objectivos principais que foram abordados, utilizando um modelo *in vitro* de OCCC (ES2). O primeiro objectivo é verificar se a neoglucogénese é a fonte de glucose, de modo a suportar as necessidades celulares. Investigámos a glutamina, lactato e butirato como substrato da neoglucogénese, bem como o perfil de expressão de enzimas chave da neoglucogénese (PCK1, PCK2, FBP1 e PFKFB1) e a modulação de características celulares como a migração e ciclo celular. O segundo objetivo, que partiu dos resultados obtidos no primeiro objetivo, e é clarificar a importância do metabolismo da glutamina e da cisteína e a sua influência na síntese de GSH. Pretendemos ainda determinar a relevância da glutamina e cisteína na via de síntese de GSH, bem como na progressão tumoral.

O perfil metabólico de ES2 por NMR revelou a presença de glicogénio não marcado, assim como também não foi detetada glucose ^{13}C marcada, o que é indicativo de que as células não estão a recorrer aos substratos testados como fonte para neoglucogénese.

Ao nível das enzimas neoglucogénicas, a acetilação de PCK1 pode ser responsável pelos resultados obtidos, onde maiores níveis de expressão de mRNA PCK1 nas condições de glucose e butirato não se refletiram num aumento dos níveis proteicos de PCK1, sendo por sua vez verificado um aumento dos níveis proteicos de PCK1 na condição lactato e glutamina. Em relação ao PCK2, os resultados suportam o descrito na literatura, em que a expressão de PCK2 permanece praticamente inalterada, sendo porém a sua expressão mais acentuada quando a neoglucogénese recorre ao lactato como substrato.

Os nossos resultados também sugerem que quando as células estão num meio privado de glucose os níveis proteicos de FBP1 encontram-se sobre expressos, enquanto que os níveis de PFKFB1 permanecem baixos, estimulando a neoglucogénese. No geral, a nível da modulação de enzimas envolvidas na neoglucogénese o lactato parece ser o principal substrato.

Como referido anteriormente, a alanina também pode ser usada como substrato da neoglucogénese, através da conversão de alanina em piruvato, via transaminação. Observámos um aumento nos níveis de mRNA de transaminase de alanina (ALT), nas condições glucose, lactato e glutamina, o que sugere que a alanina também desempenha um papel importante como precursor da neoglucogénese.

A análise de NMR permitiu ainda verificar que ES2 são capazes a metabolizar (pelo menos parte) o butirato, favorecendo o ciclo celular e a migração.

Por sua vez, e de acordo com os resultados obtidos por NMR, a glutamina parece ser o substrato mais usado. A análise metabólica revelou que a glutamina foi metabolizada em intermediários do ciclo TCA ^{13}C marcados, bem como intermediários ^{13}C marcados para a síntese de macromoléculas, o que sugere que a glutamina é metabolizada pela glutaminólise em vez de ser utilizada como substrato para a neoglucogénese. Os resultados obtidos tambem confirmam que a glutaminólise favorece a migração celular e a progressão do ciclo celular.

O perfil metabólico de ES2 revelou ainda a presença intracelular de GSH ^{13}C marcado nos resíduos de glicina e de glutamato, bem como glicina ^{13}C marcada e glutamato^{13}C livres.

Observámos que a suplementação de cisteína conduziu a um aumento dos níveis de GSH, que se encontra associado à proliferação e ciclo celular. Detetámos ainda que na presença de cisteína, ocorre um aumento da síntese GSH, que especulativamente estará associado ao decréscimo dos níveis de metionina no interior das células. Assim, o modelo *in vitro* de OCCC revelou que a glutaminólise parece ser relevante, não só ao nível da produção de energia e de

manter o potencial redox favorável, mas também está associada à síntese de GSH, sendo por sua vez, a síntese de GSH favorecida pela suplementação de cisteína.

Resumindo, o metabolismo de aminoácidos revelou-se crucial na tumorigénese de OCCC, bem como na resistência a drogas anti tumorais.

Palavras-chave: carcinoma de células claras do ovário (OCCC)**,** neoglucogénese**,** glutaminólise**,** glutatião (GSH)**,** metabolismo tumoral

Abstract

Tumor cells may exhibit different metabolic profiles compared to normal tissues from which they are derived. Those observations gave rise to the new concept that tumorigenesis requires metabolic alterations to sustain cell proliferation. Several studies reveal that increased cell proliferation is accompanied by increased glucose consumption. In OCCC, a typical morphological feature is the accumulation of glycogen in cancer cells cytoplasm this fact allows us to raise the stepwise questions: 1) Is glucose the main energy and carbon source used by OCCC?; 2) Being glucose a relevant energy and carbon source, can gluconeogenesis be working on ovarian clear cell carcinoma?, and 3) If gluconeogenesis is working on, which are the gluconeogenic substrates used by ovarian clear cell carcinoma?

In the present thesis we try to clarify, in an OCCC *in vitro* model (ES2) and in a glucose privation microenvironment, if gluconeogenesis pathway is working on, in order to support cells energy demands. Glutamine, lactate and butyrate were testes as putative gluconeogenesis substrates.

Metabolic analysis by NMR of ES2 cell line showed the presence of glycogen, characteristic of this cell line, though ^{13C} unlabelled, meaning that it was not synthesized from the tested substrates. At the same time the tested time points were not enough to clarify if glucose is *de novo* synthesized through gluconeogenesis. Nevertheless, NMR results showed that glutaminolysis was the major pathway used to sustain ES2 cell proliferation, with the production of TCA intermediates, as well as intermediates for macromolecular synthesis.

These findings prompted us to investigate the role of glutaminolysis in OCCC. In NMR analysis, we observed the synthesis of glycine and glutamate as well as the synthesis of GSH. Gathering cysteine to cells exposed to glutamine, we verified an increase in the synthesis of GSH. In cancer, GSH high levels is related to drug resistance which is in agreement with the fact that OCCC poor prognosis is also due to resistance to therapy.

Summing up, amino acids can play a central role in OCCC concerning energy and carbon metabolism as well as drug resistance.

Keywords: gluconeogenesis, glutaminolysis, glutathione (GSH), ovary clear cell carcinoma (OCCC), tumor metabolism

Table of contents

Index of figures

Index of tables

List of abbreviations

αKG – α-Ketoglutarate
AA – Antibiotic-Antimycotic
ADP – Adenosine diphosphate
AKT – Protein kinase B
ALT- Alanine transaminase
AMPK – AMP-activated protein kinase
ATP – Adenosine Triphosphate
BSA – Bovine serum albumin
cAMP – Cyclic adenosine monophosphate
cDNA – DNA copy
ChIP – Chromatin immunoprecipitation
CREB – Responsive element binding protein
CS – Citrate synthase
CTH – Cystathionine gamma-lyase
CysGly – Cysteinylglycine
ddH_2O – Bidestilled water
DMEM – Dulbecco's modified essential medium
DNA – Deoxyribonucleic acid
DTT – Dithiothreitol
EMSA – Electrophoretic mobility shift assay
ERRγ - Estrogen receptor related gamma
ETC – Electron transport chain
F1,6BP – Fructose-1, 6-biphosphate
F2,6BP – Fructose-2,6-biphosphatase
F6P – Fructose-6-phosphate
FBP1 – Fructose-1,6-bisphosphatase
FBS – Fetal bovine serum
For – Forward
FoxOs – Forkhead box class O
G6Pase – Glucose-6-phosphatase
GA – Glutaminase
GCL – γ-glutamylcysteine ligase
gDNA – Genomic DNA
GLS1 – Glutaminase isoform 1
GLS2 – Glutaminase isoform 2
GLUD1 – Glutamate dehydrogenase
GLUL – Glutamate- ammonia ligase
GPT – Glutamate pyruvate transaminase
GR – Glucocorticoids receptors
GSH – Glutathione
GSH – Glutathione
GSH-R – Glutathione reductase
GSS – Glutathione synthetase

GSSG – Glutathione disulfide (or in oxidized form)
h – Hours
H_2S – Hydrogen sulfide
HDAC – Histone deacetylase
HIF1α - Hypoxia inducible factor
HK2 – Hexokinase 2
HMDB – Human Metabolome database
HPLC – High-performance Liquid Chromatography
HPRT – Hypoxanthine phosphoribosyltransferase
HRP – Horse raddish peroxidase
LB – Luria-Bertani medium
LDH-A – Lactate dehydrogenase subunit A
LDH-B – Lactate dehydrogenase subunit B
$MgCl_2$ – Magnesium chloride
Mg2+ - Magnesium
min – Minutes
MPC – Mitochondrial pyruvate transporter
MPST – 3-mercaptopyruvate sulfurtransferase
mRNA – messenger ribonucleic acid
mTOR – Mammalian target of rapamycin
mTOR C1 – Mammalian target of rapamycin complex 1
mTOR C2 – Mammalian target of rapamycin complex 1
NADH – Nicotinamide adenine dinucleotide reduced
NaOH – Sodium hydroxide
NMR – Nuclear magnetic resonance
OAA – Oxoloacetate
OCCC – Ovarian clear cell carcinoma
ON – Overnight
OXPHOS – Oxidative phosphorylation
PBS – Phosphate buffered saline
PC – Pyruvate carboxylase
PCK1 – Phosphoenolpyruvate carboxykinase cytosolic
PCK2 – Phosphoenolpyruvate carboxykinase mitochondrial
PCR - Polymerase chain reaction
PDH – Pyruvate dehydrogenase
PDK1 – Pyruvate dehydrogenase kinase
PEP – Phosphoenolpyruvate
PFK1 – Phosphofructokinase-1
PFKFB1 – Fructose-2, 6-bisphosphatase
PI – Propidium iodite
PK – Pyruvate kinase
PKM2 – Pyruvate kinase isozymes M2
PKM2 – Pyruvate kinase-2
PPP – Pentose phosphate pathway
PS – Phosphatidyl serine

R5P – Ribose-5-phosphate
Rb – Retinoblastoma
Rev – Reverse
RIPA – Radio-Immunoprecipitation Assay
RNA – Ribonucleic acid
ROS – Reactive oxygen species
RQ-PCR – Relative quantifying polymerase chain reaction
RT – Room temperature
RTK – Tyrosine kinase receptor
RT-PCR – Reverse transcription polymerase chain reaction
SBD-F – Ammonium 7-Fluoro-2,1,3-benzoxadiazole-4-sulfonate
T75 – 75 cm^2 tissue culture flasks
TCA – Trichloroacetic acid
TCA cycle – Tricarboxylic acid cycle, also known as citric acid cycle or Krebs cycle
TCEP – Tris (2-carboxyethyl)phosphine
V – Volume
W – Weig

1. Introduction

1.1 Cancer

Cancer is considered as one of the major public health problem worldwide (Siegel et al., 2013). According to WHO (World health organization) cancer is characterized by an abnormal growth of cells and it can develop in any part of the body and spread to other organs, process known as metastasis. Metastasis is the main responsible for morbidity and mortality in cancer patients (Seyfried and Shelton, 2010).

Nowadays because tumor progression is considered a stepwise process several studies have been developed to clarify cancer initiation and progression. Biologically, normal cells can suffer changes in cell physiology that can lead to malignant tumors. Due to the complexities of neoplastic pathways, tumor progression is characterized by hallmarks. The main alterations in cell physiology sustain proliferative signaling, insensitivity to growth inhibition, resistance to cell death, replicative immortality, angiogenesis and tissue invasion (metastasis) (Hanahan and Weinberg, 2011; Seyfried and Shelton, 2010). Additionally, two other important emerging hallmarks in cancer were recently raised, reprogramming of energy metabolism and evading immune system (Hanahan and Weinberg, 2011). Malignant transformation is always conditioned by tumor microenvironment, where tumor and surrounding cells act as a functional network (Serpa and Dias, 2011).

1.2 Ovarian clear cell carcinoma (OCCC)

Epithelial ovarian cancer make up 90% of all ovarian malignancies (Feeley et al., 2001) and is the leading cause of death in women with subtypes: serous (30%–70% of cases), endometrioid (10%–20% of cases), mucinous (5%–20% of cases), clear cell (3%–10% of cases), and undifferentiated (<1% of cases) carcinomas (Bjorkholm et al., 1982; Sorbe et al., 1982; Hogberg et al.,1993). The majority of patients present with stage III and IV disease, for which the 5-year survival rates are less than 20%, however recent reports showed that 57-81% of clear cell carcinoma (CCC) were diagnosed at stage I/II being usually presents as a pelvic mass (Anglesio et al., 2011). In Portugal the incidence of ovarian cancer is 10.61/100.000 and 5-year survival rate is 40% (Registo Oncológico Regional Sul; ISSN: 1646-6675). Most of the patients with advanced disease is not cured by surgery (Kobayashi et al, 2009).

CCC has been recognized by WHO, since 1973 as a distinct histologic type in the classification of ovarian tumors (Sugiyama et al., 2000) and despite the low incidence among epithelial ovarian cancers, patients with CCC have a distinctly different clinical behaviour with significantly worse prognosis than patients with serous carcinoma, the most prevalent type (O'Brien et al., 1993; Tammela et al.,1998). One of the reasons why CCC has such a poor prognosis is its low response to standard platinum-based chemotherapy (Goff et al., 1996). CCC are characterized, in part, by their glycogen containing clear (Anglesio et al., 2011).

Substantial histopathology data, that is also supported by epidemiological studies (Prowse et al., 2006), provide evidence that endometriosis might be viewed as a pre-neoplastic process of CCC and endometrioid carcinomas, possibly via intermediary atypical borderline lesions. An atypical glandular change in endometriosis, the so called atypical endometriosis, is often present associated with CCC, while it is rare in endometriosis without a neoplasm (Czernobilsky e al.,1979; Fukunaga et al., 1997; LaGrenade et al., 1998). Thus, many clinicopathological studies have strongly suggested a malignant transformation of endometriosis to CCC, but little molecular evidence exists to support the notion that endometriosis is the precursor of CCC.

In ovarian endometriosis, especially in that associated with a neoplasm, metaplastic changes are often observed: eosinophilic metaplasia is the most common, followed by ciliated cell, hobnailand mucinous metaplasias. Papillary, squamous and clear cell metaplasias are rare (Fukunaga et al., 1998).

Molecular genetic alterations play a key role in carcinogenesis and in CCC are specifically found mutations of K-RAS and the signaling pathways of HNF-1β (hepatocyte nuclear factor β), Emi1 (early mitotic inhibitor-1) and mTOR (mammalian target of rapamycin) are upregulated (Kobayashi et al, 2009). CCC is also associated with mutations in PIK3CA encoding PI3K, being suggested that the PI3K–AKT–mTOR–HIF1α (phosphoinositide 3-kinase, v-akt murine thymoma viral oncogene homolog, mammalian target of rapamycin, and hypoxia induced factor 1α) could be useful as therapeutically target. Most recently, it was described that in almost half of CCC cases the tumor suppressor gene ARID1 was mutated. The ARID1A gene product is part of chromatin remodelling complex, which interacts with various hypoxia and cytokine related transcription factors, including HIF1α (Anglesio et al., 2011).

Understanding metabolic features and molecular alterations could help to explain many of the distinctive prognostic features of the ovarian CCC type.

1.3 Cancer Metabolism

Metabolism is one of the emerging hallmarks in cancer (Hanahan and Weinberg, 2011) and this area has gained more attention from many research groups in the whole world.

Nowadays, it is known that tumor cells may have different metabolic profiles (Fuchs and Bode, 2005) compared to normal cells.

In 1956, Otto Warburg established the first bond between metabolism and cancer, since he observed that tumor cells exhibit an increased rate of glycolysis with lactate production even in the presence of oxygen (Warburg, 1956), so called aerobic glycolysis. In these observations known as Warburg effect, Warburg hypothesized that cancer cells have a defect in mitochondria that was responsible for the abrogation of tricarboxylic acid (TCA) cycle and consequent increased rate of glycolysis (Vander Heiden et al., 2009) to sustain metabolic requirements for cell proliferation. Warburg effect gave rise to a new concept that tumorigenesis require metabolic adaptation (Deberardinis et al., 2008).

Energy metabolism in normal cells, in the presence of oxygen, is characterized by cytoplasmic glycolysis (the precursors result from glucose oxidation), TCA acid cycle and electron transport chain (ETC)/oxidative phosphorylation (OXPHOS). OXPHOS pathway is an efficient process to generate 32 moles of ddenosine triphosphate (ATP)/mole from 1 mole of glucose (Ganapathy et al., 2009a).

When cells are under hypoxic conditions the mitochondrial function is suppressed. Instead, cells have to use an alternative pathway to produce energy, that is the aerobic glycolysis with lactate as final product (Ganapathy et al., 2009). In many cancers there is an association between the deregulated and enhanced cell proliferation and survival with an increase in aerobic glycolysis (Wise and Thompson, 2010) where carbon skeletons, NADPH and ATP are produced by glycolysis (Dang, 2012). Cells using aerobic glycolysis have higher levels of ATP/ adenosine diphosphate (ADP) and $NADH/NAD^+$. In normal cells alterations on those levels can impair growth and apoptosis (Vander Heiden et al., 2009).

Many authors thought and defend that genomic mutability acquired during tumor progression lead to metabolic modifications and in some cases to the Warburg effect (Kim and Dang, 2006; Seyfried and Shelton, 2010). Studies in energy metabolism of cancer cells have demonstrated that there was a link between alteration in several oncogenes/ tumor suppressor genes and the regulation of metabolic processes (Wise and Thompson, 2010). These alterations could lead to genomic instability and DNA damage, having the potential to increased mutability of cells. Those pre-malignant cells start to display hallmarks of cancer (Figure 1) (Seyfried and

Shelton, 2010). In most cases of malignant transformation the bioenergetic demands are supported, in part, by some oncogenic mutations responsible for an increase in nutrients uptake (Vander Heiden et al., 2009).

Cell metabolism can trigger the production of toxic products like reactive oxygen species (ROS). Increase in ROS production or abolishment/decrease in detoxification can lead to membrane damage and mutagenesis which can result in malignant transformation (Dang, 2012). Increased ROS levels induce alterations in pathways, like pentose phosphate pathway (PPP). ROS oxidizes and consequently inactivates pyruvate kinase isozymes M2 (PKM2) responsible for the last step in glycolysis by modifying a critical sulphydryl group of PKM2 (Dang, 2012). Inactive PKM2 decreases the rate of PPP, reflecting in a NADPH reduction and hence in a decrease of glutathione reductase (GSH-R) responsible for glutathione (GSH) reduction (antioxidant compound) (Dhivya, 2012).

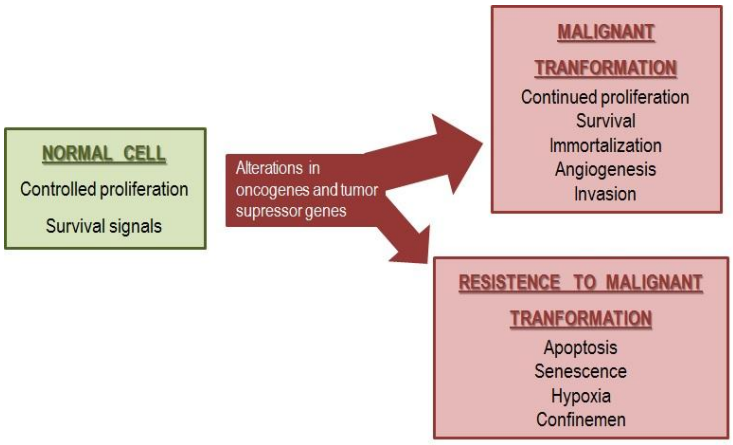

Figure 1 – Cell proliferation and survival is regulated by some pathways that can be abrogated or altered leading to malignant transformation. Cancer cells have the potential to proliferate beyond the limitations of normal cells. Some cells can resist to this alterations by blocking clonal cancer expansion and neoplastic evolution.

1.3.1 Oncogenic alterations

During malignant transformation, mutations/overexpression of oncogenes and loss of tumor suppressor genes can lead to alterations in metabolism, namely a switch from aerobic respiration to aerobic glycolysis (Warburg effect) (Dang, 2012).

In most cases, oncogenes control mitosis and cell survival by affecting steps on signaling mechanism namely by increasing signals in a cascade similar to “tyrosine kinase receptor” (RTK) (Israël and Schwartz, 2011a). One of the influences of oncogenes and tumor suppressor genes mutations is alterations in the production of ribose-5-phosphate (R5P), essential for nucleotide biosynthesis (Deberardinis et al., 2008).

Tumor suppressors are associated with DNA repair. Tumor suppressor p53 target TP53-induced glycolysis and apoptosis regulator (TIGAR) that suppresses glycolysis by inhibiting activation of phosphofructokinase-1 (PFK1). This enzyme increase substrate availability to oxidative pathway as NADPH and R5P generation, via PPP. In tumors p53 deficiency is frequent, leading to glycolysis triggering and PPP impair.

Cancer cells mostly choose an alternative mechanism to sustain cell R5P requirements. Tumors may express pyruvate kinase-2 (PKM2), a glycolytic enzyme that stimulates PPP, inducing R5P production through a non-oxidative pathway (Deberardinis et al., 2008).

Protein kinase B (AKT) is another oncogene associated with tumorigenesis. AKT encodes serine-threonine kinase protein responsible for the regulation of glucose uptake and aerobic glycolysis. This oncogene mobilizes glucose transporters to the cell surface, increasing the levels of glucose import and activating hexokinase 2 (HK2) which is responsible for glucose phosphorylation and intracellular trap. Additionally, the oncogene MYC is also associated to tumorigenesis triggering direct activation on glycolysis (Kim and Dang, 2006).

1.3.2 Nutrients uptake

Cancer cells can supply metabolites requirements due to the expression of nutrient transporters (Fuchs and Bode, 2005). In normal cells the uptake of nutrients from their environment is stimulated by growth factors avoiding uncontrolled proliferation (Vander Heiden et al., 2009).

Glucose is one of the most important nutrient for cell mass production and cell proliferation. This compound is responsible for carbon and hydrogen supply but not nitrogen, phosphorus and sulfur that are also need for cell development. Those elements essentials to build new cells are supplied by other nutrients, namely amino acids as glutamine (Dang, 2012).

Glucose, amino acids, fatty acids and vitamins are essential nutrients required for cell survival and proliferation. In cancer cells, nutrient transporters are up-regulated or altered in plasma membrane (Ganapathy et al., 2009). Amino acid transporters support metabolic needs and are essential requirements for production of nucleotides, cellular nitrogen and proteins (Ganapathy et al., 2009; Mazurek and Eigebbrodt, 2003).

Cell growth is regulated in part by mammalian target of rapamycin (mTOR) mTORC1/C2 complexes being activated by amino acids and growth factors. mTOR is a regulatory-associated protein which is located downstream of PI3K and AKT and that can also be activated by insulin-like growth factor, oxidative stress and nutrients, essentially leucine that is imported in exchange

by glutamine. (Fuchs and Bode, 2005b; Laplante et al., 2010; Wise and Thompson, 2010). Leucine mobilizes mTORC1 to lysosomal membrane by G proteins turning it active to phosphorylate substrates that will be responsible for stimulating translation, ribosome biogenesis, cell growth and autophagy inhibition. Growth signals are transmitted by RTK to activate mTORC2 and PI3K. mTORC2 and PI3K stimulate AKT initiating the pathway responsible for an increase in metabolism, survival and proliferation. This process is also responsible for a transcriptional program, namely in genes such as MYC. AKT activated by mTORC2 can also influence mTORC1 (Figure 2) (Dang, 2012; Sabatini, 2006).

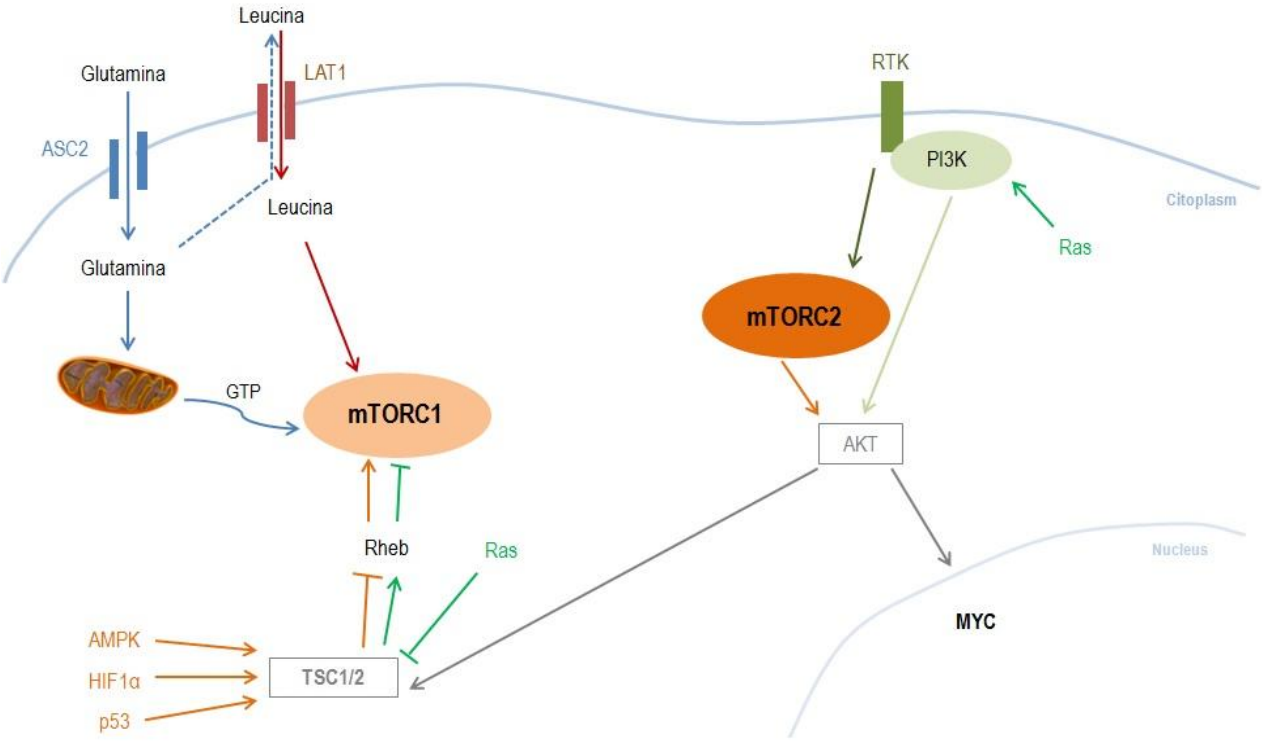

Figure 2: mTOR pathway - Glutamine (Gln) enters in the cell by neutral amino acid transporter (ASC2) membrane transporter, allowing leucine (Leu) influx by human L-type amino acid transporter 1 (LAT1). Leu actives mTORC1 (red) and in mitochondria gln realize TCA cycle with GTP production (blue). Hypoxic genes (HIF1α), DNA damage genes (p53) and energy depletion genes (AMPK) phosphorylated a negative regulator of mTORC1 (tuberous sclerosis complex - TSC1/2), overturning Rheb (orange arrows) and leading to mTORC1 activation. Ras inhibits mTORC1 by suppressing TSC1/2 (green arrows). RTK receive growth factor signaling activating PI3K and mTORC2. PI3K (also stimulated by *Ras*) and AKT induce mTORC2 (grey and dark orange arrows) resulting in *myc* activation that stimulate glycolysis and glutaminolysis. mTORC1 can also be activated by AKT expression.

1.4 Glucose and Glutamine

Glucose and glutamine are two major substrates for cell proliferation essentially because there are the two main sources of ATP and carbon skeletons required for macromolecules

synthesis. Glucose is responsible for ribose (fundamental for nucleic acid synthesis) and ATP production through pentose phosphate pathway (PPP). Glutamine that is the most abundant amino acid in bloodstream and the main bioenergetic substrate and nitrogen donnor (Dang, 2012).

In normal conditions glucose enters the cells through facilitative transport where is converted by glucose phosphorylation in hexose phosphate. This compound is phosphorylated and converted into glycerol, essential for lipid synthesis or transformed into pyruvate (Dang, 2012).

Proliferating cells in hypoxia and under glucose limitations reprogramme glutamine catabolism by TCA cycle to increase lipid synthesis. In hypoxia and in unrestricted glucose conditions the conversion of pyruvate to acetyl- CoA is switch to the conversion of pyruvate into lactate (Figure 3). This process is mediated by the inhibition of pyruvate dehydrogenase due the activation of pyruvate dehydrogenase kinase (PDK1) induced by hypoxia inducible factor (HIF1α) (Dang, 2012). HIF1α actives target genes like PDK1, consequently pyruvate is not used in mitochondrial oxidation, activating cellular responses to metabolic stresses.

Glutaminolysis, that is also increased in some tumors, is considered as a glutamate store. Glutamine is converted into glutamate by glutaminase, generating NAD+ that is essential for glycolysis (Israël and Schwartz, 2011b; Dang, 2012).

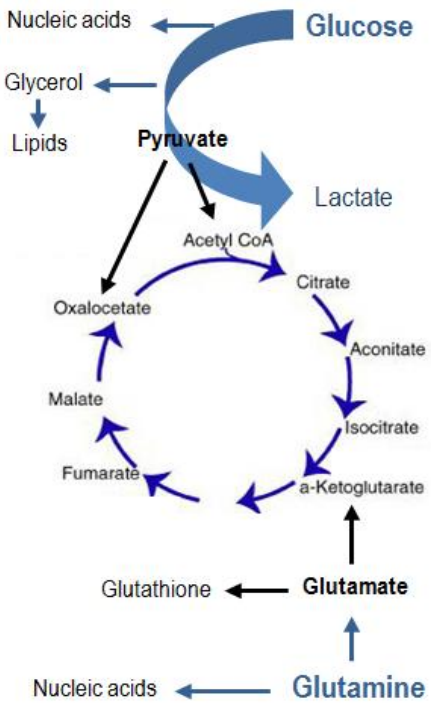

Figure 3: Pyruvate resulting from glycolysis can converted into acetyl-CoA in TCA cycle, increasing the levels of OAA and citrate which consequently permits an energy gain. Pyruvate can also be converted in lactate. Glutamine enters in TCA through conversion into glutamate. TCA can be independent of glucose or responsible for lipid synthesis via reductive carboxylation.

Decrease in glucose and glutamine levels lead to a reduction in ATP levels and an increase in AMP/ATP ratio. AMP-activated protein kinase (AMPK) is sensitive to AMP/ATP and have the potential to phosphorylate substrates to increase energy production and to decrease the activity of pathways that consume energy. On the other hand, AMPK that recycles cellular components for energy production, inhibits Acetyl-CoA carboxylase by phosphorylation and also induces mTOR pathway (Dang, 2012).

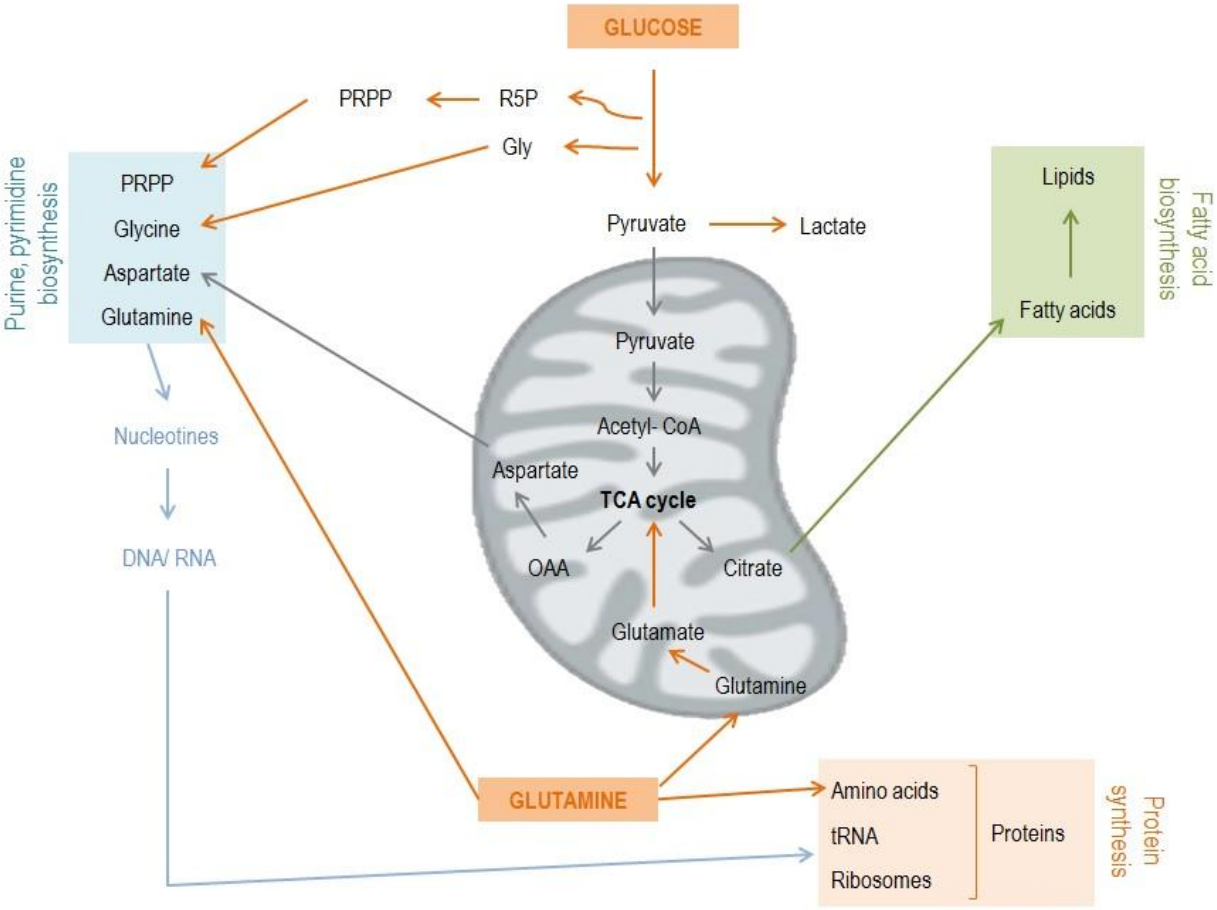

Figure 4: Cells have to duplicate genomic material, proteins and lipids to support essential requirements for replicative division, enhanced in tumors. Increase in glucose and glutamine influx is common in tumorigenesis. Glucose is converted into pyruvate with lactate production. Part of the pyruvate goes to TCA cycle in mitochondria resulting in citrate and aspartate production (TCA intermediates). Citrate is involved in fatty acids biosynthesis and asp in nucleotides production. Glucose is also responsible for amino acid precursors such as glycine and R5P. Glutamine also enters the mitochondria where is converted into glutamate that origin αKG, a TCA precursor. PRPP: phosphoribosyl pyrophosphate. Adapted from DeBerardinis et al., 2008

1.4.1 Gluconeogenesis and Glycolysis

Some enzymes are common to gluconeogenesis and glycolysis however working on different directions. Others are exclusive to gluconeogenesis or glycolysis, such as pyruvate

kinase (PK), in glycolysis, which is responsible for the conversion of phosphoenolpyruvate (PEP) into pyruvate, being transfered to mitochondria as acetyl- CoA and entering in TCA cycle and oxidative metabolism (Israël and Schwartz, 2011b).

Cells have an adaptative response to their metabolic needs, for example in starvation glycolytic enzymes, such as PK and pyruvate dehydrogenase (PDH) are phosphorylated and inactivated due to cAMP- glucagon- adrenergic signals. The inactivation of these enzymes leads to the interconnection break between glycolysis and TCA cycle and stops the oxidative metabolism (Israël and Schwartz, 2011b).

In normal cells, citrate synthase (CS) is inhibited by an increase in NADPH levels whereas in cancer cells this enzyme is active and overexpressed. Overexpression of CS increases levels of acetyl-CoA, oxoloacetate (OAA) and citrate and decrease levels of ketone bodies. On the other hand, low levels of ketone bodies are responsible for the decrease in the stimulation of pyruvate carboxylase (PC). Decreases in PC activity leads to more pyruvate to be "processed" by lactate dehydrogenase subunit A (LDHA). Overexpression of LDHA increase the levels of lactate and NAD^+, essential and required for glycolysis (Israël and Schwartz, 2011a, 2011b). This alternative pathway in tumors can explain, at least in part, the previously referred Warburg effect.

1.4.1.1 Gluconeogenesis

Gluconeogenesis accounts for 35-50% of total basal glucose production, being regulated in part by the interaction of different regulatory mechanisms discussed later on. Glucose is used by the majority of the tissues as energy source, being its production, in physiological conditions, restricted to the liver, kidneys and some cells in small intestine. Glucose-6-phosphatase (G6Pase) is an essential gluconeogenic enzyme and its expression is limited to these organs (Corssmit et al., 2001).

Glucose biosynthesis via gluconeogenesis requires ATP and NADPH for the conversion of pyruvate, lactate and amino acids, as glutamine and alanine, into the final product, *de novo* glucose. Lactate is a common substrate for kidney and liver whereas alanine conversion to glucose takes place almost exclusively in liver. In healthy humans is estimated that the contribution of lactate for total glucose production is approximately 15% (Corssmit et al., 2001).

1.4.1.1.1 Molecular regulators

In normal tissues, gluconeogenesis is activated by pos-translational modifications or by allosteric activation of key-rate limiting enzymes, responsible for the molecular events of this pathway. Liver is the most active organ for gluconeogenesis and in physiological conditions this pathway contributes to the maintenance of glucose homeostasis, controlling glucose levels between bloodstream and hepatocytes. In general and according to the metabolic requirements, this organ adjusts the regulation of glucose uptake and storage, as well as its production and release (Oh et al., 2013; Telang et al., 2012). Hormones have an important physiological role in the regulation of metabolism. Insulin inhibits gluconeogenesis while other hormones like glucagon and glucocorticoids induce the synthesis of *de novo* glucose by regulating the expression of glycolytic enzymes. Glucose concentration have also been reported to directly suppress the expression of the gene phosphoenolpyruvate carboxykinase cytosolic (PCK1) and gluconeogenesis (Weickert and Pfeiffer, 2006).

Additionally stress hormone cortisol is responsible for the initiation of signaling cascades that activate transcriptional regulators like cyclic adenosine monophosphate (cAMP), responsive element binding protein (CREB), nuclear glucocorticoids receptors (GR), estrogen receptor related gamma (ERRγ) and forkhead box class O (FoxOs) transcription factors. These transcriptional regulators promote the expression of glucogenic enzymes, namely PCK1 and G6Pase (Oh et al., 2013; Weickert and Pfeiffer, 2006).

1.4.1.1.2 Molecular pathway

The conversion of pyruvate into glucose is the major step of gluconeogenesis that is catalyzed by the action of diverse cytoplasmic and mitochondrial enzymes. Some glycogenic enzymes catalyze steps of gluconeogenesis (seven reactions in ten), in a reversible way (Figure 5).

Pyruvate is transported directly from cytoplasm to mitochondria or having alanine as a precursor, which conversion occurs in the mitochondria by transamination. Pyruvate promotes the OAA formation by the action of PC. Carnitine transporter permits the influx of Acytil-CoA in mitochondria, being an essential activator of PC due to the carboxylation of a biotin residue that occurs exclusively in the presence of acytil-CoA. OAA is then reduced to malate being transported to cytoplasm by malate-α-ketoglutarate transporter. In cytoplasm, malate is oxidized to OAA and PEP through PCK1. Nevertheless, if OAA is exported directly from the cytoplasm this reaction is catalyzed by phosphoenolpyruvate carboxykinase mitochondrial (PCK2), as it will

be depicted latter on. Another irreversible reaction in gluconeogenesis is the conversion of fructose-1, 6-biphosphate (F1,6BP) in fructose-6-phosphate (F6P), that is catalyze by fructose-1,6-bisphosphatase (FBP1) (Quintas et al., 2008a). G6Pase is then responsible for the dephosphorylation of glucose 6-phosphate (Glc-6-P) to *de novo* glucose (Figure 5) (Weickert and Pfeiffer, 2006).

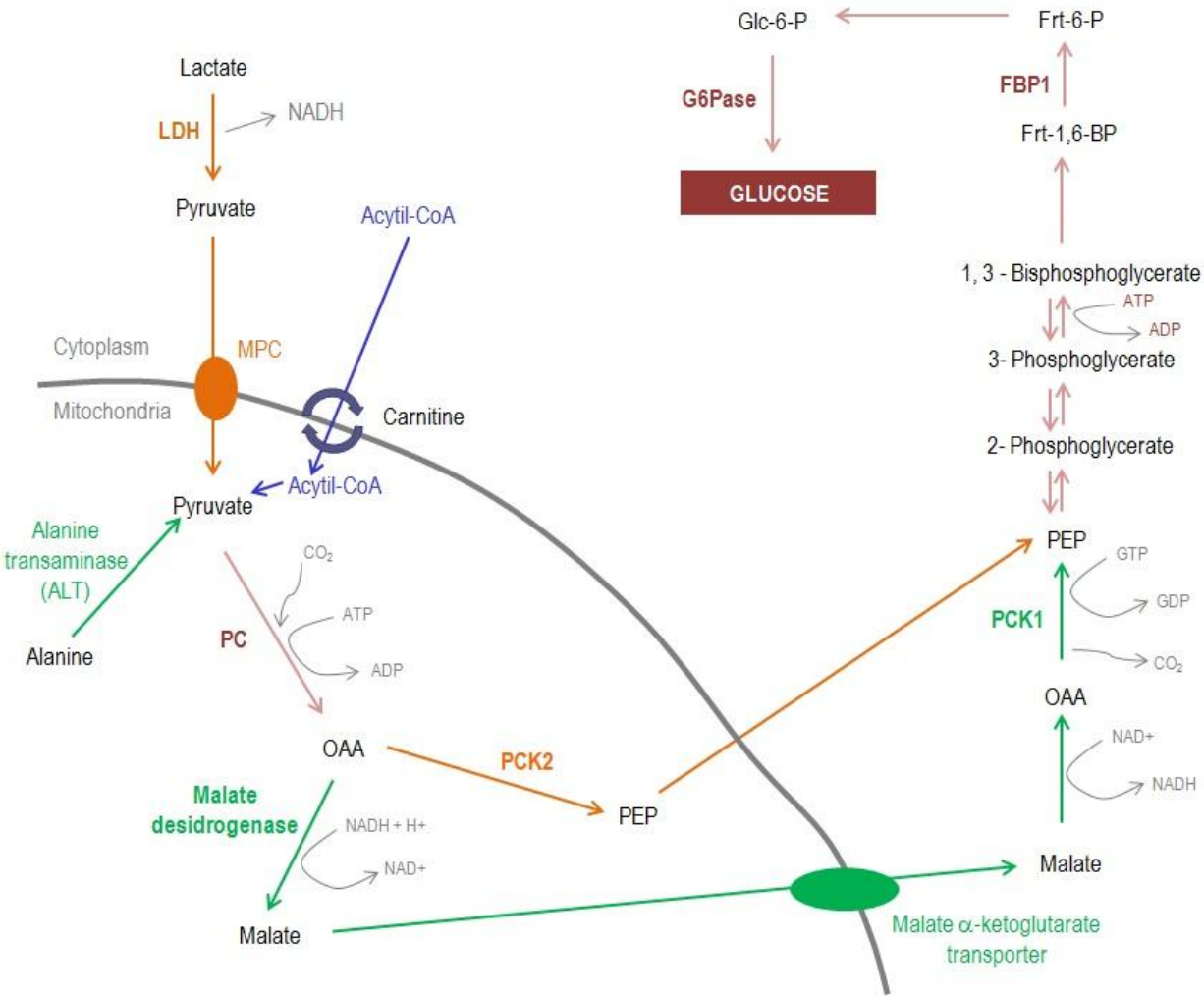

Figure 5: Gluconeogenesis Pathway - Pyruvate provided by alanine transamination or lactate dehydrogenation is converted to OAA by PC envolving the hydrolysis of one ATP molecule. Pyruvate from lactate, enters mitochondria by mitochondrial pyruvate transporter (MPC) (orange arrows). Acytil-CoA gets in mitochondria by carnitine transporter (blue arrows). OAA is reduced into malate and exported from mitochondrial by malate α-ketoglutarate transporter (green arrows) while OAA from lactate is directly converted into PEP by PCK2 and exported for cytoplasm. In cytoplasm, malate is oxidized to OAA and then converted to PEP by the action of PCK1. The conversion of PEP in 2- phosphoglycerate , 3- phosphoglycerate and 1, 3 - bisphosphoglycerate are reversible reactions with glycolysis. 1, 3 – bisphosphoglycerate are then converted to frt-1,6-BP by FBP1. Frt-1,6-BP generates Frt-6-P in a reversible way. G-6-P by the action of G6Pase origin glucose, the final product. Adapted from Quintas et al., 2008.

1.4.1.1.3 Key enzymes

The enzyme 6-phosphofructo-2-kinase/ fructose-2, 6-bisphosphatase (PFKFB1) has its function associated with the promotion of glycolysis and the inhibition of gluconeogenesis through the modulation of their kinase activity. Although, gluconeogenesis is also regulated by others rate-limiting enzymes, the PCK1 and G6Pase (Noguchi et al., 2013). The expression of PCK1 and G6Pase genes is regulated at the transcriptional level by a complex network of transcription factors and cofactors including CREB, HNF-4α and FoxO1 (Kim et al., 2011). Also the activation of AKT-signaling pathway modulates gluconeogenesis, leading to the downregulation of PCK1 and G6Pase proteins and hence the suppression of gluconeogenesis (Noguchi et al., 2013). Those enzymes could also be activated by allosteric alterations, due to the relative proportion of AMP and ATP (Oh et al., 2013).

Alanine aminotransferase (ALT) plays an important role in gluconeogenesis from alanine, being an increase in ALT activity associated with higher rates of gluconeogenic pathway (Moraes-Silva et al., 2012). Previous studies had reported that gluconeogenesis from alanine was increased in cancer patients (Moreira et al., 2013). ALT catalyses the conversion of alanine into pyruvate and then converted into OAA by the action of PC, involving the hydrolysis of one ATP molecule (Quintas et al., 2008a).

PCK1 includes two enzymes with different intracellular locations, the cytosolic and mitochondrial forms that are encoded by two nuclear genes (Greenfield et al., 2000). In human 60% of PEPCK is confined to mitochondria while 40% to cytosol (Hanson and Garber, 1972). PCK1, also known as PEPCK, is regulated by nutritional and hormonal stimuli at the transcriptional level, whereas mitochondrial form, also referred as PCK2, remains relatively unaltered appearing to be constitutive. Shifts in the ratio of PCK1 to PCK2 during feed restrictions or diabetes has been reported. PCK1 is required for gluconeogenesis from amino acids and PCK2 is more suited to gluconeogenesis from lactate. Due to the stoichiometry of gluconeogenesis, PEP formed from pyruvate and some amino acids requires the independent synthesis of NADH in cytosol (Agca et al., 2002). The reaction of conversion of lactate into pyruvate, in cytoplasm, is promoted by the enzyme lactate dehydrogenase B chain (LDH-B) with NADH production. Thereby the production of NADH by malate oxidation is not necessary and the pyruvate is directly converted into PEP by PCK2, inside mitochondria. PEP is exported to cytoplasm to sustain gluconeogenesis (Quintas et al., 2008a).

FBP1 is a magnesium (Mg2+) dependent enzyme that promote the irreversible hydrolysis of carbon 1 (C1) from fructose-1, 6-biphosphate. This reaction results in the release of an inorganic phosphate and F6P (Quintas et al., 2008a).

The molecular function of PFKFB1 is to synthesize fructose-2, 6- bisphosphate (F 2, 6 BP) from F6P. PFKFB1 activates PFK1, an essential and irreversible enzyme on controlling the glycolytic pathway. PFKFB1 expression could be stimulate by a decrease in ATP levels and by the abundance of energy stores leading to an enhancement in glycolytic flux and cell growth. When ATP levels and energy are abundant to supply cell requirements, ATP directly activates PFK1 by negative feedback. In cancer, an increase in PFKFB1 levels is commonly caused by an overexpression of HIF-1α, *myc* and activation of *ras* or loss of p53 (Yalcin et al., 2009).

G6Pase is responsible for the last step of gluconeogenesis, with glucose as final product. This enzyme promotes phosphate hydrolysis, in a Mg^{2+} dependent reaction. Glucose is then transported to bloodstream until target organs (Quintas et al., 2008a).

1.4.2 Glutaminolysis

Glutamine is a non-essential amino acid, although is a required nutrient source to maintain rapid cell division of cancer cells, being an increase of glutamine uptake and glutaminolysis associated with carcinogenesis (Matés et al., 2013). This non essential amino acid provides the anaplerotic carbon in mitochondrial TCA cycle as well as nitrogen and carbon skeletons. Glutamine is also used for glutathione (GSH) synthesis, fatty acids production, protein and nucleotide biosynthesis (Dang, 2010; Reynolds et al., 2013).

Since 1990 it has been reported that in cancer cells the activity of glutaminase is similar or higher than hexokinase from glycolysis. This result suggested that glutamine may be as important as glucose for energy generation (Board et al., 1990). More recently, it had been proved that glutamine restrictions or inhibitors of glutaminolytic enzymes decrease cell proliferation *in vitro* and *in vivo* (Reynolds et al., 2013).

MYC oncogene and tumor suppressor gene TP53 contribute to the glutamine uptake and glutaminolysis. MYC is responsible for inducing glutaminolysis through the activation of β-catenin being glutamine synthetase a direct target of activated β-catenin. Recently, dysfunctional retinoblastoma (Rb) cascate, besides promoting loss of proliferative control, it had been proposed to directly regulate the uptake and conversion of glutamine into anabolic precursors, required for neoplastic cell growth and survival (Dang, 2010; Reynolds et al., 2013).

1.4.2.1 Molecular pathway

The fundamental steps in glutaminolysis is the hydrolysis of glutamine into glutamate by glutaminase (GA) and subsequently conversion into α-KG in mitochondria. α-KG can enter TCA cycle and replenish the metabolic intermediates such as NADH (Piao et al., 2013).

GA localizes in the inner mitochondrial membrane, being responsible for the hydrolysis of the γ-amino group of glutamine, forming glutamate and ammonia. Ammonia could be used to form carbamoyl phosphate or may diffuse from the mitochondria and the cell. Glutamate can suffer deamination by glutamate dehydrogenase (GLUD1) forming α-ketoglutarate (α-KG) entering in TCA cycle for energy production. Glutamate can also be converted into pyruvate by glutamate pyruvate transaminase (GPT) (Figure 5). Hence, glutamate catabolism in TCA cycle produces reducing equivalents for the generation of ROS by OXPHOS (Matés et al., 2013).

As mentioned above glutaminolysis enables NADH production through TCA cycle; however an incomplete oxidative metabolism can lead to lactate as end product. Zagari et al. (2013) reported that glutamine has an important role in modulating the initial lactate production being this phenomenon observed *in vitro*. In this process, lactate production involves the efflux of malate from mitochondria and its conversion into pyruvate and finally into lactate, with NADH production. However, when glutamine is depleted, lactate is consumed to "refuel" the TCA cycle (Board et al., 1990; Zagari et al., 2013). The highest percentage of consumed glutamine is metabolized into molecules such as lactate (Matés et al., 2013).

1.4.2.2 Key enzymes

Glutamine could be lysed by mitochondrial GA into glutamate and ammonia and some cancer cells can survive without glutamine when provided with ammonia as nitrogen source. Cancer cells can also have an increase in glutamate-ammonia ligase (GLUL), that is responsible for the conversion of glutamate and ammonia into glutamine (Dang, 2010).

GA is a central enzyme is glutamine catabolism. Glutamate, from glutamine catabolism, is involved in mitochondrial bioenergetic via TCA cycle responsible for ATP production. GA family is composed by two isoforms, GLS and GLS2, encoded by separate genes. Only GLS enzyme is associated and increased in cancer cells whereas GLS2 plays a critical role in protection against oxidative stress by up-regulating glutathione levels. Therefore GLS up-regulation is linked with increased rates of proliferation while GLS2 is associated with resting, non-proliferative or quiescent cell states, working as a tumor suppressor (Matés et al., 2013).

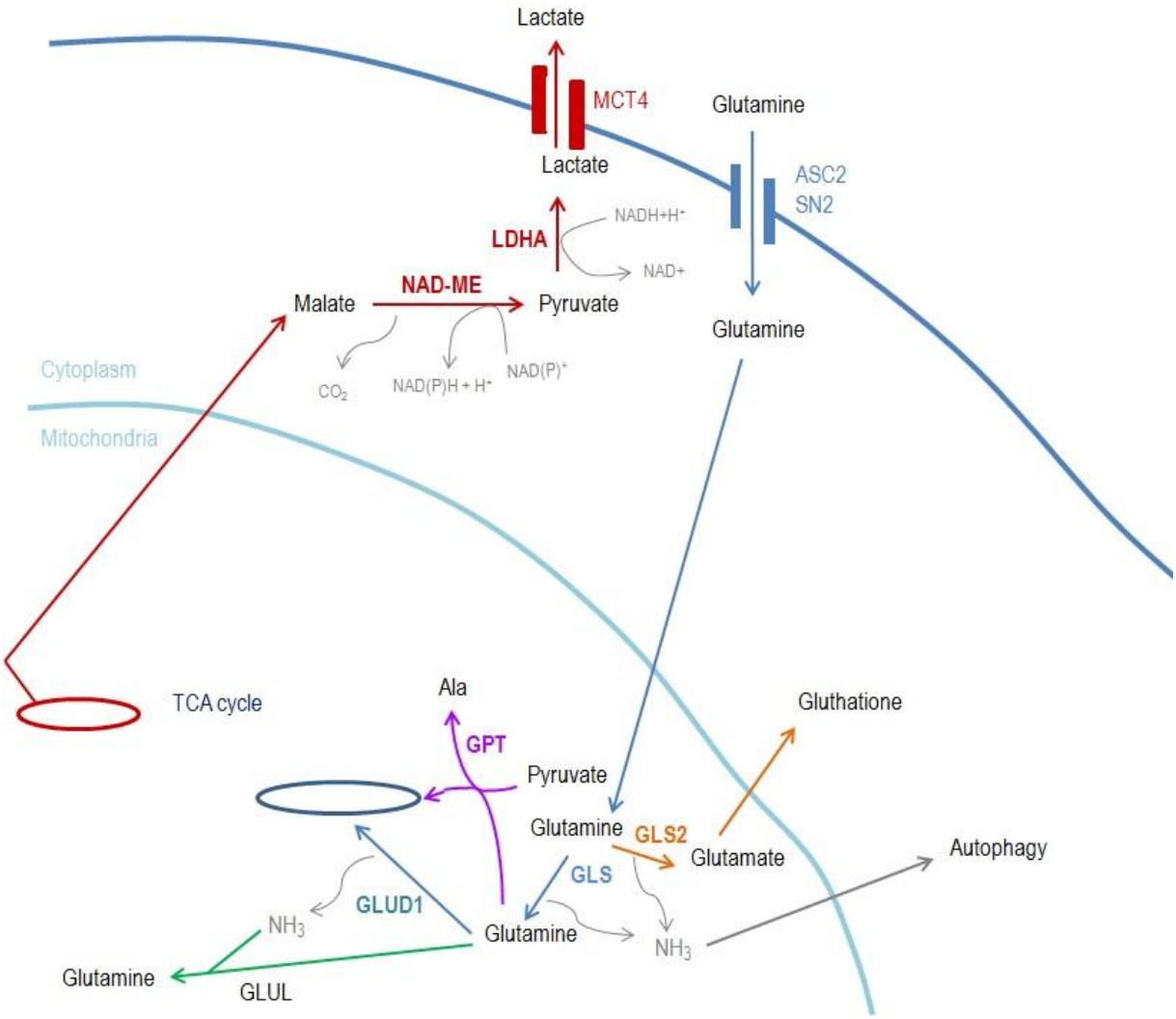

Figure 6: Glutaminolysis - Glutamine enters in the cell by cytoplasmic transporter such ASCT2 or solute carrier family 38 (SN2). Glutamine is transferred to mitochondria where is hydrolyzed by GLS (an isoform of GA) forming glutamate and ammonia (NH_3) (blue arrows). If glutamine is hydrolyzed by GLS2 (another GA isoform), in similarity to GLS reaction originates glutamate and also NH_3 but glutamate is responsible for glutathione production, a potent antioxidant agent (orange arrows). NH_3 and glutamate can be used to novo glutamine by the action of glutamine synthetase (green arrows). Glutamate is converted into α-KG (alanine production by glutamate-pyruvate transaminase – GPT is also possible), entering in TCA cycle (blue arrows). If an incomplete oxidative metabolism occurs, malate (a TCA cycle intermediate) is exported from mitochondria where originates pyruvate (by the action of malate dehydrogenase –NAD ME) and then lac (by LDHA). Lac is exported from cell through monocarboxylate transporter 4 (MCT4) (red arrows).

1.5 Glutathione (GSH)

GSH which is a tripeptide gamma-glutamyl-cysteinyl-glycine is a major free radical scavenger, immune booster and detoxifier of the body. Can be found in reduced (GSH) and oxidized forms (GSSG) (Figure 6) being the cysteine residue responsible for the readily oxidation of GSH to GSSH by electrophilic substances as free radicals and ROS. GSH is the major thiol-

containing endogenous antioxidant and acts as a redox buffer against several sources of oxidative stress (Dhivya, 2012; Matés et al., 2013). Quotient [GSH]: [GSSH] is used as indicator of the redox state of cells being values >10 verified under normal physiological conditions (Quintas et al., 2008b) where glutathione disulfide (GSSH) levels accounts for less than 1% of the intracellular content. In the cytosol, 85-90% of the GSH is freely distributed, although it can also be compartmentalized in different organelles, like mitochondria, peroxisomes and nuclear matrix (Singh et al., 2012).

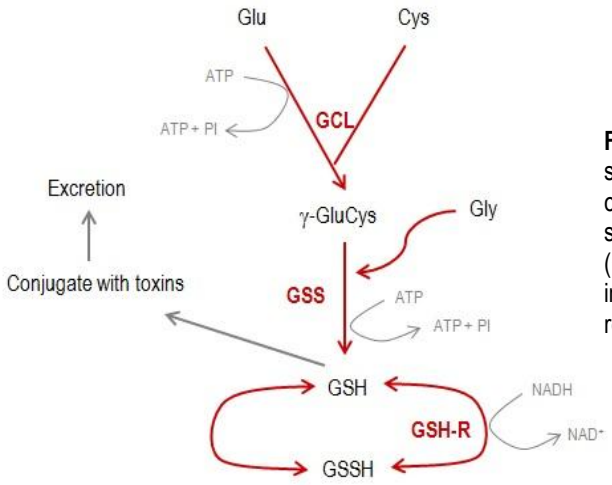

Figure 7: Gluthatione formation - γ-glutamyl cysteine synthease (GCL) that catalyzes the ligation of glu with cysteine (cys) through ATP activation. Glutathione synthetase (GSS) allowing gly ligation and glutathione (GSH) production. GSH is easily oxidized into GSSH, an inactive form. GSSH can be regenerated by glutathione reductase. Adapted from Quintas et al., 2008.

GSH provides greater antioxidant protection participating directly in ROS destruction and plays a critical role in carcinogenesis inhibition (Dhivya, 2012). Aerobic glycolysis, which is a metabolic characteristic of some tumors, is responsible for the production of ROS where their increase (higher than physiological conditions) is associated with higher levels of oxidative stress that lead to cell injury and death. Increase in ROS levels have also been implicated in cancer development and progression and molecular alterations in the components of the GSH system and in various tumors can lead to an increased survival and tumor drug resistance (Traverso et al., 2013). ROS formation and GSH depletion may also cause mitochondrial dysfunction and subsequent cytochrome c release triggering cell viability (Han et al., 2010).

GSH, beyond detoxification and cellular protection from damage by free radicals, peroxides and toxins, has also other essentials functions in metabolic and biochemical reactions, such as DNA synthesis and repair, protein and prostaglandins synthesis, amino acid transporters and enzymes activation (Dhivya, 2012). GSH is also implicated in essential functions like signal transduction, molecular regulation of cell physiology and regulation of apoptosis (Estrela et al., 2006; Singh et al., 2012).

1.6 Cysteine homeostasis

Cysteine is a semi-essential amino acid, provided through diet or trans-sulfuration pathway. High cysteine concentrations in human plasma could be cytotoxic, leading to pathologies like pre-eclampsia, premature delivery, low birth weight and cardiovascular diseases. Cysteine is used to GSH, taurine or inorganic sulphate synthesis and in similarity to GSH, taurine a most abundant free amino acid in humans, also acts as an endogenous antioxidant (Ishii et al., 2004).

Trans-sulfuration pathway is mediated, in part, by cystathionine gamma-lyase (CTH) and 3-mercaptopyruvate sulfurtransferase (MPST). CTH, a cytoplasmic enzyme and the last key enzyme in trans-sulfuration pathway, catalyze the conversion of cystathionine (derived from methionine) to cysteine, ammonia and 2-oxobutyrate. CTH protein can also accept homocysteine (HCYS) as substrate and could be responsible for hydrogen sulfide (H_2S) production (Wang and Hegele, 2003). In literature, CTH was also characterized as being able to degradate cysteine, leading to pyruvate production (Steegborn, 1999).

Under physiological conditions, oxidative stress induces an increase of HCYS flux through the trans-sulfuration pathway. As results cystathionine levels, a direct substrate of CTH, increase leading to an increase of downstream metabolites of CTH, cysteine and GSH. Then, GSH permits the maintenance of cellular redox status (Jurkowska et al., 2011).

MPST is an enzyme involved in cysteine degradation, catalyzing the transfer of sulfur ion from 3-mercaptopyruvate to cyanine or other thiol compound, yielding sulfane sulfur. In cancer had been reported a decrease in MPST activity leading to a reduction of non-oxidative metabolism of cysteine and consequently to a sulfane sulfur deficiency. Insufficient levels of sulfane sulfur induce an uncontrollable action of enzymes inactivated by sulfane sulfur (Jurkowska et al., 2011).

As referred, CTH and MPST, plays an important role in cysteine homeostasis, GSH-taurine synthesis and H_2S production. In humans, CTH mutations and deficiency levels causes cystathionimaemia, a disease characterized by accumulation of cystathionine in blood, tissue and urine with no consistent clinical consequences (Ishii et al., 2004; Jurkowska et al., 2011; Kraus et al., 2009).

2. Aims

The first main objective of this thesis is to understand if gluconeogenesis is a source of glucose supply in ovarian clear cell carcinoma (OCCC). This main objective is subdivided in 3 specific aims: 1) To verify if gluconeogenesis is working on OCCC by testing glutamine, lactate and butyrate as gluconeogenic substrates; 2); To evaluate the expression profile of key gluconeogenic enzymes (PCK1, PKC2, FBP1 and PFKF1) under these gluconeogenic substrates exposure; 3) To evaluate the modulation of cell features such as migration, cell viability and cell cycle in the presence of these gluconeogenic substrates.

The second main objective of this thesis came up from the evaluation of the results obtained from the first main objective accomplishment; and it is to clarify the role of glutamine and cysteine metabolism in OCCC. This objective is accomplished through 4 specific aims: 1) To verify if glutaminolysis is working on OCCC; 2) To evaluated cysteine degradation and synthesis as well as to determine the expression profile of genes involved in cysteine metabolism; 3) To evaluate the modulation of cell features such as migration, cell viability and cell cycle by cysteine in cells grown in glutamine, and 4) To determine the relevance of glutamine and cysteine metabolism in GSH synthesis.

3. Materials and Methods

3.1 Role of glucose, glutamine, lactate and butyrate as gluconeogenic precursor and cysteine associated with glutaminolysis

3.1.1 Cell culture

ES2 cell line, an *in vitro* model of OCCC, was obtained from American Type Culture Collection (ATCC) (CRL-1978™).

Cells were maintained at 37°C in a humidified 5% CO_2 environment in Dulbecco's modified essential medium 1X (DMEM) (41965-039, Gibco) containing 4.5g/L of D-glucose and L-glutamine 0.58 g/L. Medium was supplemented with 10% fetal bovine serum (FBS) (S 0615, Biochrom) and 1% Antibiotic-Antimycotic (AA) (15240062, Anti-Anti, Invitrogen).

Cells were grown to 75%-100% optical confluence before they were detached by incubation with 1X 0.05% trypsin- Ethylenediamine tetraacetic acid (EDTA) (25300-054, Invitrogen) at room temperature (RT) for 5 min. Whenever necessary, the cell number was determined with the help of a Bürker counting chamber.

In gluconeogenic assays cells were conditioned to DMEM without D-glucose/ L-glutamine (F 0405, Biochrom) supplemented with 1% FBS (S 0615, Biochrom), 1% AA (15240062, Anti-Anti, Invitrogen) and exposed either to 5mM glucose (G8270, Sigma), 50% lactate (1.06522.2500, Merck) at 10 mM, to 8 mM glutamine (25030-081, Gibco) or 8mM butyrate (B10 350-0, Sigma-Aldrich). Cells grown in control conditions were maintained in the absence of glucose, lactate, glutamine and butyrate. In cysteine assays, ES2 were also exposed to DMEM without glucose (11966-025, Gibco) supplemented with 1% FBS (S 0615, Biochrom), 1% Antibiotic-Antimycotic (15240062, Anti-Anti, Invitrogen) and 0.420 mM cysteine. Cells grown in control conditions were maintained in the absence of cysteine. In NMR assays cells were exposed to DMEM without D-glucose/ L-glutamine (F 0405, Biochrom) supplemented with 1% FBS (S 0615, Biochrom), 1% AA (15240062, Anti-Anti, Invitrogen) and 8mM ^{13C}-[U]-glutamine (605166, Sigma), 8mM sodium ^{13C}-[U]-butyrate (Isotec) or 10mM sodium ^{13C}-[U]-lactate (Sigma-Aldrich®).

3.1.2 Nuclear magnetic resonance (NMR) for metabolomic detection

Nuclear magnetic resonance (NMR) spectroscopy combined with advanced multivariate analyses methodologies have several advantages over classical biochemical assays. Essentially it represents a powerful, reproducible, and inexpensive technique for investigating the metabolome without extensive sample preparation that can be combined with ^{13C}-labeled substrates, alloing a noninvasive measurement of metabolic fluxes (Bodi et al., 2012).

In the context of the present thesis NMR assay was performed to identify the glutamine, lactate and butyrate metabolism in ES2 cell line and their possible influence as gluconeogenesis precursor.

ES2 cell line were plated 75 cm^2 tissue culture flasks (T75) and maintenance in DMEM (41965-039, Gibco) supplemented with 10% FBS (S 0615, Biochrom) and 1% AA (15240062, Anti-Anti, Invitrogen) until expected 60% optical confluence (~5.5x10^6 cells/mL) in incubation at 37ºC and 5% CO_2. Confluent cells were placed in starvation (DMEM without FBS) ON at 37ºC and 5% CO_2 (to synchronize cells). After that, cells were treated with 8mM ^{13C}-[U]-glutamine (605166, Sigma), 8mM sodium ^{13C}-[U]-butyrate (Isotec), and 10mM sodium ^{13C}-[U]-lactate (Sigma-Aldrich®), in DMEM without D-glucose/ L-glutamine (F 0405, Biochrom) supplemented with 1% FBS (S 0615, Biochrom), 1% AA (15240062, Anti-Anti, Invitrogen), for 16 and 48 hours. The supernatants were collected and stored at - 80ºC whereas cells were washed twice in PBS 1x, scraped and centrifuged at 1200 rpm for 2 min. Methanol and chloroform extraction was performed in cell pellets for detach organic and aqueous phases. Cell pellets were weighed to calculate the methanol volume added for sample (4ml methanol/1g weight pellet). After cold methanol mixture, the water was added (double volume of methanol), mixed and incubated for 5 min on ice. Chloroform (same volume methanol) was added to the sample and mixed. Then, water (same volume methanol) was added and samples were incubated for 10 min on ice, following centrifugation at 4000 rpm for 15min at 4ºC. Organic and aqueous phase was performed with glass pipette and stored at -20ºC until lyophilization. Lyophilization of the aqueous phase was made using Speed Vac Plus Scllon and then dissolved in deuterated water (D_2O) and 4% (v/v) azide (N3) / 4,4-dimethyl-4-silapentane-1-sulfonic acid (DSS) solution (1:10). To supernatants was also added 50µl of D_2O and 4% (v/v) N3 / DSS solution. NOESY 1DPR 1D (^{1}H), HSQC 2D (^{1}H, ^{13}C) and TOCSY 2D (^{1}H, ^{1}H) spectrums were obtained in a magnetic field of 800 MHz at 25ºC in Ultrashied™ 800 Plus (Bruker) with TXI probe and COSY 2D (^{13}C, ^{13}C) spectrum was obtained in a magnetic field of 500 MHz at 25ºC in Ultrashied™ 500 Plus (Bruker) with ^{13}C Dual probe. Software used in acquisition was Topspin 2.1 on avance 800 (Bruker) and

spectrums analysis were done according the chemical shifts supported with the Human Metabolome database (HMDB) (http://www.hmdb.ca/) and Chemomx NMR suite 7.6.

3.1.3 Gene expression

In the present thesis, gene expression of gluconeogenic enzymes (*PCK1, PCK2, FBP1* and *PFKFB1*) was determined to study the possible role of glucose, glutamine, lactate and butyrate as gluconeogenic precursors. The possible association between cysteine degradation and glutaminolysis was also evaluated (culture conditions are specified in 3.1.1).

3.1.3.1 Reverse transcription polymerase chain reaction (RT-PCR)

Reverse transcription polymerase chain reaction (RT-PCR) is one of the variant in polymerase chain reaction (PCR), used mainly for quantifying mRNA in biological samples. This technique produces a single-stranded complementary DNA copy (cDNA) of an RNA template through the action of the enzyme reverse transcriptase. Following RT reaction, cDNA is amplified by PCR (Freeman et al., 1999).

Ribonucleic acid (RNA) from biological samples was extracted using RNeasy Mini Extraction kit (74104, Qiagen) according to the manufacturer's protocol. RNA concentration was determined by measuring the absorbance at 260 nm in a *Nanodrop 2000* (Thermo Scientific).

cDNA was synthesized from 1µg RNA, which was reversely-transcribed by SuperScript II Reverse Transcriptase (18080-44, Invitrogen). Firstly, to complete a final volume of 8µl, 0.5µl of random hexamers (11034731001, Roche) and bidestilled water (ddH_2O) were added to 1µg RNA. The reaction mixture was incubated at 70ºC for 10 min, in order to occur the annealing between RNA and primers. Then the reaction mixture was refreshed until 4ºC in order to add the following mixture: 4 µl first Strand Buffer 5X (Y00146, Invitrogen), 2 µl dithiothreitol 0.1M (DTT) (Y00147, Invitrogen), 2 µl deoxynucleotides (dNTPs) mix (10mM) (28-4065-22V, 28-4065-02V, 28-4065-12V and 28-4065-32V, GE Healthcare), 1 µl RNAse OUT™ Recombinant RNase Inhibitor 40 U/µl (10777-019, Invitrogen), 1 µl Superscript II® 200 U/µl (18064-022, Invitrogen) and ddH_2O to complete a total volume 12µl. cDNA synthesis was performed in a *T3000 thermocycler* (Biometra), using the following conditions (Table 1).

Table 1- Program used for cDNA synthesis

Stage	Cycles	Temperature (ºC)	Time (min)
Denaturation	1	70	10
Cooling	1	4	3
cDNA synthesis	1	42	90
Inactivation	1	75	15
Cooling		4	∞

3.1.3.2 Relative quantifying PCR (RQ-PCR)

Relative Quantifying PCR (RQ-PCR) consists in gene expression analysis with accuracy, sensitive and fast results, allowing the absolute or relative quantification of messenger ribonucleic acid (mRNA transcription) (Derveaux et al., 2010). RQ-PCR analysis is normalized for an endogenous control also known as housekeeping gene (gene expressed constitutively) (Gubern et al., 2009).

For RQ-PCR a reaction mixture was performed for all genes of interest for each sample. A reaction mixture was made in triplicate, for a total volume of 7 µl per reaction, containing 1µl cDNA, 3.5 µL LightCycler 480 SYBR Green I master (04707516001, Roche), 2 µL LightCycler 480 SYBR Green II master H_2O (04707516001, Roche) and 0.5 µL of both forwad and reverse primers (5 µM), according to the program described in table 2, using LightCycler 480 instrument (Roche). In all assays, the housekeeping gene used to normalize the samples was *Hypoxanthine phosphoribosyltransferase* (HRPT) gene.

Table 2- Relative quantifying PCR program

Stage	Cycles	Temperature (ºC)	Time
Heat activation	1	95	10 min 15 sec
PCR			
Denaturation		95	15 sec
Annealing	45	60	15 sec
Elongation		72	20 sec
Melting	1	60	14 sec
		95	14 sec
Cooling		40	10 sec

3.1.4 Protein levels

Cells were exposed to glucose, glutamine, lactate and butyrate to understand the role of these compounds as precursors of gluconeogenesis in ES2. The levels of gluconeogenic proteins (PCK1, PCK2, FBP1 and PFKFB1) were evaluated by western blot for all experimental conditions (culture conditions specified in 3.1.1).

3.1.4.1 Western Blotting

Western blotting is one of the gold standard protein analytical techniques. This assay allows target proteins to be specifically detected in complex biological samples, by interaction with antibodies after separating the proteins by SDS-PAGE and transferring them to a membrane (Liu et al., 2011).

Cell pellets were lysed in Radio-Immunoprecipitation Assay (RIPA) buffer (Appendix A) and stored at -20ºC, ON. The lysates were centrifuged at 14000 rpm for 4 min at 4ºC. Supernatants were used, in part, for determination of protein concentration, based on Bradford method, using Bio-Rad protein assay reagent (500-0006, Bio-Rad) through spectotrophometric quantification (595 nm). Following quantification, Loading buffer 5x (Appendix A) with 10% β-mercaptoethanol (M3148, Sigma) was added to each lysate and boiled at 95-100ºC for 10 min, to denature proteins. After that, samples were centrifuged at 14000 rpm for 2 min at 4ºC and then placed in ice.

The same amount of total protein from each sample was loaded in 15% polyacrylamide gel (Tris-glycine SDS-Polyacrylamide gel) (Appendix A) and electrophoresis was carried out in MINI-PROTEAN Tetra Electrophoresis System (Bio-Rad) at 150V for 1h30, into 1X TGS buffer (Tris-Glycine-SDS 10x (TGS), 161-0772, Bio-Rad) and then transferred to a Immun-Blot® PVDF membrane with a Mini Trans-Blot® Electrophoretic Transfer Cell (Bio-Rad), at 60V and at 4ºC, overnight (ON). Non-specific bindings to the membrane were blocked using 5% (weight (w)/volume(v)) non-fat milk in phosphate buffered saline 1x (PBS) 0.1% (v/v) Tween 20 (Appendix A) for 2 h at room temperature (RT), with gentle shaking. For protein detection, membranes were incubated with primary specific antibodies (Anti-PCK1, R04368, Sigma; Anti-FBP1, R07412, Sigma; Anti-PFKFB1, SAB1408617, Sigma), at appropriate concentrations (1:250 in 5% (w/v) non-fat milk in PBS 0.1% (v/v) Tween 20 (Appendix A)) at 4ºC, ON, with shaking.

The membrane was rinsed 3 times, for 5 min, with PBS 1x 0.1% (v/v) Tween 20, to remove unbound primary antibody. Membranes were then incubated for 2 h at RT with secondary antibody IgG-conjugated Horse raddish peroxidase (HRP) (anti-rabbit (31460, Thermo Scientific))

in appropriate concentrations (1:5000 in 5% (w/v) skin milk in PBS 0.1% (v/v) Tween 20 (Appendix A)). After rinsing the membrane 3 x 5 min with PBS 1x 0.1% (v/v) Tween 20, immunoreactive bands were detected by using ECL western blotting substrate (SuperSignal® West Pico Chemiluminescent Substrate (34080, Thermo Scientific) in a ChemiDoc XRS System (Bio-Rad) with Image Lab software. To normalize the protein levels in samples, membranes were rinsed 3 times, for 5 min, with PBS 1x 0.1% (v/v) Tween 20 and reprobed using anti β-actin (A5441, Sigma) at 1:1000 in 5% (w/v) skin milk in PBS1x 0.1% (v/v) Tween 20 (Appendix A), at 4ºC, ON, and then revealed as describe above. Bands were analyzed and quantified using *Image J* software (rsb.info.nih.gov/ij/).

3.1.5 Promoter activity using Luciferase reporter gene assay

Promoters are important regulatory elements that contain the necessary sequence features for cells to initiate transcription. Transient transfection promoter activity assay using a luciferase reporter gene is considered as a direct method for characterizing functional promoter sequences, providing a rapid, sensitive, and quantitative basis in the analysis of factors that potentially regulate mammalian gene expression *in vitro*. This technique, based on plasmid constructs, is characterized by the fusion of a reporter gene, such as firefly (*Photinus pyralis*) luciferase with a putative promoter sequence (inserted upstream from the reporter gene), allowing the measurement of the transcription activity of the reporter genes, and, thus, the inference about the promoter activity of the inserted regulatory fragment (Landolin et al., 2010).

Bioluminescence permits the high sensitive analysis of transient transfection assay, being the luciferase protein concentration proportional to the luminescence output. To minimize errors, it is desirable to include a co-transfected internal control with a second reporter gene constitutively active, for example Renilla (*Renilla reniformis*) as an internal control for normalization. The sequential measurement of these two luciferases (dual luciferase reporter system) from a single sample minimizes experimental variability, such as differences in cell viability, transfection efficiency, pipetting errors, cell lysis efficiency, and assay efficiency (Solberg and Krauss, 2013).

3.1.5.1 Amplification of promoter sequences

Genomic DNA (gDNA) was extracted using DNA Purification Protocol for 1-2 Million Cells (Citogene) from HCT15 cells, according to manufacturer's protocol. Starting from this DNA, PCR amplification was performed, using specific primers (with and without restriction) (Table 8) to flank

the sequences of interest (PCK1, PCK2, FBP1, PFKFB1, CTH and MPST promoter sites). PCR reaction mixture had 0.1 µg DNA, 2.5 µl PCR Rxn Buffer 10x (-MgCl2) (Y02028, Invitrogen), 2µl dNTPs (28-4065-22V, 28-4065-02V, 28-4065-12V and 28-4065-32V, GE Healthcare), 1.5 µl 50 mM magnesium chloride ($MgCl_2$) (P/N Y02016, Invitrogen), 0.1 µl 5 U/µl Taq DNA Polymerase (18038-026, Invitrogen), 1 µl reverse and forward primer (10 µM) and sterile ddH_2O to complete a total volume of 25 µl, in a *T3000 thermocycler* (Biometra) as described in table 3.

Table 3- PCR program used for amplification of promoters sequences

State	Cycles	Temperature (ºC)	Time
Initial denaturation	1	95	5 min
Denaturation	10	94	50 sec
Annealing		T_{ann}[1]	30 sec
Elongation		72	50 min
Denaturation	25	94	50 sec
Annealing		T_{ann}[2]	30 sec
Elongation		72	50 min
Final elongation	1	72	7 min
Cooling		15	∞

1Annealing temperature (Tann) of primers without restriction sites: PCK1 Forward(For)Reverse(Rev) 59.6ºC; PCK2 ForRev 59.9 ºC; FBP1 ForRev 61.4ºC; PFKFB1 60.1ºC; CTH ForRev 60.6 ºC; MPST ForRev 60.4 ºC

[2]T_{ann} of primers with restriction sites: PCK1 ForRev 66.8ºC; PCK2 ForRev 68.1 ºC; FBP1 ForRev 68.9ºC; PFKFB1 68.1ºC CTH ForRev 67.5 ºC; MPST ForRev 67.4 ºC

The annealing temperature (T_{ann}) of the primers was determined using the following equation:

$$Annealing\ temperature\ \ ^{o}C\ = \%\ CG\ x\ 0.41 + 69.3 - \frac{650}{mer}$$

The amplified PCR products were analyzed by electrophoresis, on a 2% (w/v) SEA KEM ® GTG ® agarose (50074, FMC BioProducts) gel (in TBE buffer 1x, diluted from TBE buffer 10 x, EC-860, National diagnostics) labelled with 0.05% (v/v) ethidium bromide 10 mg/ml (15585-011, Invitrogen), under UV (BioDocAnalyse Transilluminator, Biometra). DNA fragments with expected size were extracted from agarose gel and purified resorting to Illustra™ GFXTM PCR DNA and Gel Band Purification kit (28-9034-71, GE Healthcare), according to the manufacturer's protocol. After purifying, the DNA fragments were sequenced by automated sequencing.

3.1.5.2 DNA automate sequencing of promoter sequences

DNA automated sequencing was used to confirm the nucleotide sequences of the PCR products. Sequencing reaction mixture contained 3 µL of Big dye™ Terminator v1.1, 2 µL of Big dye sequencing buffer 5x (BigDye® Terminator v3.1 Cycle Sequencing kit, 4337456, Applied Biosystems), 1 µL of forward or reverse primer (at 3.33 µM) (Table 8), about 100 ng of template DNA and ddH_2O up to 20 µL. Sequencing reaction was carried out in a T3000 thermocycler (Biometra), according to the program described in table 4. Sequencing reaction mixture was purified with *AutoSeq G-50 dye terminator removal* kit (27-5340-02, *GE Healthcare Life Sciences*), according to manufacturer's instructions and then evaluated in an *ABI Prism™ 310 Genetic Analyzer* (*Applied Biosystems*).

Table 4- Automate sequencing program

Stage	Cycles	Temperature (ºC)	Time
Initial denaturation	1	96	5 min
Denaturation	30	96	10 sec
Annealing		T_{ann}[1]	5 sec
Elongation		72	4 min
Cooling		4	∞

[1]T_{ann} of primers without restriction sites: PCK1 For 59.4 ºC; PCK1 Rev 59.8 ºC; PCK2 For 60.3 ºC; PCK2 Rev 59.4 ºC; FBP1 For 60.9 ºC, FBP1 Rev 59.4 ºC; PFKFB1 For 60.3 ºC; PFKFB1 Rev 59.8 ºC; CTH For 61.4 ºC; CTH Rev 59.8 ºC; MPST For 61.4 ºC; MPST Rev 59.4 ºC. When temperature was higher than 60ºC, the temperature used was 59.5ºC.

3.1.5.3 Plasmid generation and cloning

In the present experimental work, luciferase plasmid pGL3-Basic (Figure 8 a) was used as a negative control and pGL3-Control (Figure 8 b) as a positive control. pGL3-Basic vector lacks eukaryotic promoter and enhancer sequences, allowing maximum flexibility in cloning putative regulatory sequences. Expression of luciferase activity in cells transfected with this plasmid depends on the insertion and proper orientation of a functional promoter upstream from *luc*+; the vector contains a modified coding region for firefly (Photinus pyralis) luciferase, optimized for monitoring transcriptional activity in transfected eukaryotic cells. pGL3-Control vector contains SV40 promoter and enhancer sequences, resulting in strong expression of *luc*+ in many types of mammalian cells. This plasmid is useful in monitoring transfection efficiency, in

general, as it is a convenient internal standard for promoter and enhancer activities expressed by pGL3 recombinants (Technical Manual - pGL3 Luciferase Reporter Vectors, Promega).

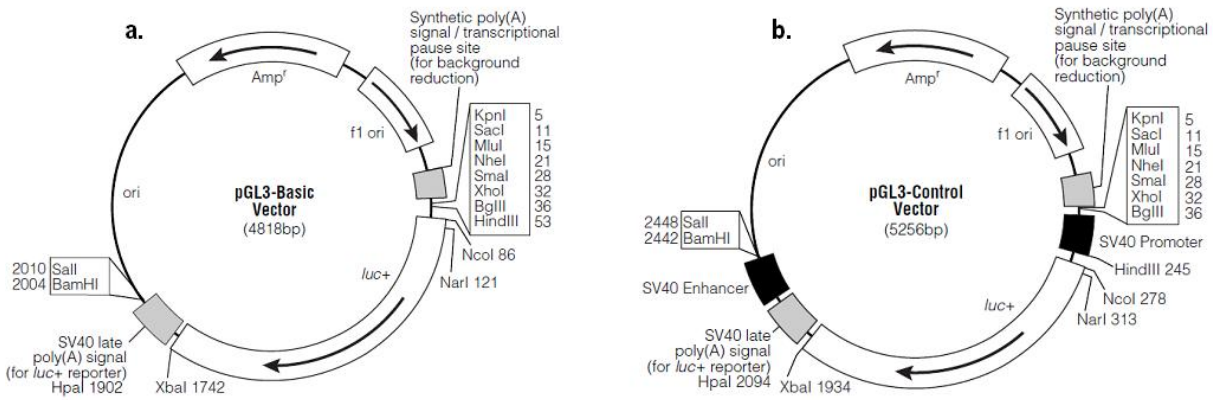

Figure 8: a) pGL3-Basic Vector. b) pGL3-Control Vector. Adapted from Technical Manual - pGL3 Luciferase

Amplified promoter sequences (PCK1, PCK2, FBP1, PFKFB1, CTH and MPST) (Table 8) and pGL3 basic vector (Figure 8 a) were digested with BglII 40 U/ µl (1175068, Boehringer Mannheim GmbH), HindIII 10 U/ µl (#ER0505, Fermentas) or MluI 10 U/ µl (#ER0561, Fermentas) restriction enzymes, depending on the fragment. The digestion reaction was performed at 37ºC, ON, in a T3000 thermocycler (Biometra) and then purified with IllustraTM GFXTM PCR DNA and Gel Band Purification kit (28-9034-71, GE Healthcare), according to the manufacturer's protocol. The digested fragments were then inserted into PGL3 basic vector, also digested, through the ligation reaction containing 1.8 µL 10x T4 DNA ligase buffer (B69, Fermentas), 1µL T4 DNA ligase (EL0011, Fermentas), 0.2 µL pGL3 basic vector, 15 µL of digested DNA and ddH_2O to complete a total volume of 20 µl, in a T3000 thermocycler (Biometra), ON, at 16ºC.

After ligation reaction, recombinant plasmids were cloned into One-shot TOP 10 Chemically Competent *Escherichia coli* (C4040-10, Invitrogen), according to the manufacturer's instructions.

3.1.5.4 Plasmid isolation

Positive colonies were selected by ampicillin resistance (Figure 8 a) and from each plate, 10 colonies were cultured in 5 ml of Luria-Bertani medium (LB) medium (with 50 µg/ml ampicillin) (Appendix A), at 37ºC, ON, with shaking. The isolation of recombinant plasmids from each culture were purified using Plasmid DNA MiniPreps kit (SP-PMN-100, EasySpin, Citomed), according to

the manufacturer's protocol. Following isolation, plasmid DNA concentration was obtained spectrophotometrically in a Nanodrop 2000 (Thermo Scientific). Recombinant plasmids were digested once again with the restriction enzymes previously used, with the purpose of confirm the insertion of the fragments of interest. After electrophoresis, the digestion products were visualized on a 2% (w/v) SEA KEM ® GTG ® agarose (50074, FMC BioProducts) gel (in TBE buffer 1x, diluted from TBE buffer 10x, EC-860, National diagnostics) stained with 0.05% (v/v) ethidium bromide 10 mg/ml (15585-011, Invitrogen), under UV (BioDocAnalyse Transilluminator, Biometra). In positive colonies for fragments of interest, PCR amplification was performed with RVprimer3 and GLprimer2 (pGL3 sequencing primers – table 8) (Table 5).

Table 5- PCR program for plasmid constructs amplification

Stage	Cycles	Temperature (ºC)	Time
Initial denaturation	1	94	5 min
Denaturation	35	94	50 sec
Annealing		56,9	30 sec
Elongation		72	1 min
Final elongation	1	72	7 min
Cooling		4	∞

Automated sequencing was used to confirm the exact position and the nucleotide sequence of the DNA inserted into pGL3 vector. The sequencing reaction mixture was performed using 10 ng of plamid DNA, 1 µL sequencing primers (at 3.33 µM) (Table 6), 4 µl of Big dye™ Terminator v1.1, 2 µL of 5X Big dye sequencing buffer (BigDye® Terminator v3.1 Cycle Sequencing kit, 4337456, Applied Biosystems) and ddH_2O to complete a total volume of 25 µl, in a *T3000 thermocycler* (Biometra) as described in table 6. Sequencing reaction products were purified using AutoSeq G-50 GFX (27-5340-03, GE Healthcare) accordingly to manufacturer's protocol, and then analyzed in a ABI Prism 3130 Genetic Analyzer.

Table 6- Automate sequencing program

Stage	Cycles	Temperature (ºC)	Time
Initial denaturation	1	96	5 min
Denaturation	30	96	10 sec
Annealing		56,9	5 sec
Elongation		60	4 min
Cooling		4	∞

To amplify the selected plasmid DNA, in which the fragment was inserted properly, a second transformation of One-shot TOP 10 Chemically Competent *Escherichia coli* (C4040-10, Invitrogen) was performed, according to the manufacturer's protocol. The colonies were cultured in 30 ml LB medium (with 50 µg/ml ampicillin) and purified using Plasmid DNA Midipreps Kit (12143, Qiagen) according to manufacturer's protocol.DNA concentration was then determined spectrophotometrically in a Nanodrop 2000 (Thermo Scientific).

3.1.5.5 Transient transfection of promoters constructs into ES2 cell line

Before transfection, ES2 cells were trypsinized with 1x 0.05% trypsin-EDTA (25300-054, Invitrogen) and plated at $2.5x10^5$ cells/mL in 24-well plates, with DMEM supplemented with 10% FBS and 1% AA. For transfection, per well, 3 µl of Lipofectamine 2000 (11668, Invitrogen), 0.5 µg of each plasmid construct (PCK1, PCK2, FBP1, PFKFB1, CTH and MPST) and 0.1 µg Renilla plasmid (1:5 ratio) were used in DMEM, at 3:1 ratio. pGL3-Control Vector (Figure 8 b) was used as positive control and pGL3-Basic Vector (Figure 8 a) as negative control, at the same concentration used for plasmid constructs. Plasmids and liposomes into DMEM were incubated separately for 5 min, at RT, and then mixed and incubated for another 20 min. One hundred µl of transfection complex were added to each well. Cells exposed to transfection complex were kept at 37ºC for 4-6h. After that time, 500 µl DMEM (41965-039, Gibco) supplemented with 10% FBS (S 0615, Biochrom) and 1% AA (15240062, Anti-Anti, Invitrogen) were added to each well, followed by incubation ON at 37ºC and 5% CO_2. For PCK1, PCK2, FBP1 and PFKFB1 constructs, 24h after transfection cells were exposed to DMEM without D-glucose/ L-glutamine (F 0405, Biochrom) supplemented with 1% FBS, 1% AA and 5 mM D-glucose (G8270, Sigma), 8 mM L-Glutamine (25030-081, Gibco), 10 mM NaLac (1.06522.2500, Merck), 8 mM Butyric acid (B10 350-0, Sigma-Aldrich) for PCK1, PCK2, FBP1 and PFKFB1 plasmid constructs. For CTH and MPST constructs, cells were exposed to DMEM without glucose (11966-025, Gibco) supplemented with 1% FBS, 1% AA and 0.402 mM cysteine. Cells transfected in control conditions were maintained in DMEM without glucose (11966-025, Gibco) supplemented with 1% FBS, 1% AA. Cells were harvested 48h post-transfection and lysed with Passive lysis buffer 1x (Passive lysis buffer 5x, E194A, Promega) and frozen at - 80ºC, ON. The experiments were performed in triplicates.

3.1.5.6 Luciferase activity

To evaluate the luciferase activity of constructs, Firefly and Renilla luciferase activities were measured sequentially from a single cell lysate in a Victor^3 1420 Multilabel Counter Luminoter (Perkin Elmer), using the Dual Luciferase Assay System (E1910, Promega) according to the manufacturer's protocol. The experiments were made in triplicates and the results were normalized to the pGL3-Basic vector activity, as a ratio of firefly luciferase activity to Renilla luciferase activity.

3.2. Role of glucose, glutamime, lactate, butyrate and cysteine in cell migration, cell cycle and apoptosis regulation

3.2.1 Cell migration - *In vitro* wound healing assay

In vitro wound healing assay is an easy, low-cost and well-developed method to measure cell migration *in vitro*. The basic steps involve an "injury" by ''scratching'' a cell monolayer, Images must be captured at the beginning and at regular timepoints during cell migration until the scratch closure, and then compared to quantify cell migration rates. This method permits the study of directional cell migration *in vitro* that mimics the migration of cells during wound healing *in vivo* (Liang et al., 2007). In the present experimental work, this assay was performed to identify a possible role of glucose, glutamine, lactate, butyrate and glutamine plus cysteine on cell migration, by comparison to control conditions (culture conditions specified in 3.1.1).

ES2 were plated in twelve-well culture plates at a 2.5 x 10^5 cells/mL concentration and maintained in DMEM (41965-039, Gibco) supplemented with 10% FBS (S 0615, Biochrom) and 1% AA (15240062, Anti-Anti, Invitrogen) until a confluent monolayer. In order to inhibit cell proliferation that could mask migration results, when cells were in expected optical confluence, they were treated with 5 µg/mL Mitomycin-C (M4287, Sigma), an antiproliferative agent, for 3 h at 37ºC, 5% CO_2. After that, in each well a tip of micropipette (P200 tip) was used to make a linear scratch along the well biggest diameter, creating a wound in the cell layer. The culture medium was replaced after the scratch in order to remove detached cells and to expose cells to the different experimental conditions, as described above. Cell were photographed under an *Olympus CK2* inverted optical microscope (Olympus) at the following time points: 0, 8, 24, 36 and 48 h. Photographs were analyzed with *Image J* software (rsb.info.nih.gov/ij/) to estimate wound closure in the different experimental conditions.

3.2.2 Cell cycle analysis by Flow Cytometry

Loss of control of cell proliferation underlies the pathology of diseases like cancer. As such there is a great need to investigate cell proliferation and cell cycle activity (Cecchini et al., 2012). Cell division consists of two consecutive processes, mainly characterized by DNA replication and segregation of replicated chromosomes into two separate cells. Replication of DNA occurs in a specific part of the interphase called S phase. S phase is preceded by a gap called G1 during which the cell is preparing DNA synthesis and is followed by a gap called G2 during which the cell prepares for division**.** G1, S, G2 and M phases are the traditional subdivisions of the standard cell cycle (Vermeulen et al., 2003).

DNA content in cells can be readily quantitated by flow cytometry of cells stained with propidium iodide (PI) - a fluorescent DNA intercalating dye – which binds to DNA in cells fixed with ethanol. In flow cytometry four distinct phases could be recognized in a proliferating cell population: G1, S, G2 and M, however G2 and M cannot be distinguished (Cecchini et al., 2012).

In the present experimental work, this assay was performed to identify a possible role of glucose, glutamine, lactate, butyrate and glutamine plus cysteine (culture conditions specified in 3.1.1) in the regulation of cell cycle.

ES2 cell lines were plated in six-well plate tissue dishes at a 2.5 $x10^5$ cells/ mL concentration, and maintained in DMEM (41965-039, Gibco) supplemented with 10% FBS (S 0615, Biochrom) and 1% AA (15240062, Anti-Anti, Invitrogen). When cells were adherent (~8 h later) they were kept under starvation (DMEM without FBS) (to synchronize cells). After that, at time point 0h some cells were harvested (control) and others were stimulated with the different media, as described above (culture conditions specified in 3.1.1). Cells were collected at 6, 24, 30 , 48 and 60 h after stimulation, and fixed in 70% ethanol (100983, Merck) at 4ºC. Cells were centrifuged at 1500 rpm for 5 min and then stained with 100 µl 50 µg/mL PI solution (Appendix A) and incubated at 37ºC for 40 min. 1X PBS was added after incubation and the cells were centrifuged at 1500 rpm for 5 min at 4ºC. The supernatant was discarded and cells were resuspended in 200 µl PBS 1x 0.1% (w/v) bovine serum albumin (BSA) (Appendix A) and analyzed by flow cytometry (FACScalibur – Becton Dickinson). The experiments were made in triplicates. In flow cytometric analysis death cells and cell aggregates were excluded.

3.2.3 Apoptosis analysis by Flow Cytometry

Apoptosis is distinguished from necrosis, or accidental cell death, by characteristic morphological and biochemical changes, including compaction and fragmentation of the nuclear

chromatin, shrinkage of the cytoplasm, and loss of membrane asymmetry. In normal live cells, phosphatidyl serine (PS) is located on the cytoplasmic surface of the cell membrane. However, in apoptotic cells, PS is translocated from the inner to the outer leaflet of the plasma membrane, thus exposing PS to the external cellular environment. Labeled Annexin V allows the identification of apoptotic cells by binding to PS exposed on the outer leaflet, and PI, which is impermeant to live and apoptotic cells, stains dead cells binding tightly to the nucleic acids in the cell (Technical Manual - Alexa Fluor® 488 annexin V/Dead Cell Apoptosis Kit with Alexa® Fluor 488 annexin V and PI for Flow Cytometry, Invitrogen).

In the context of the present thesis apoptosis assay was performed to identify a potential role of glutamine and glutamine plus cysteine in the regulation of apoptosis in ES2 cell line.

ES2 cells were plated in twelve-well plate tissue dishes at a 2.5 $x10^5$ cells/ mL concentration and maintained in DMEM supplemented with 10% FBS and 1% AA. After adhering (~8 h later) cells were kept under starvation (DMEM without FBS) ON at 37ºC and 5% CO_2. After that, at time point 0 h some cells were harvested (control) and others were stimulated with glutamine and glutamine plus cysteine (culture conditions specified in 3.1.1). Cells exposed to the different experimental conditions were collected at 6, 24, 30, 48 and 60 h, by harvesting with 100 µl of 1X 0.05% trypsin-EDTA (25300-054, Invitrogen) per well. Cells were centrifuged at 1200 rpm for 2 min and stained with 1.25 µl Alexa Fluor® 488 annexin V and 1.25 µl PI solution (50µg/mL) and incubated at RT and in dark for 15 min. After incubation, samples were resuspended in 200 µl PBS 1x 0.1% (w/v) BSA (Appendix A) twice and centrifuged at 1200 rpm for 2 min. The supernatant was removed and cells were resuspended in 100 µl of annexin V binding buffer 1X (Appendix A) and analyzed by flow cytometry (FACScalibur – Becton Dickinson). The experiments were made in duplicates.

3.3 Role of cysteine in aminothiols production

3.3.1 High-performance Liquid Chromatography (HPLC) for aminothiols detection

Thiols are chemically and biochemically very active components and low molecular-mass thiols, such as homocysteine (HCY), cysteine (CYS), cysteinylglycine (CysGly) and glutathione (GSH) are critical cellular components that play numerous roles in metabolism, cell signaling, detoxification and homeostasis, being important in a variety of physiological and pathological processes (Nolin et al., 2007). Intracellular thiols such as GSH are essential in

maintaining the highly reduced environment inside the cell, while extracellular thiols such as CYS also constitute an important component in antioxidant defense (Kuśmierek et al., 2009).

HPLC with fluorescence detection (HPLC–FD) is the most commonly used method for determination of aminothiols due to its high sensitivity, relative simplicity, ease of automation, and high throughput capability. Sample preparation usually involves disulfide reduction, protein precipitation, and derivatization prior to chromatographic separation (McMenamin et al., 2009).

In the present thesis this assay was performed to understand the possible role of L-cysteine addiction comparatively to the control (only glutamine presence) in aminothiols production, namely in the influence in endogenous antioxidant GSH pathway.

ES2 cells were plated in 75 cm^2 tissue culture flasks (T75) and maintained in DMEM (41965-039, Gibco) supplemented with 10% FBS (S 0615, Biochrom) and 1% AA (15240062, Anti-Anti, Invitrogen) until expected 70% optical confluence (~$6.4x10^6$ cells/mL). Confluent cells were exposed to DMEM without glucose (11966-025, Gibco) supplemented with 10% FBS (S 0615, Biochrom) and 1% AA (15240062, Anti-Anti, Invitrogen) and 0.402 mM cysteine (culture conditions specified in 3.1.1), for 16 h. The supernatants were collected and cells were harvested with 1X 0.05% trypsin-EDTA (25300-054, Invitrogen), centrifuged at 1200 rpm for 2 min, rinsed twice in 1X PBS (Appendix A) and frozen at -80ºC.

In order to perform cell lysis, pellets were resuspended in 250 µl 1X PBS - 0.01% (v/v) Triton x-100 and centrifuged at 10000 rpm for 2 min. After that, cell supernatants were filtered in Amicon Ultra-15 Centrifugal Filter Units (Merck Millipore) by centrifugation at 3800 rpm for 20 min at 4ºC. Cells, cell supernatants and crude culture medium were reduced by the addiction of 10 µl 100g/L Tris (2-carboxyethyl)phosphine (TCEP) per 100 µl of sample and incubated for 30 min at RT. After that, 90 µl 100g/L Trichloroacetic acid (TCA) 1mM EDTA were added and samples centrifuged at 13000 rpm for 10 min at 4ºC. TCA acid stops the reduction reaction and induces protein precipitation. The resultant supernatants were collected and derived due to the addiction of 10 µl 1.55M Sodium hydroxide (NaOH), 125 µl 0.125M Sodium tetraborate- 4mM EDTA (Borate tampon) and 50 µl 1g/L Ammonium 7-Fluoro-2,1,3-benzoxadiazole-4-sulfonate (SBD-F). The samples were incubated at 60ºC for 1 hour, protected from ligth.

After samples processing, aminothiols quantification by HPLC was performed in Schimadzu (Kyoto, Japan) system, consisting of a LC 9-A solvent delivery pump, a 7725i injector, a RF-10AXL fluorescence detector and a CTO-10AS VP column oven. A LiChrospher 100 RP-18 (250 x 4 mm; 5 µm) column protected by a LiChrospher 100 RP-18e (4x 4mm; 5 µm) guard-column, both from Merck (New Jersey, USA), was used, at 29^oC. The detector was set at excitation and emission wavelengths of 385 nm and 515 nm. Data acquisition and processing

were performed in Shimadzu Class VP 7.X software. Calibration curves were constructed six standard concentrations of the five aminothiols (HCY, CYS, CysGly, GSH and NAC) in PBS 1X and, for each curve, the absolute peak-area ratios were calculated and plotted against the nominal aminothiol concentration.

3.4 Statistical analysis

Results were analyzed by student's t test or 2-way ANOVA to evaluate the statistical significance of results, using GraphPad Prism 6 software. Data's were considered significant when $p<0.05$.

Table 7 - Primers used during the experimental work

Reference/Target	Primer (5'-3')	Tm (ºC)	Technique
BglII pPCK1.For	ATGAGATCTGGATGGGTCGCATTTAGGAC	66.7	PCR Automate sequencing
HindIII pPCK1.Rev	ATGAAGCTTCTTCCATGGAAGCCTCTCTAC	66.8	
MluI pPCK2.For	TGAGGCGTGATGTGGGGGTGACAACATTAG	69.5	
BglII pPCK2.Rev	ATGAGATCTGCTCTGTGTCAGCAACTCTG	66.7	
MluI pFBP1.For	ATGACGCGTCTCCCCTCCACATTCCGTG	71	
HindIII pFBP1.Rev	ATGAAGCTTGACTCTGCCAGAGAGAAAGC	66.7	
MluI pPFKFB1.For	ATGACGCGTCCCTGTAAGGCTAACAAGGATG	69.5	
HindIII pPFKFB1.Rev	ATGAAGCTTCCCTCCTTAGGACTGTTGAAG	66.8	
BglII pCTH.For	ATGAGATCTCAGCCAATAAGGAGCGGGAG	68.1	
HindIII pCTH.Rer	ATGAAGCTTGCTGAACCGCGAAAGAAGAAG	66.8	
BglII pMPST.For	ATGAGATCTCGTAGGTCTTGAGCAGGGAG	68.1	
HindIII pMPST.Rev	ATGAAGCTTGGAGGGAGAAAGAGCTTCTC	66.7	
RVprimer3	CTAGCAAAATAGGCTGTCCC	57.0	PCR Automate sequencing
GLprimer2	GGAAGACGCCAAAAACATAAAG	56.0	
PCK1.For	GCGGATCATGACGCGGATG	58.8	RQ-PCR
PCK1.Rev	GAGCGTCAGCTCCGGGTTG	63.1	
PCK2.For	CAAGACCAACCTGGCTATGATG	60.3	
PCK2.Rev	GAGTCGACCTTCACTGTCAAAC	60.3	
FBP1.For	GCTACGCACTGTATGGCAGTG	61.8	
FBP1.Rev	CGTAGCCCTCGTTAAGGCTG	61.4	
PFKFB1.For	CCAGTATCGACGAGAGGCAG	61.4	
PFKFB1.Rev	CTCTGGTAGTGTTGGTGGCATC	62.1	
ALT.For	CGTGACGGTGCTGAAGCTG	61.0	
ALT.Rev	CTCGTCCAGGTAGTAATCCAC	59.8	
CTH.For	GCAGCCACTGTAACTATTACCC	60.3	
CTH.Rev	CTGGTGTAATTGCTGCCTCTAG	60.3	
MPST.For	CTTCATCAAGACCTACGAGGAC	60.3	
MPST.Rev	GGTAGTGGCCAGGTTCAATG	59.4	
mTOR.For	CAATGTGAGCGTCCTGCAG	58.8	
mTOR.Rev	GACTCCTCTTGACTCATCTCTC	60.3	

Tm: melting temperature
RQ-PCR: Relative quantifying PCR

4. Results

4.1 Role of glucose, glutamine, lactate and butyrate as gluconeogenic precursor

4.1.1 Nuclear magnetic resonance (NMR) for metabolic detection in ES2 cell line

To evaluate gluconeogenesis in ES2 cell lines, NMR spectroscopy was used. Different ^{13C}-labeled carbon source were used: ^{13C}-[U]-glutamine, ^{13C}-[U]-lactate and sodium ^{13C}-[U]-butyrate.

In ES2 cell extracts no ^{13C} labeled glucose was detected. The profile of ^{13}C-labeled compounds varied, depending of the carbon source used (Figure 9).

It was observed the presence of ^{13C}-labelled glutamine, glutamate, alanine and lactate when glutamine was a carbon source. Glycogen was only observed with butyrate as carbon source, but it was not ^{13C}-labelled (Figure 9 b).

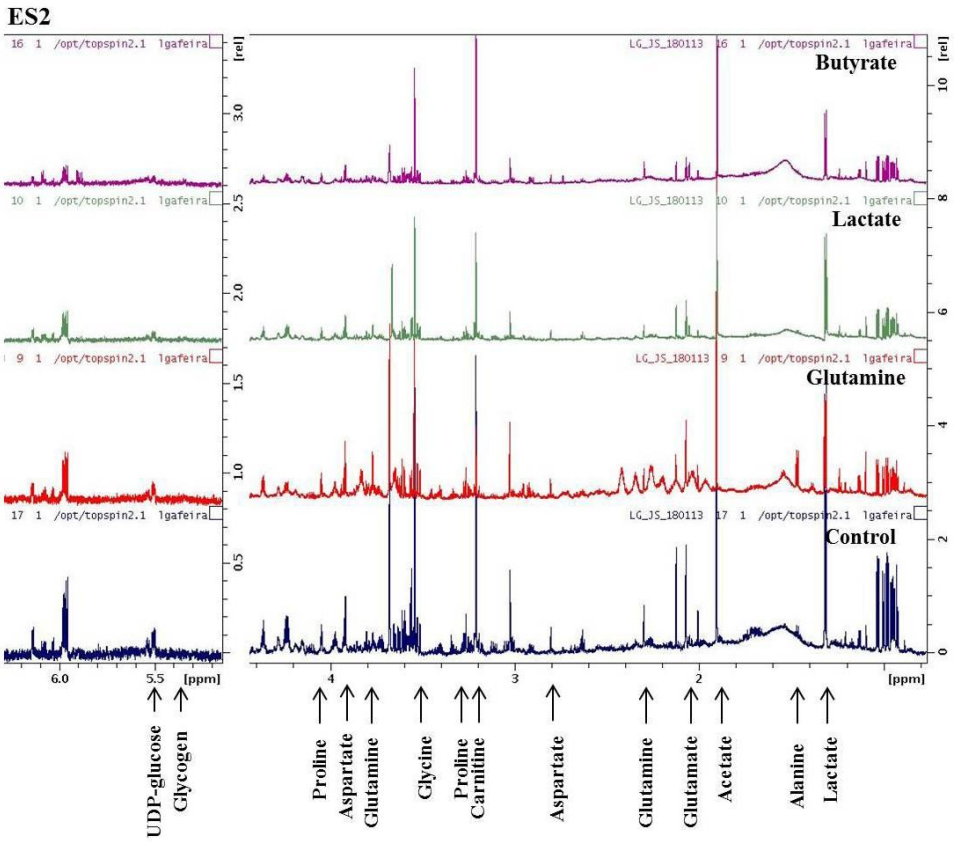

Figure 9- NOESY 1D (1H) spectra for ES2 cell line. Cells were exposed to sodium ^{13C}-[U] –butyrate, sodium ^{13C}-[U] –lactate and ^{13C}-[U] –glutamine, ON at 37ºC. Control were cells grown in DMEM without D-glucose/ L-glutamine, supplemented with 1% FBS and 1% AA

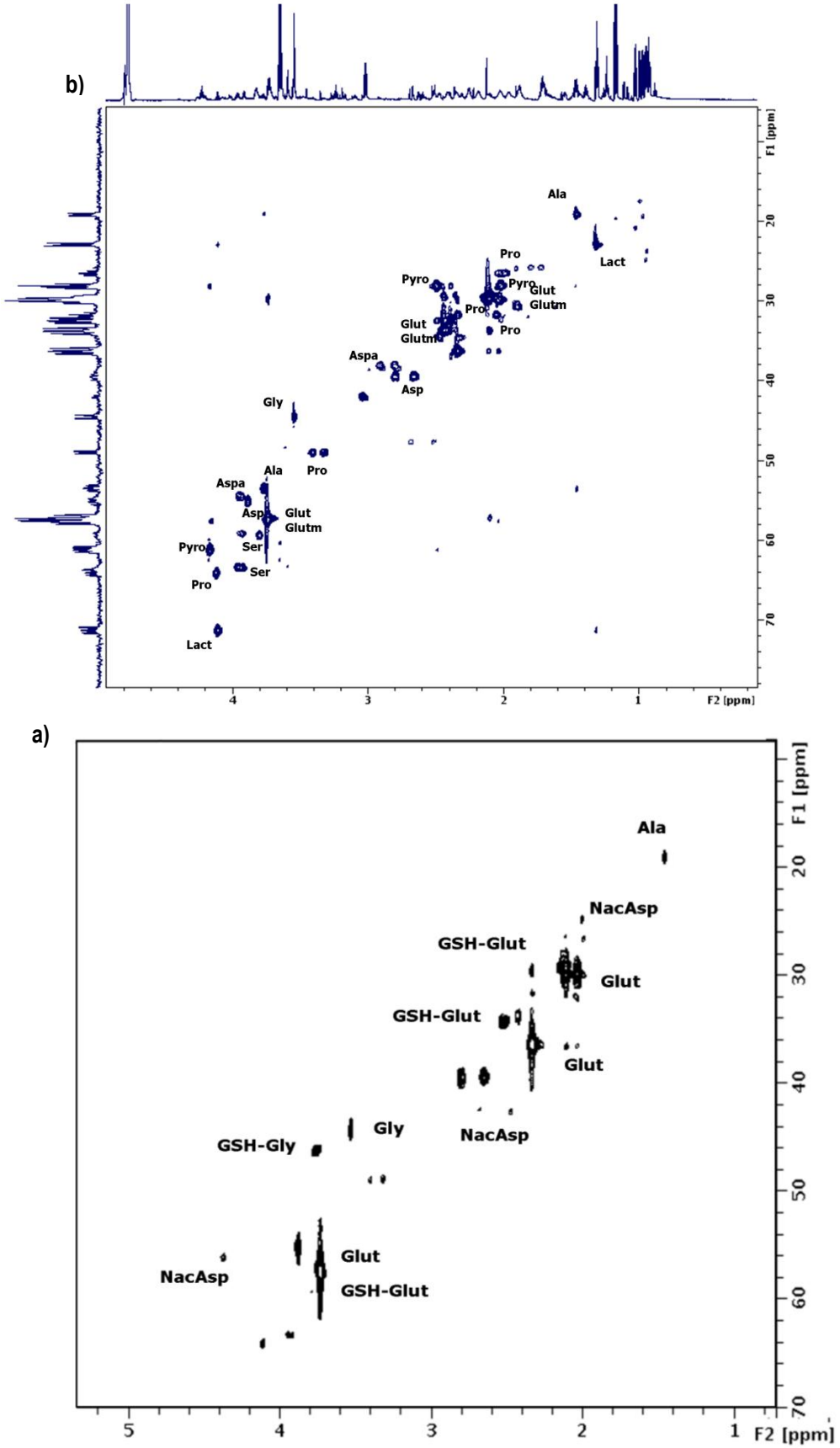

Figure 10: ^{13}C-^{1}H-HSQC spectra of ES2 supernant (A) and cell extracts (B) incubated with ^{13}C-glutamine. Cells in starvation were exposed to ^{13C}-[U] –glutamine, for 48 at 37ºC. The ^{13C} labeled compounds identified were: Lact- lactate; Pro- proline; Ser- serine; Asp-aspartate; Pyro- pyroglutamate; Aspa- asparagine; Ala- alanine; Gly- glycine; Glut- glutamate; Glutm- glutamine. In panel B, it is indicated the resonances of the free glutamate(Glut) and glutamate moiety of GSH (GSH-Glut), free glycine (Gly) and glycine moiety of GSH (GSH-Gly), and the N-acetyl-aspartate (NacAsp).

The glutamine metabolism was further studied in starvation conditions. Cells in starvation were incubated 48 hours with ^{13C}-U-glutamine, and further analyzed.

As control, it was used cells incubated with unlabelled glucose. In these cases, the growth media were also analyzed, in order to evaluate the secreted metabolites.

In supernatants of ^{13C} glutamine ES2 cells were detected ^{13C} labeled metabolites, namely formate, lactate, alanine, pyroglutamate, aspartate, asparagine, glycine, proline, glutamine and glutamate (Figure 10). In the cells, the same ^{13}C labeled metabolites were present besides glutathione (GSH) and N-acetlylaspartic acid (Figure 10). The results show that ^{13C} from glutamine were incorporated in glycine and glutamate moieties of GSH, but not in the cysteine moiety (Figure 11).

Organic phase of ES2 cells incubated with ^{13C} glutamine were also analyzed, indicated that the glutamine is preferentially used for the synthesis of glycerol backbone of triglycerides and phospholipids, and not for the fatty acids synthesis (data not shown).

4.1.2 *PCK1, PCK2, FBP1, PFKFB1* and *ALT* gene expression and protein levels in ES2 cell line

The metabolic reprogramming capacity of tumor cells was evaluated in ES2 cells grown in glucose and in glucose privation with glutamine, lactate or butyrate, using as control cells grown in medium without both glucose and glutamine and supplemented with 1% FBS. The expression of gluconeogenic (*PCK1, PCK2, FBP1* and *ALT*) and glycolytic gene (*PFKFB1*) were assessed by Real Time-PCR (Figures 11) and Western Blotting (Figures 12).

In ES2 it was observed a statistically significant increase in *PCK1* expression after glucose and butyrate treatment and a decrease after lactate and glutamine (statistically significant) treatment, comparing to cells grown in control conditions (Figure 11). The dynamics at mRNA levels did not correspond to PCK1 protein levels assessed by Western Blotting (Figure 12 a). Comparing to control condition, PCK1 protein profile showed exactly the opposite, lower levels of PCK1 with glucose and butyrate treatment and higher in glutamine and lactate conditions (Figure 11 and 12 a).

Regarding *PCK2* gene expression, after butyrate treatment it was verified an increase in mRNA levels while glucose (statistically significant) and lactate treatment induced a decrease in mRNA levels, comparing to control condition. Glutamine treatment led to an expression level of *PCK2* almost equivalent to control condition (Figure 11).

The levels of FBP1 protein in ES2 cells was also detected in all conditions although glucose, glutamine and lactate exposure led to higher levels of expression. Butyrate exposure and control condition showed low levels of FBP1 protein (Figure 12 b).

A statistically significant increase of mRNA levels of PFKFB1 was observed in glucose, butyrate and lactate conditions while in glutamine condition it was verified a decrease in mRNA levels of *PFKFB1*, comparing to cells grown in control condition (Figure 11). Concerning protein levels of PFKFB1 assessed by Western Blotting, the dynamics was not the same observed at the mRNA levels (Figure 12 c). Lactate condition showed a decrease in PFKFB1 protein levels in comparison with control condition while butyrate, glutamine and glucose exposure led to higher levels of PFKFB1 protein expression (Figure 12 c).

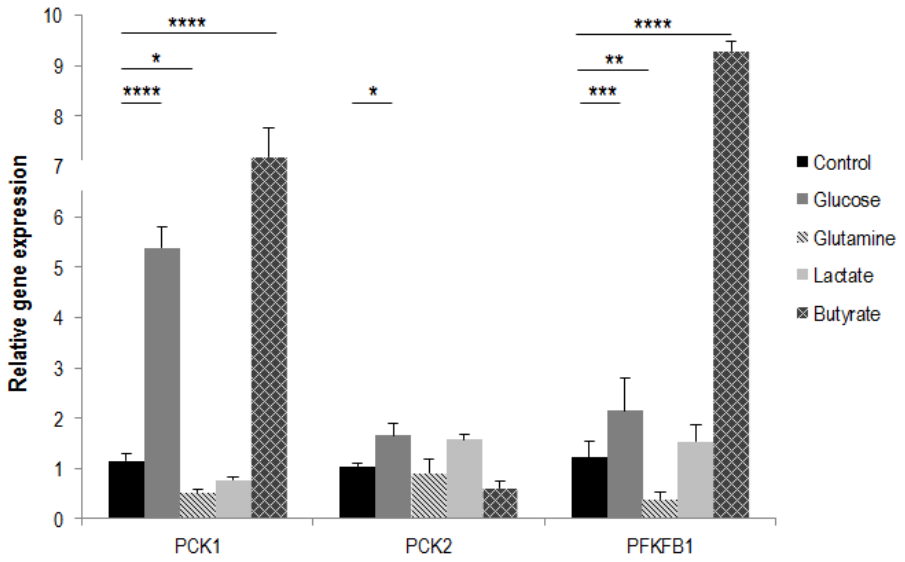

Figure 11- Relative gene expression of *PCK1, PCK2* and *PFKFB1*. Cells were grown in control, glucose, glutamine, lactate and butyrate conditions. HPRT gene was used as endogenous control. Expression levels were normalized to control condition. Data are mean ± error bars of triplicates. *p≤0.05 **p ≤0.01 ***p ≤0.001 ****p<0.0001

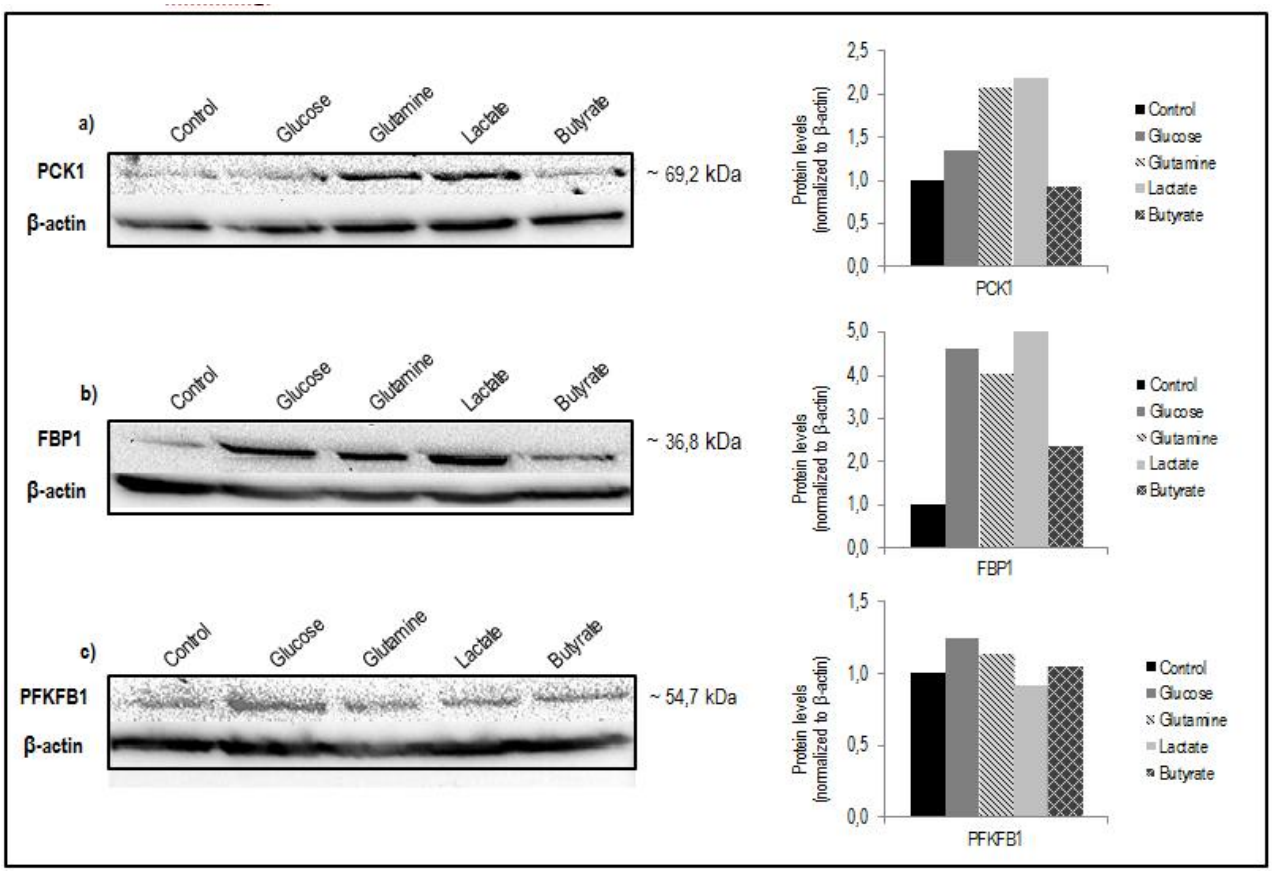

Figure 12– PCK1 (a), FBP1 (b) and PFKFB1 (c) protein levels in ES2cells assessed by western-blotting. Cells were grown in control, glucose, glutamine, lactate and butyrate conditions. Protein levels were normalized to β-actin and are relative to those obtained for cells grown in control conditions.

In the present thesis it was also important to evaluate the expression of alanine transaminase (ALT), since it catalyses the conversion of glutamine into alanine, which can be canalized to produce glucose, becoming also an important enzyme in gluconeogenesis context.

It was observed an increase in *ALT* expression after glucose, lactate, butyrate and glutamine treatment, although this increase was statistically significant in glucose and lactate conditions (Figure 12). However, when glutamine exposure time was increased from 16 to 30h a statistically significant increase in mRNA levels of ALT was observed (Figure 12).

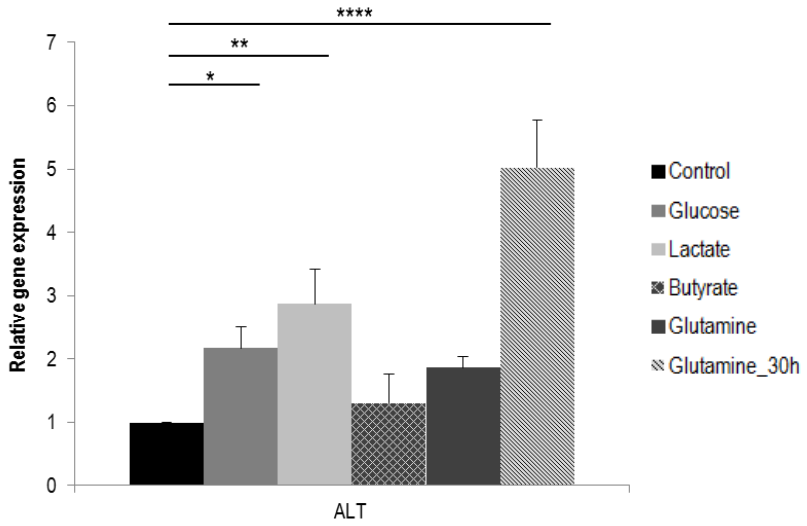

Figure 13- Relative gene expression of ALT. Cells were grown in control, glucose, glutamine, lactate and butyrate conditions. HPRT gene was used as endogenous control. Expression levels were normalized to those obtained for cells grown in control conditions. Data are mean ± error bars of triplicates. *p≤0.05 **p ≤0.01 ****p<0.0001

4.1.3 Activity of PCK1, PCK2, FBP1 and PFKFB1 promoters in ES2 cell line

In order to evaluate the influence of different nutrients in the regulation of the expression of gluconeogenic and glycolytic genes PCK1, PCK2, FBP1 and PFKFB1, promoters activity was evaluated by using Luciferase reporter gene assay in cells grown in glucose privation medium and further stimulated with glucose, glutamine, lactate and butyrate. Different constructs were generated using conventional molecular cloning techniques and cells were transfected with cationic liposome (Lipofectamine).

Regarding PCK1 promoter, glucose and butyrate conditions, showed the same level of activity verified in control (Figure 14). Higher PCK1 promoter activity was observed in cells exposed to lactate, whereas in cells exposed to glutamine a decrease in PCK1 promoter activity was observed. Both differences were statistically significant.

For PCK2 promoter, cells grown in all conditions except glutamine showed higher promoter activity comparing to control, being butyrate exposure the condition more favorable to PCK2 promoter activity (Figure 14).

FBP1 promoter activity was higher in cells exposed to lactate and glucose, whereas butyrate and glutamine exposure induced a decrease in PFKFB1 promoter activity, in relation to control all these differences were statistically significant. (Figure 14).

Finally, for PFKFB1 promoter only lactate condition induced a statistically significant increase in luciferase activity, comparing to control. In glucose, glutamine and butyrate the levels were equivalent to control (Figure 14).

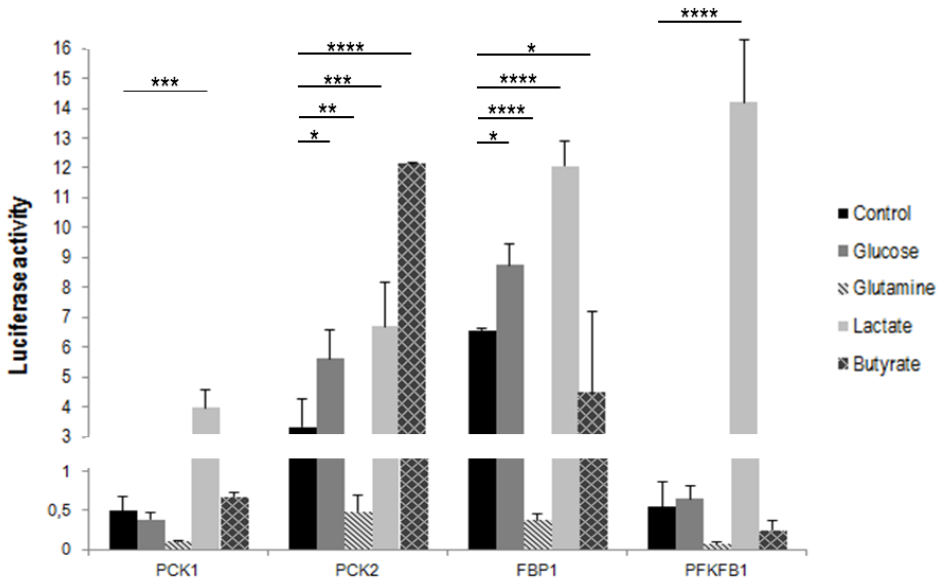

Figure 14 - Luciferase activity of PCK1, PCK2, FBP1 and PFKFB1 constructs in transfected ES2 cells. Cells were grown in control, glucose, glutamine, lactate and butyrate conditions. Data are mean ± error bars of triplicates. *p≤0.05 **p ≤0.01 ***p ≤0.001 ****p<0.0001

4.2 Role of glucose, glutamine, lactate, butyrate in cell migration and cell cycle in ES2 cell line

4.2.1 Cell migration - *In vitro* wound healing assay

In vitro wound healing assay was performed to assess a putative role of glucose, glutamine, lactate and butyrate on ES2 cells migration. The migration rate was monitorized in cells previously submitted to glucose privation at the following time points: 0, 8, 24, 32 and 48 h (Figure 15).

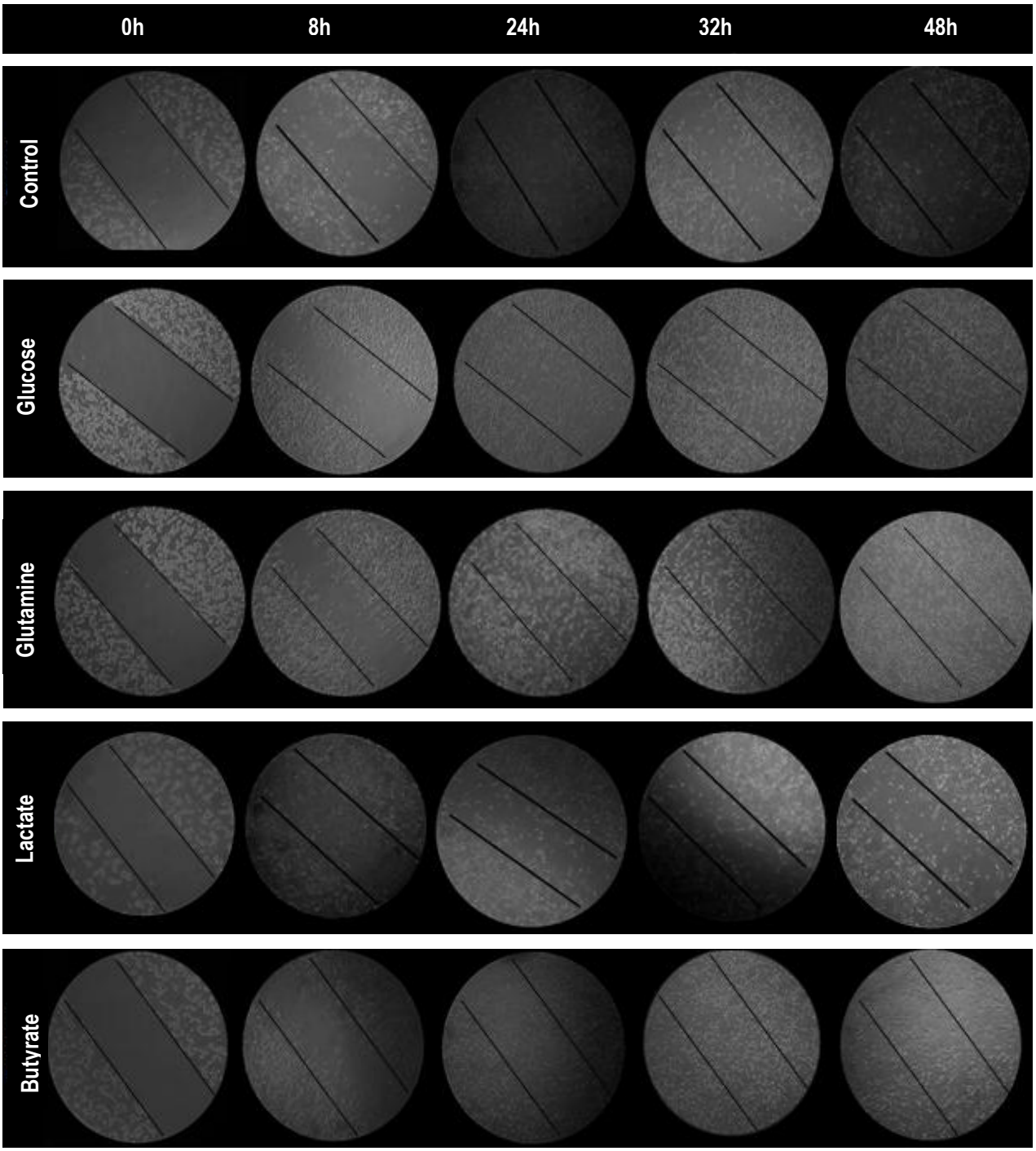

Figure 15- *In vitro* Wound Healing assay in ES2 cells. Comparison between cells grown in control, glucose, glutamine, lactate and butyrate conditions at 0, 8, 24, 32 and 48 h. Phase microscopy (original magnification: 200x).

During the assay, it was observed a higher cell migration rate (faster wound closure) in cells exposed to glucose, glutamine and butyrate, comparing to control (Figure 15 and 16). In lactate condition cells showed the same migration rate as the control (Figure 15 and 16).

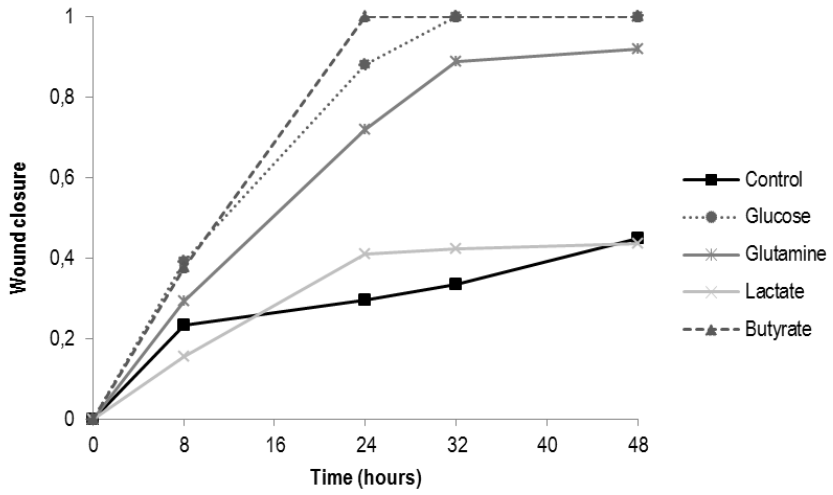

Figure 16- Quantification of wound closure in ES2 cells. Cells were maintained in control, glucose, glutamine, lactate and butyrate conditions at 0, 8, 24, 32 and 48 h

4.2.2 Cell cycle analysis by Flow Cytometry

Cell cycle analysis was performed to assess the influence of glucose, glutamine, lactate and butyrate in cell cycle regulation. Cells were submitted previously to glucose privation.

The percentage of cells after 6 h in culture (control_6h), showed few alterations in S and G2-M phase (44.7% and 15.95%) compared to time point 0 h (S phase 44.7% and G2-M phase 15.94%) (Figure 17). Butyrate, glutamine and lactate conditions, after 6 h, express an identical percentage of cells in S phase (42.57%, 39.41% and 36.79% respectively) and G2-M phase (18.03%, 13.02%, 15.35%, respectively) comparing with control (S phase 44.7% and G2-M phase 15.95%) whereas in glucose condition S phase (42.15%) and G2-M phase (12.47%) was slightly lower (Figure 17 b, c and d).

In time point 24 h, the conditions showing to be more favorable to cell cycle progression were butyrate and glutamine (Figure 17 b and d). Under these conditions, S phase (7.72% and 19.58%) and G2-M phase (32.52% and 7.81%) were higher than control (S phase 5.84% and G2-M phase 11.35%) (Figure 17 b and d). Identical results were observed in the same conditions with 30 h of exposure (Figure 17 b and d).

Glucose and lactate exposure did not show relevant alterations on cell cycle profile, comparing to control condition (Figure 17 a).

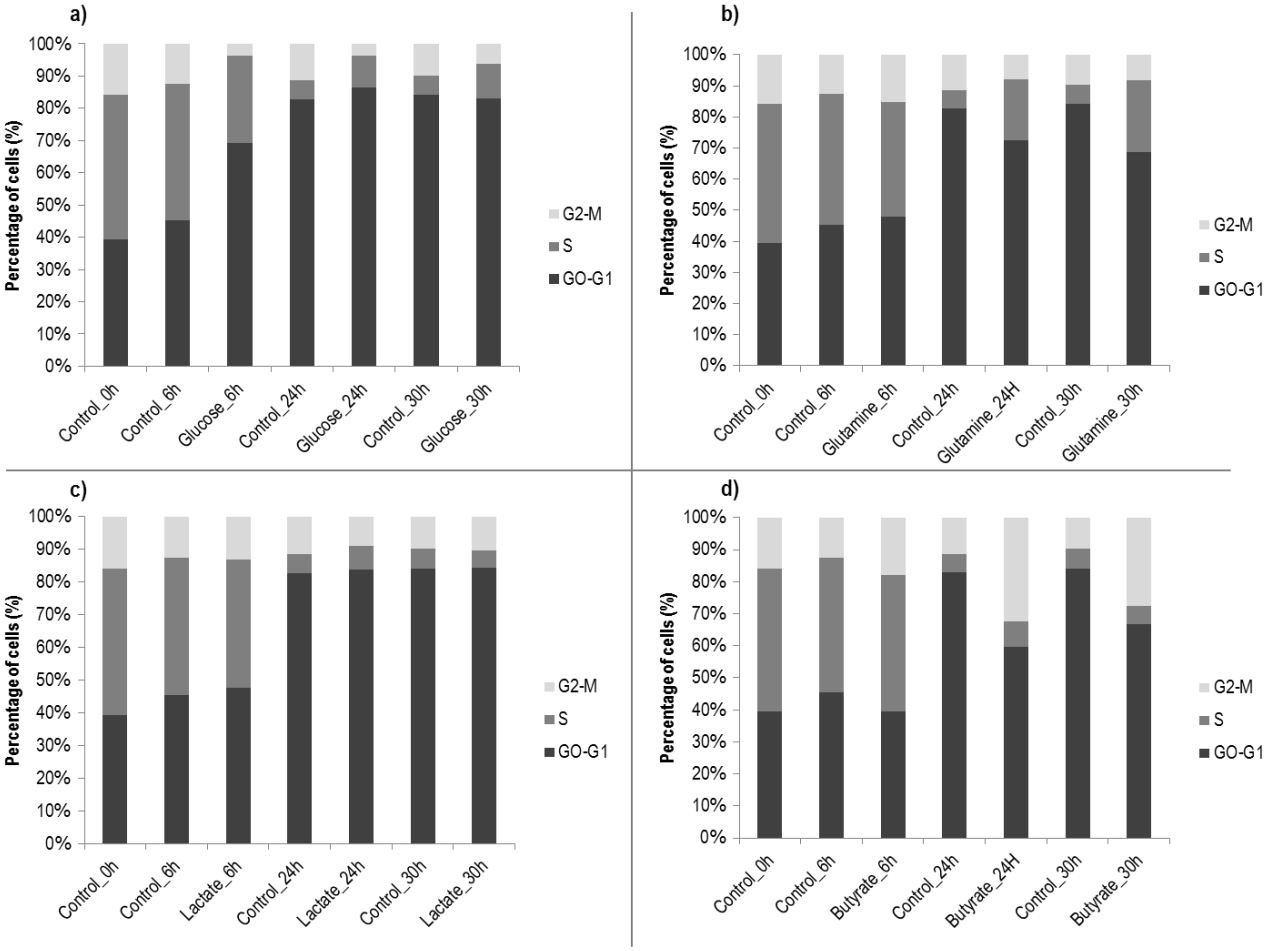

Figure 17– Cell cycle analyzes by flow cytometric (PI staining) in ES2 cells. Cells were grown in control, glucose (a), glutamine (b), lactate (c) and butyrate (d) conditions at 0, 8, 24, 32 and 48 h. Data are means of triplicates.

4.3 Role of cysteine associated with glutamine and endogenous antioxidant synthesis

4.3.1 *CTH, MPST* and *mTOR* gene expression in ES2 cell line

Cysteine is one of the amino acids used in the synthesis of GSH (glutathione). In the literatures it is reported that the levels of free cysteine is associated with an increase in antioxidative responses and cysteine metabolism. The effects of cysteine exposure in cell features and in antioxidative pathways were evaluated.

The expression of genes involved in cysteine synthesis (*CTH*), in cysteine degradation (*MPST*) was assessed by RQ-PCR (Figures 18). The assays were performed because was observed by NMR (described above) the presence ^{13C} partially labeled GSH (^{13C} labeled glycine and ^{13C} labeled glutamate were detected) in cells exposed with ^{13C} glutamine for 30 h. Because of

this, it becomes important to understand the behavior of ES2 cells (in glucose privation medium) with additional resources of free cysteine.

In ES2 it was not observed significant differences in *CTH* expression after cysteine supplement, comparing to cells grown in glutamine condition (DMEM without glucose/ with glutamine) (Figure 18 a) while in *MPST* mRNA levels it was verify an increase in cells exposed to cysteine supplement (Figure 18 b).

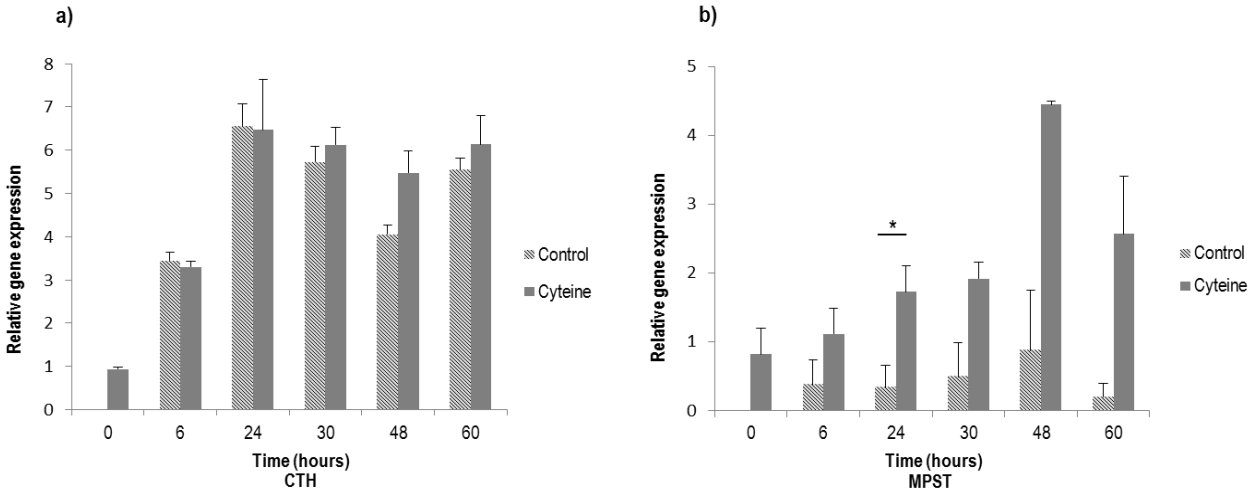

Figure 18- Relative gene expression of CTH (a) and MPST (b). Cells were grown in control and in cysteine condition. HPRT gene was used as endogenous control. Expression levels were normalized to those obtained for cells grown in control conditions. Data are mean ± error bars of triplicates. *p≤0.05

Because mTOR pathway is sensitive to amino acids, namely glutamine, we evaluate the expression of *mTOR* by RQ-PCR, in ES2 cells grown in glutamine in the presence and absence of glutamine. Few differences were detected in glutamine and in cysteine condition (Figure 19). Although, with 6 h of exposition the *mTOR* mRNA levels were lightly increased with cysteine supplementation whereas when cells were exposed to cysteine for 30 h the mRNA levels were increased in glutamine condition (Figure 19).

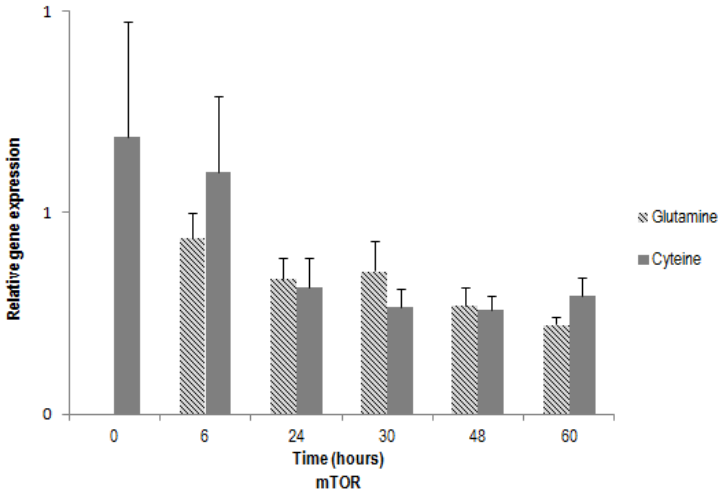

Figure 19- Relative gene expression of mTOR. Cells were grown in control and in cysteine condition. HPRT gene was used as endogenous control. Expression levels were normalized to those obtained for cells grown in control conditions. Data are mean ± error bars of triplicates.

4.3.2 Activity of CTH and MPST promoters in ES2 cell line

To evaluate the role of cysteine in the activity of CTH and MPST promoter, cells were grown in glutamine and glutamine plus cysteine conditions. Cells were transfected with different constructs using cationic liposome (Lipofectamine) and then, promoter activity was detected using the Dual Luciferase Assay System.

CTH promoter showed identical luciferase activity in glutamine plus cysteine condition, comparatively to glutamine condition being the same verified in MPST promoters (Figure 19). Although, these results showed that CTH promoter was about 5 fold more active than MPST promoter, in ES2 cell line (Figure 20).

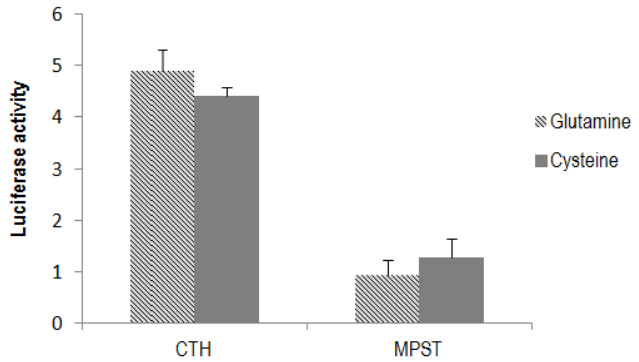

Figure 20- Luciferase activity of CTH and MPST constructs in transfected ES2 cells. Cells were grown in glutamine and cysteine condition. Data are mean ± error bars of triplicates

4.4 Role of cysteine in cell migration, cell cycle and apoptosis in ES 2 cell line

4.4.1 Cell migration - *In vitro* wound healing assay

In vitro wound healing assay was performed to evaluate the additional effect of cysteine in the migration rate of ES2 cells grown in glutamine. The migration rate was evaluated at the following time points: 0, 8, 24 and 32 h (Figure 21).

It was verified a higher cell migration rate in cells grown in glutamine plus cysteine condition, comparing to glutamine condition (Figure 22).

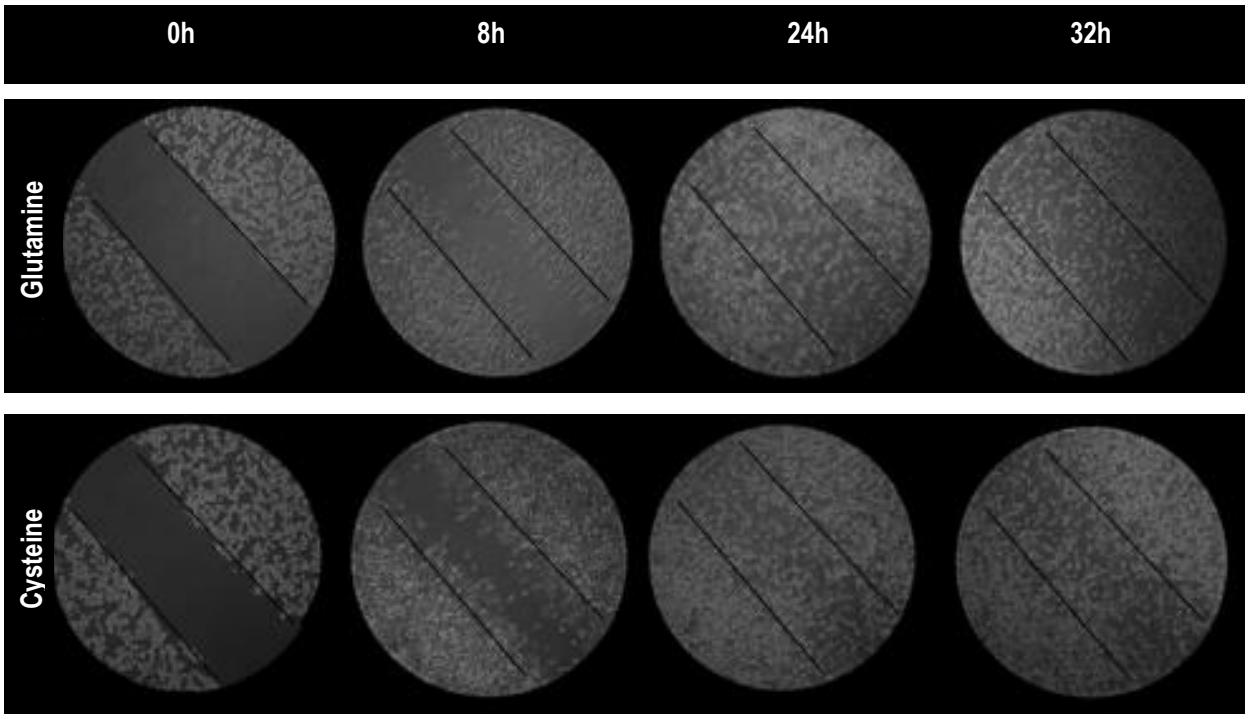

Figure 21 - *In vitro* Wound Healing assay in ES2 cells. Comparison between cells cultured in glutamine and in cysteine supplement conditions at 0, 8, 24 and 32 h. Phase microscopy (original magnification: 200x).

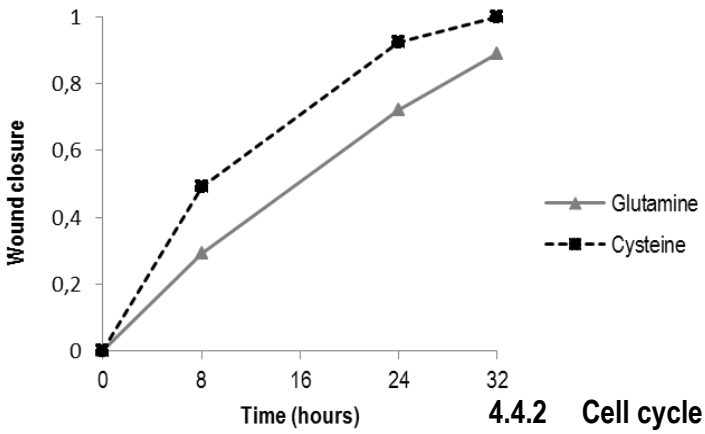

Figure 22- Quantification of wound closure in ES2 cells. Cells were cultured in glutamine and in cysteine supplement conditions at 0, 8, 24 and 32 h

4.4.2 Cell cycle analysis by Flow Cytometry

Cell cycle analysis was performed to evaluate the additional effect of cysteine in cell cycle regulation of ES2 cells grown in glutamine.

In cell cycle analyzes, few differences were detected between glutamine condition and cells exposed to cysteine (Figure 23). At time point 30 h there is an increase in the percentage of cells in S phase in glutamine plus cysteine condition (glutamine 11.94% and glutamine plus cysteine 15.33%). In both conditions, after 48 h it was observed a significant decrease in S phase (glutamine condition 4.5% and glutamine plus cysteine condition 5.85 %) that might be related to medium depletion (Figure 23). Summing up, in all time points except at 24h, cells grown in the presence of glutamine plus cysteine have a slight increase in the percentage of cells dividing (S + G2-M phases).

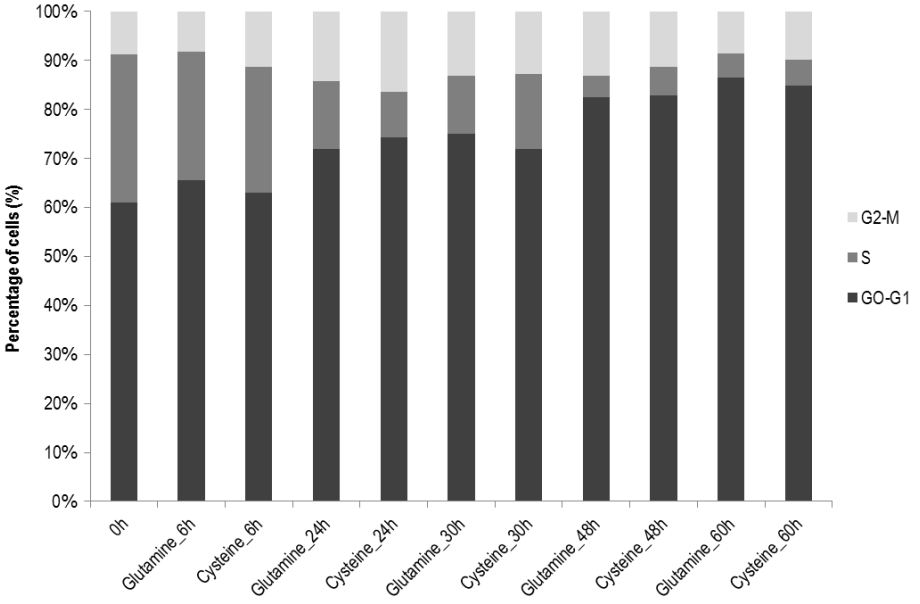

Figure 23– Cell cycle analyzes by flow cytometric (PI staining) in ES2 cells. Cells were grown in control and in cysteine conditions at 0, 6, 24, 30, 48 and 60 h. Data are means of triplicates.

4.4.3 Cell death analysis by Flow Cytometry

Cell death analysis was performed to evaluate the effect of cysteine in apoptosis and/or necrosis regulation in cells grown in glutamine.

ES2 cells, after 24 h in culture, showed higher percentage of apoptosis (annexin V positive cells) in glutamine plus cysteine condition (Figure 24 a). This result was more evident in time point 30 h where the percentage of apoptosis was approximately 6 fold higher than in glutamine condition (Figure 24 a). It was also detected after 48h in culture, in both conditions, a decrease in

the levels of apoptosis, essentially in glutamine condition (Figure 24 a). An identical behavior in both conditions was verified in necrosis (PI positive cells) (Figure 24 b).

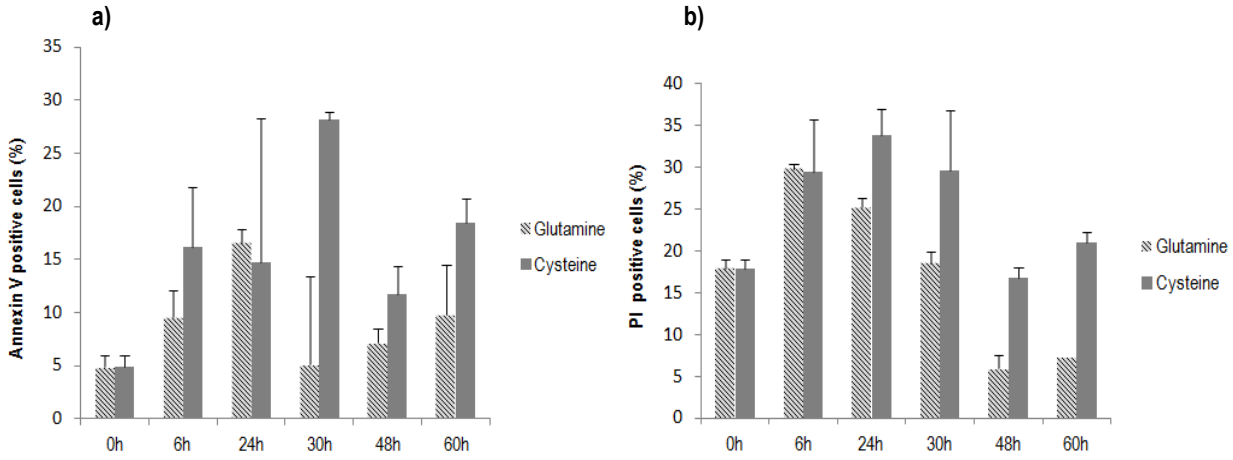

Figure 24– Apoptosis and necrosis analyzes by flow cytometric (Annexin V and PI staining) in ES2 cells. Cell mortality were analyzed in cells were grown in control and in cysteine conditions at 0, 6, 24, 30, 48 and 60 h. Data are means of triplicates ± error bars of triplicates.

4.5 Role of cysteine in aminothiols production

4.5.1 High-performance Liquid Chromatography (HPLC) for aminothiols detection in ES2 cell line

HPLC was performed to detect thiols levels (cysteine (CYS), homocysteine (HCYS), cysteinylglycine (CysGly), glutathione (GSH) and N-Acetyl Cysteine (NAC)), in ES2 cells exposed to glutamine plus cysteine condition, comparing to the glutamine condition. ^{13C} GSH partially labeled (^{13C} glycine and ^{13C} glutamate labeled) was detected in ES2 cells by NMR (described above) and as GSH, an endogenous antioxidant, results, in part, by the degradation of cysteine it becomes important to clarify the possible role of cysteine in GSH production. GSH is essential in antioxidant defenses, implicated in cancer progression and under normal conditions it maintains physiological levels of ROS, preventing cell damage and death.

Firstly, glutamine and glutamine plus cysteine crude media were analyzed in order to understand which thiols were presented initially in crude medium formulation and which of them were excreted by cells. By HPLC, we detected the presence of cysteine, HCYS and NAC in both crude mediums (Figure 23 a and b, Figure A1 (Appendix II)) although with different levels. In

glutamine condition, cysteine levels was detected, due to the fact that crude medium contain approximately 200 µM of cystine, the reduced form of cysteine (Figure 23 a, Figure A1 (Appendix II)) while in cysteine supplemented crude medium the supplementation addiction was 402 µM resulting in the final levels of free cysteine of about 602 µM (Figure 23 b, Figure A1 (Appendix II)).

Comparing the supernatants of glutamine with glutamine plus cysteine condition (Figure 23 a and b, Figure A2 and A3 (Appendix II)) the levels of HCYS (retention time - 7.9 min), CysGly (retention time – 8.9 min) and GSH (retention time - 12.8 min) were, respectively, 2.5, 3.3 and 3.4 fold higher in glutamine plus cysteine condition, which is in agreement with the cysteine supplement (Figure 23 a and b, Figure A2 and A3 (Appendix II)). In relation to the NAC presence (retention time – 17.9), in glutamine plus cysteine condition the levels were unchanged while in glutamine condition it was verified a decrease in NAC levels (Figure 23 a and b, Figure A2 and A3 (Appendix II)).

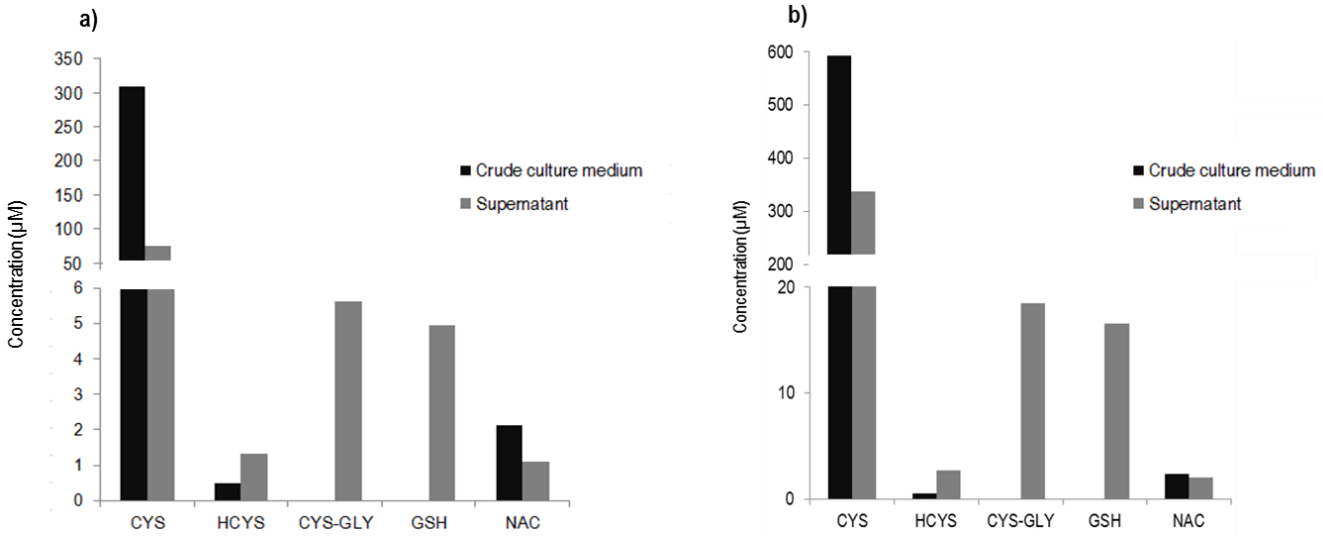

Figure 25 –Thiols quantification in crude culture medium and supernatant in ES2 cell line. Cells were grown in glutamine (a) and cysteine (b) conditions.

In the cell, cysteine levels were almost similar in both conditions whereas CysGly and HCYS levels were, respectively, 1.4 and 2.4 fold higher in glutamine plus cysteine condition than glutamine (Figure 24, Figure A4 (Appendix II)). In glutamine condition, GSH levels detected were 1.6 fold higher comparing to glutamine plus cysteine condition (Figure 24, Figure A4 (Appendix II)). In both conditions, NAC levels were lower than the limit of HPLC quantification (<0.313 µM).

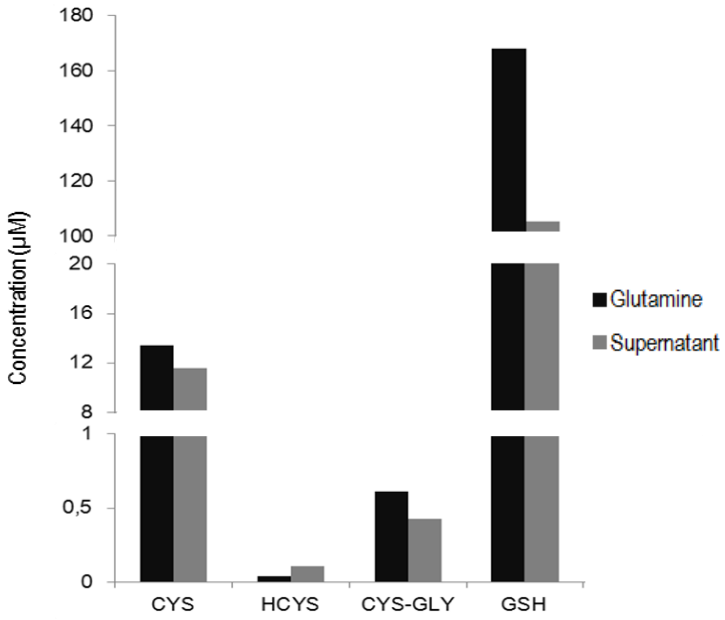

Figure 26 – Aminothiols quantification in ES2 cell line. Cells were grown in glutamine and cysteine conditions.

5. Discussion

Research in tumor cell metabolism has recently entered in a new age. The metabolic alterations in cancer cells compared to normal cell confer a selective advantage for their survival and proliferation (Draoui and Feron, 2011).

Nowadays it is well known that neoplastic cells metabolize abundant glucose to support their energetic and anabolic requirements, namely when tumor metabolism switch the glucose consumption from oxidative phosphorylation to aerobic glycolysis (Liu et al., 2010; Shapot and Blinov, 1974). Those alterations verified in tumors metabolism show the critical relevance of understanding the regulation of enzymes implicated in glucose metabolism, anabolism and catabolism. The regulation of gluconeogenic enzymes occurs on multiple levels as gene expression, posttranslational modifications and allosteric regulation (Xiong et al., 2011).

Many studies in cancer research have their focus in the identification of genes related to human cancers. As several studies had reported that gluconeogenesis is increased in cells surrounding tumors to support their glucose requirements is important to understand the regulation of gluconeogenic genes in tumor cells when their microenvironment is exposed to glucose privation (Feron, 2009; Liu et al., 2010; Shapot and Blinov, 1974; Yalcin et al., 2009) .

In the present thesis, at first by NMR we performed a metabolic profile of ovarian cell clear carcinoma (ES2) when exposed to ^{13C}-[U]-glutamine, ^{13C}-[U]-lactate and ^{13C}-[U]-butyrate, in a glucose privation medium. ^{13C} unlabeled glycogen was detected in ^{13C} butyrate condition (Figure 9 b) corroborating previous studies in which the OCCC signature was related to intracellular glycogen storage in the cytoplasm, in the form of massive aggregation or diffuse distribution (Hkaw et al., 1977; Yamaguchi et al., 2010). In NMR analyzes no ^{13C} labeled glucose was detected which indicates that cells was not using ^{13C} glutamine, ^{13C} lactate and ^{13C} butyrate as gluconeogenesis substrate. Glutamine appeared to be the major substrate used in glucose privation, although our results showed that glutamine was metabolized into TCA ^{13C} labeled intermediates instead of be used as gluconeogenic substrate (Figure 10).

In order to evaluate the expression of key genes involved in gluconeogenesis, ES2 cells in glucose privation medium were exposed to different substrates: lactate, glutamine, glucose and butyrate.

Lactate is considered as an alternative metabolic fuel for cancer cells, that often reduce pyruvate, the last glycolytic metabolite, to lactate. In some tumors, lactate is also produced in response to genetic features of tumors and to stimuli from the surrounding tumor microenvironment (Draoui and Feron, 2011; Xiong et al., 2011). Glutamine is the most abundant

amino acid in the plasma and can support essential requests for tumor cells proliferation, the bioenergetics needs (ATP production) and macromolecules synthesis. Identically to glucose consume, tumor cells in culture metabolize glutamine in higher rates than others amino acids (DeBerardinis and Cheng, 2010). Butyrate is a short chain fatty acid that can also act as a histone deacetylase (HDAC) inhibitor, acting as an epigenetic modulator. Increase in butyrate levels active the expression of several genes (as p53 and methylase inhibitory genes), sustaining tumorigenesis process (Israël and Schwartz, 2011b). Moreover, Serpa et al., 2010 had reported that tumor cells that are able to metabolize butyrate, in a butyrate-rich microenvironment, are phenotypically more aggressive.

Regarding the expression of phosphoenolpyruvate carboxykinase cytosolic (PCK1) and mitochondrial (PCK2) that catalyze the rate-limiting reaction in gluconeogenesis, our results are not in agreement with previous studies that correlate the induction of PCK1 mRNA levels with an increase in protein levels (Blouin et al., 2010). We verified that the higher increase in PCK1 mRNA levels, compared to control, was observed when cells were exposed to glucose and butyrate (Figure 11). Although the protein levels of glucose and butyrate conditions was, respectively, slightly higher and equal to the protein levels detected in control condition (Figure 12 a). The increase in mRNA levels in butyrate (Figure 11) can be related to the role of butyrate as HDAC inhibitior, which can induce an increase in gene transcription. In lactate and glutamine condition the opposite was verified, PCK1 mRNA levels were lower than control (Figure 11) whereas PCK1 protein levels were approximately 2 fold higher than control (Figure 12 a).

Extracellular levels of nutrient regulate PCK1 expression activating its acetylation which is a major post-translational modifier responsible for metabolic enzyme regulation, acting through protein degradation. In normal cells, glucose increase PCK1 acetylation while amino acids that can serve as gluconeogenic precursors decrease PCK1 acetylation. PCK1 acetylation correlates directly with decreases in PCK1 protein levels, having no direct effect on PCK1 enzymatic activity (Blouin et al., 2010; Weickert and Pfeiffer, 2006; Xiong et al., 2011). In our case, acetylation could be responsible for results observed in ES2 cell line, where higher levels of PCK1 mRNA expression in glucose and butyrate conditions was not reflected in higher PCK1 protein levels (Figure 11 and 12 a). This decrease in protein levels occurs maybe because acetylation promotes PCK1 ubiquitination and degradation, in both conditions.

Lactate and glutamine can server as gluconeogenic precursor and, as referred, gluconeogenic precursors decrease PCK1 acetylation. As observed in ES2 cell line, an increase in PCK1 protein levels comparing to control (Figure 12 a) could be explained by a decline in PCK1 acetylation and consequently reflected in an increase in PCK1 protein levels. In lactate

condition was also detected a higher activity in luciferase activity of PCK1 promoter construct, comparing to control (Figure 14).

In the literature, PCK2 was described as constitutively expressed, remaining relatively unaltered although their expression is more suited to gluconeogenesis from lactate (Hanson, 2009; Hanson and Garber, 1972). Our results also support these evidences, we observed an increase in PCK2 mRNA expression in lactate condition, comparing to PCK1 mRNA levels (Figure 11). This result was also obtained in luciferase activity of PCK2 promoter that showed higher activity than PCK1 promoter (Figure 14). Although, the evaluation luciferase activity of promoter is an artificial assay that has to be complemented with functional assays, as chromatin immunoprecipitation (ChIP) or electrophoretic mobility shift assay (EMSA).

Fructose-1,6-bisphosphatase (FBP1) is a gluconeogenic enzyme responsible for the irreversible reaction of fructose-2,6-biphosphatase (F1,6BP) into fructose-6-phosphate (F6P). In the literature, it was described that in gastric, liver and colon cancer this key enzyme is silenced by promoter methylation (Gerhäuser, 2012; Quintas et al., 2008a). Several studies reported that FBP1 is commonly downregulated in cancer cells due to the significant increase in methylation of FBP1 gene promoter (Chen et al., 2011). Gerhäuser, 2012 demonstrate in gastric cancer that when FBP1 expression is restored by promoter demethlyation, the cell cycle is arrested. However, in cancer cells any study in this field was performed under glucose privation microenvironment.

In the present thesis, we observed that ES2 cells need to modify their endogenous metabolism in order to supply metabolic requirements. We observed in all conditions, essentially in lactate condition and in contrast with the literature, that FBP1 protein levels were upregulated (Figure 12 b) under glucose privation, as well as luciferase activity of FBP1 promoter (Figure 14).

ES2 results obtained under glucose privation (Figure 12 b and 14) may be related to the fact that cells in culture need to increase their levels of glucose production. Glucose is an essential nutrient for cancer cells because is the initial substrate of glycolysis. In cancer cells, in normal growing conditions FBP1 antagonizes glycolysis and as previously described, high rates of glycolysis are a metabolic characteristic of cancer cells that justifies the downregulation of FBP1 in tumors (Chen et al., 2011; Liu et al., 2010). However, in our case the high levels of FBP1 expression is essential for glucose synthesis that subsequently will serve as aerobic glycolysis substrate and support cancer metabolism.

PFKFB is an enzyme associated with the promotion of glycolysis and the inhibition of gluconeogenesis through the activation or inhibition, respectively, of their kinase activity (Noguchi et al., 2013). The molecular function of PFKFB is to synthesize F 2, 6 BP from F6P. Fructose-2,

6-bisphosphatase (PFKFB1) activates 6-phosphofructo-1-kinase (PFK1), an essential and irreversible enzyme on controlling the glycolytic pathway (Yalcin et al., 2009).

PFKFB have four isozymes (PFKFB 1-4) with high sequence homology in their catalytic domains, although with different regulatory and kinetic properties. Previous studies in four isoforms had demonstrated that when organs were exposed to hypoxia it's verified an increase in PFKFB mRNA levels. However, PFKFB3 mRNA demonstrated the highest induction in several organs as lungs, liver, kidney, brain, heart and testis while PFKFB1 is mainly expressed in liver (Yalcin et al., 2009). PFKFB3 expression was also detected in proliferating tissues and transformed cells of various tumors (Bartrons and Caro, 2007).

In the present thesis the PFKFB1 isoform was evaluated since it is the isoform up regulated in the liver, and as it was mentioned before OCCC has the up regulation of HNF1β, a liver specific gene. Previous studies had reported that an increased in PFKFB3 expression favors the progression of aerobic glycolysis, however as in our work ES2 cells were in glucose conditioned microenvironment, cells have the need to increase their glucose levels by favoring gluconeogenesis and inhibiting aerobic glycolysis.

In ES2 cell line we verified that the levels of PFKFB1 mRNA in glutamine and lactate conditions remains, respectively, lower and almost equal to control condition while in butyrate it was detected an increase in PFKFB1 mRNA levels (Figure 11). In luciferase activity of PFKFB1 promoter, lactate condition induced a luciferase activity approximately 14 fold higher than control whereas glutamine and butyrate condition the luciferase activity decreased in comparison to control (Figure 14). Although, as gene expression are subject to posttranslational modifications and epigenetic regulation, PFKFB1 mRNA levels and luciferase activity of PFKFB1 promoter activity was not reflected in protein levels, being PFKFB1 protein expression almost equivalent and lower in all conditions (Figure 12 c).

Furthermore, our results suggest that when cells were in glucose privation the levels of PFKFB1 remains lower (Figure 12) in order to stimulate gluconeogenesis. As consequence of an increase in stimulatory gluconeogenic enzymes (Figure 12 a and b) and a decrease in inhibitory enzymes (Figure 12 c), the glucose synthesis by gluconeogenesis is favored to support the metabolic requirements for cancer cell survival.

Alanine also can be a gluconeogenic substrate, through transamination that coffers the conversion of alanine into pyruvate. This reaction catalyzed by alanine aminotransaminase (ALT), which expression was evaluated. It was observed an increase in ALT mRNA levels in glucose, lactate and glutamine conditions (Figure 13) although as glutamine condition NMR analyzes showed the presence of alanine ^{13C} labeled (Figure 10) we also detect the ALT expression with

30 hours of glutamine exposure, suggesting that alanine may play an important role as gluconeogenic precursor.

After the evaluation of gluconeogenic genes expression in cells when exposed to different substrates (glucose, glutamine, lactate and butyrate) with previous glucose privation, the evaluation of migration rate and cell cycle were performed. In *wound healing assay*, glucose, butyrate and glutamine condition appeared to be more favorable to cell migration, compared to control (Figure 16) which can correspond to a more invasive phenotype.

Our results in cell cycle analyze showed that butyrate and glutamine conditions were more favorable to cell cycle progression (Figure 17 b and d). In those conditions, an increase of cell percentage in S and G2-M phases indicates an increase in the rate of DNA synthesis and mitosis, meaning the stimulation of cell cycle progression. Previous studies reported that the donation of the amido nitrogen from glutamine to nucleotides might become essential during the cell cycle, since it occurs transient increases in nucleotide biosynthesis, sustaining the in an enhanced proliferation (Braga-Neto et al., 2008; DeBerardinis and Cheng, 2010). Contrary to our findings, in fibroblasts butyrate inhibited cell cycle progression (Chang et al., 2012). However observations made by Serpa et al., 2010 demonstrate that colon cancer cells that metabolize butyrate showed a more aggressive fenotype, associated with a high proliferative rate and a more *in vivo* metastatic behavior. We saw by NMR that ES2 cell are able to metabolize butyrate, at least in part, favoring cell cycle progression and migration (Figure 16 and 17 d).

ES2 results also showed that in glutamine condition the mRNA levels of gluconeogenic enzymes remain relatively lower than control (Figure 11) being the same verified in luciferase activity of promoter constructs (Figure 14). Although, cells exposed to glutamine had higher cell migration (Figure 15 and 16) and cell cycle progression favored (Figure 17 b). Glutamine seems to promote cell cycle progression and proliferation. Results obtained also confirm that glutamine instead of being used as gluconeogenic precursor was metabolized by another pathway, the glutaminolysis.

Our observations in ES2 cells are in agreement with other studies saying that glutamine metabolism is one of the major component of metabolic phenotype of proliferating tumor cells, showing that proliferative cells display an intense appetite for glutamine consumption (DeBerardinis and Cheng, 2010). An increase in glutamine metabolism or glutaminolysis is associated with carcinogenesis. Inside cell, glutamine is metabolized into glutamate which generates NAD+ (essential for glycolysis). Then, glutamate enter in TCA cycle by their conversion into α-Ketoglutarate (α-KG), providing NADH, nitrogen and carbon skeletons, essential for cell proliferation (Dang, 2012; Israël and Schwartz, 2011a; Matés et al., 2013)

As described above, NMR analyzes in ES2 cells (Figure 9 and 11) also proves that glutamine was metabolized. The TCA intermediates as aspartate, glutamate and lactate were ^{13C} labeled, as well as, intermediates for macromolecules synthesis as alanine, proline and formate (Figure 10). The NMR results also detected intracellular ^{13C} labeled GSH, in the glycine and glutamate moiety, but not in the cysteine moiety of GSH (Figure 11). The NMR results also detected intracellular ^{13}C labeled GSH as well as ^{13}C labeled glycine (Figure 10) which allowed, in part, the formation of GSH metabolite.

Recent studies have demonstrated that GSH levels play an important role in endogenous antioxidant defenses, implicated in cancer progression. GSH allows the maintenance of the redox state of cells, drug detoxification and prevention of cellular damage by free radicals, peroxides and toxins (Singh et al., 2012; Traverso et al., 2013). Alterations in cysteine and GSH levels are considered relevant in cancer development and progression. Mani et al., (2011) described that it is common in cancer patients a decrease in cysteine and GSH plasma levels, preceded by loss of body weight (cachexia) which compromise the quality of life and increases patients morbidity and mortality. At a molecular level, alterations in cysteine and GSH levels could be correlated with an oxidative shift in plasma redox state of cells reflected by a decrease ratio of reduced/oxidized cysteine form (Mani et al., 2011; Tozer et al., 2008).

As several *in vitro* and *in vivo* studies demonstrated, cysteine is as a rate-limiting factor for GSH synthesis (Mani et al., 2011), in the present work it is also evaluated the possible role of cysteine supplementation in ES2 cell line and their effect in proliferation, evasion and intracelular antioxidant levels.

In order to evaluate the role of cysteine metabolism in ES2 cells exposed to glutamine in the presence or absence of cysteine, gene expression of cystathionine gamma-lyase (CTH) (Figure 18 a), assessed by RQ- PCR, was evaluated as well as CTH promoter activity (Figure 20). CTH, a pyridoxal 5'-phosphate dependent enzyme, is responsible for cysteine production under transsulfuration pathway where methionine, an essential amino acid, is catabolized into cysteine. CTH is also able to degradate cysteine, leading to pyruvate production (Steegborn, 1999). Thus, evaluation of CTH becomes important because, as referred, CTH is involved in cysteine metabolism and had been reported that CTH deficiency leads to a decrease in cysteine, GSH, taurine and hydrogen sulfide (H_2S) levels. Mani et al., 2011 described that the treatment of hepatocytes with 2 mM propargylglycine (PPG), an irreversible inhibitor of CTH activity, was responsible for the decrease of cysteine and GSH levels in 89% and 93%, respectively.

It was verified, in ES2 cell line, that CTH gene expression (Figure 18 a) and promoter activity (Figure 20) of CTH were identical in glutamine and glutamine plus cysteine conditions,

allowing to speculate that CTH activity is independent of extracellular levels of cysteine. In the literature many authors try to clarify the relationship between cysteine supplementation and CTH activity, although this subject has been unclear, in part because the most studies only had focused in CTH elimination or inhibition, without considering the exogenous uptake of cysteine (Mani et al., 2011). Moreover, CTH has two different and contradictory enzymatic activities since it is able to catalyze both cysteine synthesis and degradation (Steegborn, 1999).

As described, CTH activity plays an essential role in cysteine synthesis and decreases in CTH activity have also influence in the reduction of H_2S levels, very important for many physiological functions as vasorelaxation, stimulation of cellular bioenergetics and promotion of angiogenesis (Szabo et al., 2013) .

Studies developed by Szabo et al., (2013) reported that in colorectal carcinoma lower levels of H_2S were associated with a decrease in cell proliferation, migration and invasion. Although we have not measure H_2S, in cell cycle analyzes by flow cytometric (Figure 23), few differences in both conditions were detected (Figure 18 a) perhaps by the fact that CTH expression is identical in glutamine and glutamine plus cysteine conditions, which can reflect in identical H_2S levels in both conditions.

It was also observed that CTH gene expression increase their modulation over the course of the experiment (Figure 18 a). Extracellular cysteine resources in culture medium were consumed by the cells, although when cysteine levels in culture becomes limited cells had to development an alternative way to increase the intracellular levels of cysteine.

MPST activity, responsible for cysteine degradation was as expected increased in glutamine plus cysteine condition (Figure 18 b).

In the present work the analysis of mTOR pathway (Figure 19) also becomes important because this regulatory-associated protein complex was activated in part by amino acids and oxidative stress. Glutamine plays an important role in mTOR activation due to the fact that glutamine export allows leucine import, responsible for mTOR activation and consequently an increase in cell metabolism, survival and proliferation (Fuchs and Bode, 2005; Laplante et al., 2010). Comparing glutamine to glutamine plus cysteine condition there was no significant differences (Figure 19) indicating that cysteine do not have influence in mTOR pathway.

The GSH levels and their precursors were assessed by HPLC, allowing the association between extracellular cysteine levels and the endogenous antioxidant potential of ES2 cell line (Figure 25 and 26).

Cystine, the reduced form of cysteine, is composed by two cysteine molecules joined by a disulfide bond and as referred in results (specification in section 4.5.1) the media formulation

contains by 200 μM of cystine. Cystine levels where responsible for cysteine detection in glutamine crude culture medium (Figure 25 a). Zhang et al., (2012) described that cystine can enter in cell by the association with glutamate. In ES2 cells was detected by NMR (Figure 10) the presence of glutamate ^{13C} labeled, resultant from glutamine metabolism. Thereafter, cystine and glutamate could be conjugated in γ-Glumate-Cystine, allowing cystine entry, by Xc-transporter, into the cell and their posterior conversion in cysteine (Pompella et al., 2006; Zhang et al., 2012).

In the literature, GSH is described as essential in eliminating ROS such as hydrogen peroxide and other organic peroxide, essential in many antioxidant defenses systems. GSH also forming conjugates with electrophilic xenobiotics and is associated with the storage and cysteine transport, participating in many metabolic processes (Traverso et al., 2013; Wang et al., 1997).

Oxidative stress has been implicated in cancer development and progression in many studies having their focus in GSH synthesis and release. GSH system is a possible target for medical intervention against cancer progression and chemoresistance (Traverso et al., 2013).

Increased in GSH levels is a normal response to cysteine supplement, and some previous studies in cancer patients have reported and associated the decrease in intracellular cysteine levels with a decrease in GSH synthesis (Mani et al., 2011). In ES2 cell line, we observed that cysteine supplement led to an increase in GSH synthesis (Figure 25 and 26), corroborating the observations made in patients, where lower cysteine levels were associated with lower GSH levels.

Increase in GSH levels is associated with a proliferative response and is essential for cell cycle progression, however the molecular mechanism of GSH modulation remains largely speculative. In many tumor types high GSH levels were observed, promoting chemotherapy resistance. Increases in GSH levels are typically associated with an increase in GSH-related enzymes, such as γ-glutamylcysteine ligase (GCL) and γ-glutamyl-transpeptidades (GGT) activites, as well as a higher expression of GSH-transporting export pumps (Traverso et al., 2013).

GGT is a cell surface enzyme involved in GSH homeostasis which affect intracellular and extracellular microenvironment. In tumors, the GGT activity is significantly higher than normal cells, increasing and affecting GSH efflux. This phenomenon have been observed in cancer of ovary, colon, liver and leukemias, affecting cell sensitivity to anticancer drugs and increased tumor progression and invasion (Pompella et al., 2006). Corti et al., (2010) observed in *in vivo* and *in vitro* assays performed in melanomas cells that an increased in GGT expression is followed by an increase in tumor invasion. In human breast cancer, GGT overexpression and an increase in GSH efflux was associated in an unfavorable prognosis (Bard et al., 1986).

As referred, ES2 cells in glutamine plus cysteine condition had higher GSH efflux, comparing to glutamine condition (Figure 25 and 26). This phenomenon could be associated with a decrease in methionine influx. Rao et al., (1990) observed the effects of this essential amino acid when freshly isolated hepatocytes incubated with L-[^{35}S] methionine and observed an increase in intracellular levels of ^{35}S-labeled cysteine and GSH. We speculate that methionine, present in the formulation of crude medium in glutamine and cysteine conditions, could be responsible for the inhibition of GSH efflux, in ES2 cell line. Cells with cysteine supplement have less methionine requirements for cysteine synthesis by CTH. This fact decrease influx of methionine in cysteine condition, remaining methionine levels lower than glutamine condition and consequently the inhibition of GSH efflux was lower in glutamine (Figure 25 and 26).

Due to this fact, cells cultured in glutamine had an increase in intracellular levels of methionine, responsible for an inhibition of GSH efflux (Figure 25 and 26). These observations was also showed by Wang et al., (1997), who had reported that intracellular GSH levels were lower in cells treated with lower concentrations of methionine. Roh et al., (2012) also detected that an increase in methionine influx induced an increase of GSH intracellular levels. The inhibition of GSH efflux by the levels of methionine was also verified in HeLa cells (Meredith et al., 1998).

GSH efflux was also considered as a saturable process regulated in part by positive feedback (more extracellular GSH levels, more GSH efflux). As referred, GSH is released by cells through GGT-mediated metabolism which is implicated in tumor development *in vivo* where the increase in GSH efflux is associated with an increased invasive behavior (Traverso et al., 2013). *In vitro*, in ES2 cell line, the same phenomenon was observed in *wound healing assay* (Figure 21 and 22), where cells in glutamine plus cysteine condition presented more GSH extracellular levels (Figure 25 and 26), and an increase in the migration rate.

Homocysteine (HCYS) levels, a cysteine precursor in transsulfuration pathway, which is synthesized from methionine and further catabolized to cysteine, was increased in glutamine condition (Figure 25 a). This fact occurs because cells that do not have cysteine supplement suffer an increase in cysteine synthesis, comparing to glutamine plus cysteine condition, originates an increase in cysteine intermediates, namely HCYS (Figure 25 a). N-acetyl cysteine (NAC), commonly present in medium formulation, serves as cysteine source. NAC could be internalized by cells, being transformed into cysteine inside cells. In ES2 cell line, as glutamine present less cysteine sources, NAC levels in supernatant were lower, comparing to cysteine condition (Figure 25 a), due to cysteine requirements for cell survival.

GSH levels also can be associated with changes in cell viability, observed in cysteine and glutamine conditions. In ES2 cell line it was verified a decrease in cell viability in cysteine condition (Figure 24). This fact can be explained by a decrease in intracellular GSH levels (Figure 25), because GSH affects significantly cell survival by inhibiting apoptosis through mechanisms that do not involve directly ROS modulation. Activity of GGT may contribute to modulate the apoptotic process, due to the fact that GGT overexpression induces and increases in GSH release for extracellular medium, leading to a decrease in intracellular GSH levels (Corti et al., 2010).

6. Conclusions

Nowadays it is known that cell proliferation is sustained by an adapted tumor cell metabolism, favoring carbon and energy demanding, being relevant for tumor progression and metastasis. During this thesis we tried to clarify in an ovary cell clear carcinoma *in vitro* model (ES2) if gluconeogenesis is a source of glucose supply as well as the role of amino acid metabolism.

NMR analyzes in ES2 cell line revealed that glucose is not synthesized from the tested compounds. Nevertheless NMR assay showed that glutamine was the major substrate used for sustain carbon and energy demands. It was verified that glutaminolysis was responsible for the incorporation of glutamine into TCA intermediates that are canalized directly into oxidative metabolism leading to energy production and precursors for macromolecules synthesis, essential to support metabolic requirements for tumor progression. In NMR analyzes it was also detected the presence of not labeled glycogen, characteristic of OCCC.

NMR analysis did not show glucose and/or glycogen ^{13C} labeled in the tested cell culture conditions maybe because: 1) glucose is a very labile nutrient; 2) other carbon sources can be preferentially used; 3) gluconeogenesis is not occuring, or 4) the timepoints evalued are not long enough to occur glycogen turnover.

However, the evaluation of gluconeogenic genes (PCK1, PCK2, FBP1 and PFKFB1) expression was more favorable for glucose using lactate as substrate. Butyrate condition showed higher mRNA levels and lower proteins levels that can be related to the role of butyrate as HDAC inhibitor, increasing transcription. Contrary to verified in normal cells, the glucose did not acts by negative feedback since we verified that the increased glucose levels also stimulate the expression of gluconeogenic enzymes.

As referred above, we detected by NMR that glutaminolysis lead to the production of amino acids as glycine and glutamate and consequently GSH. The additional stimulation of cells with cysteine (also a substrate for GSH synthesis) leads to an increase in GSH levels, with a concomitant increase in cell proliferation, cell cycle progression and migration.

Our findings suggest that glutaminolysis is a central metabolic pathway. In our *in vitro* model of OCCC glutaminolysis seem to be relevant not only for carbon and energy supply but also for sustain favorable redox potential through GSH synthesis. GSH synthesis is also favored by the additional exposure to cysteine.

Summing up, amino acid metabolism can be crucial for OCCC tumorigenesis and drug resistance.

7. Future Perspectives

To better understand the regulatory molecular mechanism of gluconeogenesis, as future perspectives, it would be important to investigate the enzymatic activity of gluconeogenic enzymes, in order to determinate the functional relevance of gluconeogenic pathway in OCCC. The evaluation of mechanisms of regulation of gluconeogenic gene expression must be completed with ChiP and/or EMSA.

As glutamine revealed to be a key amino acid in tumor metabolism, we ought to determine which transporters are mediating glutamine uptake.

The confirmation that glutamine activates mTOR pathway must be addressed by analyzing the phosphorylation levels of mTOR.

In order to clarify the role of amino acids metabolism in GSH increase and consequent drug resistance, we must evaluate ES2 cell line the effect of convential chemotherapy (ie cis-platin and paclitaxel) in cell viability and DNA demage in the presence of glutamine and/or cysteine. Other cell lines from ovarian carcinomas must be also tested.

The evaluation of H_2S production must be quantified in order to confirm the association with cell proliferation and migration.

Overall, we must validate our findings in animal models, in order to confirm the physiopathological relevance of amino acid metabolism in tumor growth and metastasis as well as in drug resistance.

Bibliography references

Agca, C., Greenfield, R.B., Hartwell, J.R., and Donkin, S.S. (2002). Cloning and characterization of bovine cytosolic and mitochondrial PEPCK during transition to lactation. Physiological Genomics *11*, 53–63.

Anglesio, M.S., Carey, M.S., Köbel, M., Mackay, H., and Huntsman, D.G. (2011). Clear cell carcinoma of the ovary: a report from the first Ovarian Clear Cell Symposium, June 24th, 2010. Gynecologic Oncology *121*, 407–415.

Bard, S., Noël, P., Chauvin, F., and Quash, G. (1986). gamma-Glutamyltranspeptidase activity in human breast lesions: an unfavourable prognostic sign. British Journal of Cancer *53*, 637–642.

Bartrons, R., and Caro, J. (2007). Hypoxia, glucose metabolism and the Warburg's effect. Journal of Bioenergetics and Biomembranes *39*, 223–229.

Bjorkholm E, Pettersson F, Einhorn N, Krebs I, Nilsson B, Tjernberg B (1982). Long-term followup and prognostic factors in ovarian carcinoma. The radiumhemmet series 1958 to 1973. Acta Radiol Oncol *9*; 21:413.

Blouin, J.-M., Bortoli, S., Nacfer, M., Collinet, M., Penot, G., Laurent-Puig, P., and Forest, C. (2010). Down-regulation of the phosphoenolpyruvate carboxykinase gene in human colon tumors and induction by omega-3 fatty acids. Biochimie *92*, 1772–1777.

Board, M., Humm, S., and Newsholme, E. a (1990). Maximum activities of key enzymes of glycolysis, glutaminolysis, pentose phosphate pathway and tricarboxylic acid cycle in normal, neoplastic and suppressed cells. The Biochemical Journal *265*, 503–509.

Bodi, V., Sanchis, J., Morales, J.M., Marrachelli, V.G., Nunez, J., Forteza, M.J., Chaustre, F., Gomez, C., Mainar, L., Minana, G., et al. (2012). Metabolomic profile of human myocardial ischemia by nuclear magnetic resonance spectroscopy of peripheral blood serum: a translational study based on transient coronary occlusion models. Journal of the American College of Cardiology *59*, 1629–1641.

Braga-Neto, M.B., Warren, C. a, Oriá, R.B., Monteiro, M.S., Maciel, A. a S., Brito, G. a C., Lima, A. a M., and Guerrant, R.L. (2008). Alanyl-glutamine and glutamine supplementation improves 5-fluorouracil-induced intestinal epithelium damage in vitro. Digestive Diseases and Sciences *53*, 2687–2696.

Cecchini, M.J., Amiri, M., and Dick, F. a (2012). Analysis of cell cycle position in mammalian cells. Journal of Visualized Experiments : JoVE *7*, 1–7.

Chang, M.-C., Tsai, Y.-L., Chen, Y.-W., Chan, C.-P., Huang, C.-F., Lan, W.-C., Lin, C.-C., Lan, W.-H., and Jeng, J.-H. (2012). Butyrate induces reactive oxygen species production and affects cell cycle progression in gengival fibroblasts. Journal of Periodontal Research *48*, 66–73.

Chen, M., Zhang, J., Li, N., Qian, Z., Zhu, M., Li, Q., Zheng, J., Wang, X., and Shi, G. (2011). Promoter hypermethylation mediated downregulation of FBP1 in human hepatocellular carcinoma and colon cancer. PloS One *6*, e25564.

Corssmit, E.P., Romijn, J. a, and Sauerwein, H.P. (2001). Review article: Regulation of glucose production with special attention to nonclassical regulatory mechanisms: a review. Metabolism: Clinical and Experimental *50*, 742–755.

Corti, A., Franzini, M., Paolicchi, A., and Pompella, A. (2010). Gamma-glutamyltransferase of cancer cells at the crossroads of tumor progression, drug resistance and drug targeting. Anticancer Research *30*, 1169–1181.

Czernobilsky B, Morris WJ. (1979). A histologic study of ovarian endometriosis with emphasis on hyperplastic and atypical changes. Obstet Gynecol *53*, 318–323.

Dang, C. V (2012a). Links between metabolism and cancer. Genes & Development *26*, 877–890.

Dang, C. V (2012b). Links between metabolism and cancer. Genes & Development *26*, 877–890.

Dang, C. V. (2010). Glutaminolysis: Supplying carbon or nitrogen, or both for cancer cells? Cell Cycle *9*, 3884–3886.

DeBerardinis, R.J., and Cheng, T. (2010). Q's next: the diverse functions of glutamine in metabolism, cell biology and cancer. Oncogene *29*, 313–324.

Deberardinis, R.J., Sayed, N., Ditsworth, D., and Thompson, C.B. (2008). Brick by brick: metabolism and tumor cell growth. Current Opinion in Genetics & Development *18*, 54–61.

Derveaux, S., Vandesompele, J., and Hellemans, J. (2010). How to do successful gene expression analysis using real-time PCR. Methods *50*, 227–230.

Dhivya, H. (2012). Glutathione — a master antioxidant and an immune system modulator. *1*, 13–15.

Draoui, N., and Feron, O. (2011). Lactate shuttles at a glance: from physiological paradigms to anti-cancer treatments. Disease Models & Mechanisms *4*, 727–732.

Estrela, J.M., Ortega, A., and Obrador, E. (2006). Glutathione in cancer biology and therapy. Critical Reviews in Clinical Laboratory Sciences *43*, 143–181.

Feeley KM, Wells M. (2001). Precursor lesions of ovarian epithelial malignancy. Histopathology *95*; 38:87.

Feron, O. (2009). Pyruvate into lactate and back: from the Warburg effect to symbiotic energy fuel exchange in cancer cells. Radiotherapy and Oncology *92*, 329–333.

Freeman, W.M., Walker, J., and Vrana, K.E. (1999). Review Quantitative RT-PCR : Pitfalls and Potential. BioTechiques *26*.

Fukunaga M, Nomura K, Ishikawa E, et al. (1997). Ovarian atypical endometriosis: its close association with malignant epithelial tumours. Histopathology *30*; 249–255.

Fuchs, B.C., and Bode, B.P. (2005). Amino acid transporters ASCT2 and LAT1 in cancer: partners in crime? Seminars in Cancer Biology *15*, 254–266.

Ganapathy, V., Thangaraju, M., and Prasad, P.D. (2009). Nutrient transporters in cancer: relevance to Warburg hypothesis and beyond. Pharmacology & Therapeutics *121*, 29–40.

Gerhäuser, C. (2012). Cancer cell metabolism , epigenetics and the potential influence of dietary components – A perspective. Biomedical Research *23*.

Goff BA, Sainz de la Cuesta R, Muntz HG, Fleischhacker D, Ek M, Rice LW, Nikrui N, Tamimi HK, Cain JM, Greer BE, Fuller Jr AF (1996). Clear cell carcinoma of the ovary: a distinct histologic type with poor prognosis and resistance to platinum-based chemotherapy in stage III disease. Gynecol Oncol *60*, 412–417.

Greenfield, R.B., Cecava, M.J., and Donkin, S.S. (2000). Changes in mRNA expression for gluconeogenic enzymes in liver of dairy cattle during the transition to lactation. Journal of Dairy Science *83*, 1228–1236.

Gubern, C., Hurtado, O., Rodríguez, R., Morales, J.R., Romera, V.G., Moro, M. a, Lizasoain, I., Serena, J., and Mallolas, J. (2009). Validation of housekeeping genes for quantitative real-time PCR in in-vivo and in-vitro models of cerebral ischaemia. BMC Molecular Biology *10*, 57.

Han, Y.H., Moon, H.W.A.J.I.N., You, B.O.R.A., Kim, S.Z.O.O., Kim, S.H.E.E., and Park, W.O.O.H. (2010). The effects of N-acetyl cysteine on the MG132 proteasome inhibitor-treated lung cancer cells in relation to cell growth , reactive oxygen species and glutathione. 657–662.

Hanahan, D., and Weinberg, R. a (2011). Hallmarks of cancer: the next generation. Cell *144*, 646–674.

Hanson, R.W. (2009). A Perspective on the Biology of Phosphoenolpyruvate Carboxykinase 55 Years After Its Discovery 1–6.

Hanson, R., and Garber, A. (1972). Phosphoenolpyruvate. Its role role in gluconeogenesis. The American Journal of Clinical Nutrition 1010–1021.

HIROSHI KOBAYASHI, HIROTAKA KAJIWARA, SEIJI KANAYAMA, YOSHIHIKO YAMADA, NAOTO FURUKAWA, TAKETOSHI NOGUCHI, SHOJI HARUTA, SHOZO YOSHIDA, MARIKO SAKATA, TOSHIYUKI SADO AND HIDEKAZU OI (2009). Molecular pathogenesis of endometriosis-associated clear cell carcinoma of the ovary (Review). Oncology Reports *23* 233-240

Hogberg T, Carstensen J, Simonsen E (1993). Treatment results and prognostic factors in a population-based study of epithelial ovarian cancer. Gynecol Oncol *48*; 38-49.

Vander Heiden, M.G., Cantley, L.C., and Thompson, C.B. (2009). Understanding the Warburg effect: the metabolic requirements of cell proliferation. Science (New York, N.Y.) *324*, 1029–1033.

Hkaw, K., Asaki, H., Rashi, O., Zawa, S., and Shika, E. (1977). CLEAR CELL CARCINOMA OF THE OVARY: Light and Electron Microscopic Studies. Cancer *6*, 3010–3029.

Ishii, I., Akahoshi, N., Yu, X.-N., Kobayashi, Y., Namekata, K., Komaki, G., and Kimura, H. (2004). Murine cystathionine gamma-lyase: complete cDNA and genomic sequences, promoter

activity, tissue distribution and developmental expression. The Biochemical Journal *381*, 113–123.

Israël, M., and Schwartz, L. (2011a). On the metabolic origin of cancer : substances that target tumor metabolism . *22*, 132–166.

Israël, M., and Schwartz, L. (2011b). The metabolic advantage of tumor cells. Molecular Cancer *10*, 70.

Jurkowska, H., Placha, W., Nagahara, N., and Wróbel, M. (2011). The expression and activity of cystathionine-γ-lyase and 3-mercaptopyruvate sulfurtransferase in human neoplastic cell lines. Amino Acids *41*, 151–158.

Kim, J., and Dang, C. V (2006). Cancer's molecular sweet tooth and the Warburg effect. Cancer Research *66*, 8927–8930.

Kim, H., Jee, H.J., and Yun, J. (2011). DNA damage induces down-regulation of PEPCK and G6P gene expression through degradation of PGC-1a. *43*, 589–594.

Kraus, J.P., Hasek, J., Kozich, V., Collard, R., Venezia, S., Janosíková, B., Wang, J., Stabler, S.P., Allen, R.H., Jakobs, C., et al. (2009). Cystathionine gamma-lyase: Clinical, metabolic, genetic, and structural studies. Molecular Genetics and Metabolism *97*, 250–259.

Kuśmierek, K., Chwatko, G., Głowacki, R., and Bald, E. (2009). Determination of endogenous thiols and thiol drugs in urine by HPLC with ultraviolet detection. Journal of Chromatography B *877*, 3300–3308.

LaGrenade A, Silverberg S. (1988). Ovarian tumors associated atypical endometriosis. Hum Pathol *19*, 1080–1084.

Landolin, J.M., Johnson, D.S., Trinklein, N.D., Aldred, S.F., Medina, C., Shulha, H., Weng, Z., and Myers, R.M. (2010). Sequence features that drive human promoter function and tissue specificity. Genome Research *20*, 890–898.

Laplante, M., Sabatini, D., Natl, P., and Sci, A. (2010). Correction for Laplante et al., mTORC1 activates SREBP-1c and uncouples lipogenesis from gluconeogenesis. Proceedings of the National Academy of Sciences *107*, 7617–7617.

Liang, C.-C., Park, A.Y., and Guan, J.-L. (2007). In vitro scratch assay: a convenient and inexpensive method for analysis of cell migration in vitro. Nature Protocols 2, 329–333.

Liu, X., Wang, X., Zhang, J., Lam, E.K.Y., Shin, V.Y., Cheng, a S.L., Yu, J., Chan, F.K.L., Sung, J.J.Y., and Jin, H.C. (2010). Warburg effect revisited: an epigenetic link between glycolysis and gastric carcinogenesis. Oncogene *29*, 442–450.

Liu, Y., Gu, J., Hagner-McWhirter, Å., Sathiyanarayanan, P., Gullberg, M., Söderberg, O., Johansson, J., Hammond, M., Ivansson, D., and Landegren, U. (2011). Western blotting via proximity ligation for high performance protein analysis. Molecular & Cellular Proteomics : MCP *10*, O111.011031.

Mani, S., Yang, G., and Wang, R. (2011). A critical life-supporting role for cystathionine γ -lyase in the absence of dietary cysteine supply. Free Radical Biology and Medicine *50*, 1280–1287.

Matés, J.M., Segura, J. a, Martín-Rufián, M., Campos-Sandoval, J. a, Alonso, F.J., and Márquez, J. (2013). Glutaminase isoenzymes as key regulators in metabolic and oxidative stress against cancer. Current Molecular Medicine *13*, 514–534.

Mazurek, S., and Eigebbrodt, E. (2003). The tumor metabolome. Anticancer Research *23*, 1149–1154.

McMenamin, M.E., Himmelfarb, J., and Nolin, T.D. (2009). Simultaneous analysis of multiple aminothiols in human plasma by high performance liquid chromatography with fluorescence detection. Journal of Chromatography B *877*, 3274–3281.

Meredith, M.J., Cusick, C.L., Soltaninassab, S., Sekhar, K.S., Lu, S., and Freeman, M.L. (1998). Expression of Bcl-2 Increases Intracellular Glutathione by Inhibiting Methionine-Dependent GSH Efflux. Biochemical and Biophysical Research Communications *248*, 458–463.

Moraes-Silva, L., Bueno, T.M., Franciscato, C., de Oliveira, C.S., Peixoto, N.C., and Pereira, M.E. (2012). Mercury chloride increases hepatic alanine aminotransferase and glucose 6-phosphatase activities in newborn rats in vivo. Cell Biology International *36*, 561–566.

Moreira, C.C.L., Cassolla, P., Dornellas, A.P.S., de Morais, H., de Souza, C.O., Borba-Murad, G.R., Bazotte, R.B., and de Souza, H.M. (2013). Changes in liver gluconeogenesis during the development of Walker-256 tumour in rats. International Journal of Experimental Pathology *94*, 47–55.

Noguchi, R., Kubota, H., Yugi, K., Toyoshima, Y., Komori, Y., Soga, T., and Kuroda, S. (2013). The selective control of glycolysis, gluconeogenesis and glycogenesis by temporal insulin patterns. Molecular Systems Biology *9*, 664.

Nolin, T.D., McMenamin, M.E., and Himmelfarb, J. (2007). Simultaneous determination of total homocysteine, cysteine, cysteinylglycine, and glutathione in human plasma by high-performance liquid chromatography: application to studies of oxidative stress. Journal of Chromatography. B, Analytical Technologies in the Biomedical and Life Sciences *852*, 554–561.

O'Brien ME, Schofield JB, Tan S, Fryatt I, Fisher C, Wiltshaw E (1993). Clear cell epithelial ovarian cancer (mesonephroid): bad prognosis only in early stages. Gynecol Oncol *49*, 250–254.

Oh, K.-J., Han, H.-S., Kim, M.-J., and Koo, S.-H. (2013). Transcriptional regulators of hepatic gluconeogenesis. Archives of Pharmacal Research *36*, 189–200.

Piao, L., Fang, Y.-H., Parikh, K., Ryan, J.J., Toth, P.T., and Archer, S.L. (2013). Cardiac glutaminolysis: a maladaptive cancer metabolism pathway in the right ventricle in pulmonary hypertension. Journal of Molecular Medicine (Berlin, Germany).

Pompella, A., De Tata, V., Paolicchi, A., and Zunino, F. (2006). Expression of γ-glutamyltransferase in cancer cells and its significance in drug resistance. Biochemical Pharmacology *71*, 231–238.

Prowse AH, Manek S, Varma R, et al (2006). Molecular genetic evidence that endometriosis is a precursor of ovarian cancer. Int J Cancer *119*, 556-562.

Quintas, A., Freire, A., and Halpern, M. (2008a). Biossíntese de Oses e Ósidos. In Bioquímica - Organização Molecular Da Vida, (Lisboa: LIDEL), pp. 431–446.

Quintas, A., Freire, A., and Halpern, M. (2008b). Via dos Fosfatos de Pentose. In Bioquímica - Organização Molecular Da Vida, (Lisbon: LIDEL), pp. 357–358.

Rao, A.M., Drake, M.R., and Stipanuk, M.H. (1990). Role of the transsulfuration pathway and of gamma-cystathionase activity in the formation of cysteine and sulfate from methionine in rat hepatocytes. The Journal of Nutrition *120*, 837–845.

Reynolds, M.R., Lane, a N., Robertson, B., Kemp, S., Liu, Y., Hill, B.G., Dean, D.C., and Clem, B.F. (2013). Control of glutamine metabolism by the tumor suppressor Rb. Oncogene 1–11.

Roh, T., Kwak, M.Y., Kwak, E.H., Kim, D.H., Han, E.Y., Bae, J.Y., Bang, D.Y., Lim, D.S., Ahn, I.Y., Jang, D.E., et al. (2012). Chemopreventive mechanisms of methionine on inhibition of benzo(a)pyrene–DNA adducts formation in human hepatocellular carcinoma HepG2 cells. Toxicology Letters *208*, 232–238.

Sabatini, D.M. (2006). mTOR and cancer: insights into a complex relationship. *6*, 729–734.

Serpa, J., and Dias, S. (2011). Metabolic cues from the microenvironment act as a major selective factor for cancer progression and metastases formation. Cell Cycle *10*, 180–181.

Serpa, J., Caiado, F., Carvalho, T., Torre, C., Gonçalves, L.G., Casalou, C., Lamosa, P., Rodrigues, M., Zhu, Z., Lam, E.W.F., et al. (2010). Butyrate-rich colonic microenvironment is a relevant selection factor for metabolically adapted tumor cells. The Journal of Biological Chemistry *285*, 39211–39223.

Seyfried, T.N., and Shelton, L.M. (2010). Cancer as a metabolic disease. Nutrition & Metabolism *7*, 7.

Shapot, V.S., and Blinov, V.A. (1974). Blood Glucose Levels and Gluconeogenesis in Animals Bearing Transplantable Tumors Blood Glucose Levels and Gluconeogenesis in Animals Bearing Transplantable Tumors. Cancer Research *34*, 1827–1832.

Siegel, R., Desantis, C., Virgo, K., Stein, K., Mariotto, A., Smith, T., Cooper, D., Gansler, T., Lerro, C., and Fedewa, S. (2013). Cancer Treatment and Survivorship Statistics , 2012.

Singh, S., Khen, A., and Gupta, A. (2012). Role of glutathione in cancer pathophysiology and therapeutic interventions. Journal of Experimental Therapeutics and Oncology *9*, 303–316.

Sorbe B, Frankendal B, Veress B (1982). Importance of histologic grading in the prognosis of epithelial ovarian carcinoma. Obstet Gynecol *82*; 59:576.

Solberg, N., and Krauss, S. (2013). Luciferase Assay to Study the Activity of a Cloned Promoter DNA Fragment. In Methods in Molecular Biology, M. Bina, ed. (Totowa, NJ: Humana Press), pp. 65–78.

Steegborn, C. (1999). Kinetics and Inhibition of Recombinant Human Cystathionine gamma - Lyase. TOWARD THE RATIONAL CONTROL OF TRANSSULFURATION. Journal of Biological Chemistry *274*, 12675–12684.

Sugiyama, T., Kamura, T., Kigawa, J., Terakawa, N., Kikuchi, Y., Kita, T., Suzuki, M., Sato, I., and Taguchi, K. (2000). Clinical characteristics of clear cell carcinoma of the ovary: a distinct histologic type with poor prognosis and resistance to platinum-based chemotherapy. Cancer *88*, 2584–2589.

Szabo, C., Coletta, C., Chao, C., Módis, K., Szczesny, B., Papapetropoulos, A., and Hellmich, M.R. (2013). Tumor-derived hydrogen sulfide, produced by cystathionine-β-synthase, stimulates bioenergetics, cell proliferation, and angiogenesis in colon cancer. Proceedings of the National Academy of Sciences of the United States of America *110*, 12474–12479.

Telang, S., Clem, B.F., Klarer, A.C., Clem, A.L., Trent, J.O., Bucala, R., and Chesney, J. (2012). Small molecule inhibition of 6-phosphofructo-2-kinase suppresses t cell activation. Journal of Translational Medicine *10*, 95.

Tozer, R.G., Tai, P., Falconer, W., Ducruet, T., Karabadjian, A., Bounous, G., Molson, J.H., and Dröge, W. (2008). Cysteine-Rich Protein Reverses Weight Loss in Lung Cancer Patients Receiving Chemotherapy or Radiotherapy. Antioxidants & Redox Signaling *10*, 395–402.

Traverso, N., Ricciarelli, R., Nitti, M., Marengo, B., Furfaro, A.L., Pronzato, M.A., Marinari, U.M., and Domenicotti, C. (2013). Role of glutathione in cancer progression and chemoresistance. Oxidative Medicine and Cellular Longevity *2013*, 972913.

Vermeulen, K., Van Bockstaele, D.R., and Berneman, Z.N. (2003). The cell cycle: a review of regulation, deregulation and therapeutic targets in cancer. Cell Proliferation *36*, 131–149.

Wang, J., and Hegele, R. a (2003). Genomic basis of cystathioninuria (MIM 219500) revealed by multiple mutations in cystathionine gamma-lyase (CTH). Human Genetics *112*, 404–408.

Wang, S., Chen, H., Sheen, L., Lii, C., and Al, W.E.T. (1997). Methionine and Cysteine Affect Glutathione Level , Glutathione-Related Enzyme Activities and the Expression of Glutathione S-Transferase. Biochemical and Molecular Roles of Nutrients 2135–2141.

Warburg, O. (1956). On the origin of cancer cells.

Weickert, M.O., and Pfeiffer, a F.H. (2006). Signalling mechanisms linking hepatic glucose and lipid metabolism. Diabetologia *49*, 1732–1741.

Wise, D.R., and Thompson, C.B. (2010). Glutamine addiction: a new therapeutic target in cancer. Trends in Biochemical Sciences *35*, 427–433.

Xiong, Y., Lei, Q.-Y., Zhao, S., and Guan, K.-L. (2011). Regulation of glycolysis and gluconeogenesis by acetylation of PKM and PEPCK. Cold Spring Harbor Symposia on Quantitative Biology *76*, 285–289.

Yalcin, A., Telang, S., Clem, B., and Chesney, J. (2009). Regulation of glucose metabolism by 6-phosphofructo-2-kinase/fructose-2,6-bisphosphatases in cancer. Experimental and Molecular Pathology *86*, 174–179.

Yamaguchi, K., Mandai, M., Oura, T., Matsumura, N., Hamanishi, J., Baba, T., Matsui, S., Murphy, S.K., and Konishi, I. (2010). Identification of an ovarian clear cell carcinoma gene signature that reflects inherent disease biology and the carcinogenic processes. Oncogene *29*, 1741–1752.

Zagari, F., Jordan, M., Stettler, M., Broly, H., and Wurm, F.M. (2013). Lactate metabolism shift in CHO cell culture: the role of mitochondrial oxidative activity. New Biotechnology *30*, 238–245.

Zhang, W., Trachootham, D., Liu, J., Chen, G., Pelicano, H., Garcia-Prieto, C., Lu, W., Burger, J. a, Croce, C.M., Plunkett, W., et al. (2012). Stromal control of cystine metabolism promotes cancer cell survival in chronic lymphocytic leukaemia. Nature Cell Biology *14*, 276–286.

Appendices

Appendix I

Solutions prepared for the experimental work:

Luria-Bertani (LB) medium (Sambrook & Russel, 2001)
For 1L: 10g Tryptone (L42, Oxoid) 5g Yeast extract (403 687, Cultimed) 10g NaCl (106404, Merck) ddH2O to 1L

10X PBS (pH 7.4-7.6) (Sambrook & Russel, 2001)
For 1L: 80g NaCl (1.37M) (106404, Merck) 2g KH2PO4 (14.7mM) (104873, Merck) 11.1g Na2HPO4 (78.1mM) (S-0876, Sigma) 2g KCl (26.8mM) (104936, Merck) ddH2O to 1L

10X TBS (pH 7.4-7.6)
For 1L: 8g NaCl (106404, Merck) 0.63g Tris (15504-038, Gibco BRL) 4.4 mL hydrochloric acid (1M) ddH2O to 1L

5X SDS gel loading buffer (Sambrook & Russel, 2001)
250 mM Tris HCl (pH 6.8) (0.5M 161-0799, Bio-rad) 10% SDS (V6551, Promega) 0.5% bromophenol blue

50% glycerol (1.04094.1000, Merck)

Transfer buffer
For 5L: 75g glycine (US16407, USB) 15g Trizma-base (T-8524, Sigma) ddH2O to 4L 1L Metanol (107018, Merck) 5mL 10% SDS (V6551, Promega)

15% resolving gel and 5% stacking gel for Tris-glycine SDS-Polyacrylamide Gel Electrophoresis prepared accordingly to Sambrook & Russel, 2001

PBS 0.1% (v/v) Tween 20
For 1L: 1mL Tween 20 (20605, USB) 1X PBS to 1L

PBS 0.2% (w/v) BSA
0.4g BSA (A9647, Sigma) 200 mL 1X PBS

PBS 0.2% (w/v) BSA 0.1% (v/v) Triton X-100
For 4mL: 3.96 mL PBS 0.2% (w/v) BSA 40 µL 10% Triton X-100 diluted in ddH2O (100% Triton X-100, T8787, Sigma)

5% (w/v) skim milk in PBS 0.1% (v/v) Tween 20
5g skim milk (Molico, Nestlé) 100 mL PBS 0.1% (v/v) Tween 20

RIPA buffer
For 10 mL: 20 mM Tris-HCl pH 7.5 150 mM NaCl (106404, Merck) 5mM KCl (104936, Merck) 5mM MgCl2 (M-8266, Sigma) 1% Triton X-100 (T8787, Sigma) ddH2O to 10 mL 1 Complete, Mini, EDTA-free Protease Inhibitor Cocktail Tablet (11836170001, Roche) 1 mM Orthovanadate (Na3VO4) 1 mM Sodium fluoride (NaF) (201154, Sigma)

50 µg/mL Propidium Iodide (PI) solution – Cell cyle assay
For 50 mL: 1 mL of 2.5 mg/mL PI solution (P4170, Sigma) (prepared in 1X PBS) 49 mL 1X PBS 0.1 mg/mL RNase A (Easy spin kit, Citomed) 0.05% Triton X-100 (T8787, Sigma)

50 µg/mL Propidium Iodide (PI) solution – Apoptosis assay
For 50 mL: 1 mL of 2.5 mg/mL PI solution (P4170, Sigma) (prepared in 1X PBS) 49 mL 1X PBS

Annexin binding buffer 1X
0.01 M Hepes (pH 7.4) (391333, Millipore) 0.14 M NaCl (106404, Merck) 2.5 mM $CaCl_2$ (449709, Sigma)

Appendix II

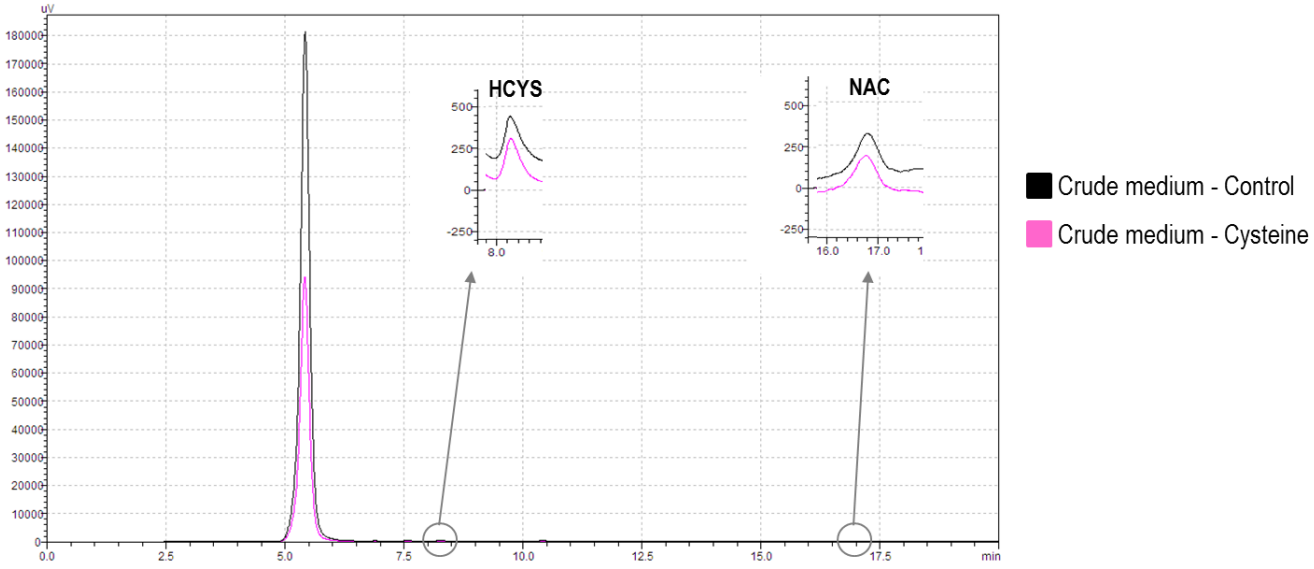

Figure A1: HPLC spectrum in control crude medium and in cysteine crude medium.

Control is referent to glutamine condition whereas cysteine is referent to glutamine plus cysteine.

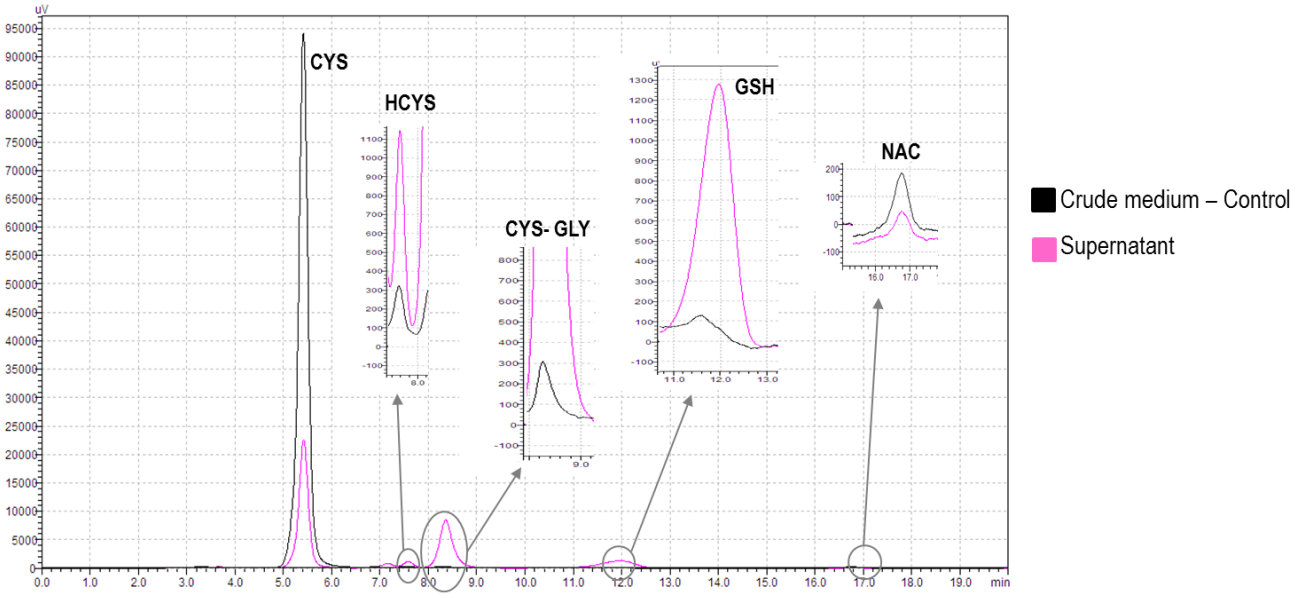

Figure A2 - HPLC spectrum in control crude medium and supernatant..

Control is referent to glutamine condition.

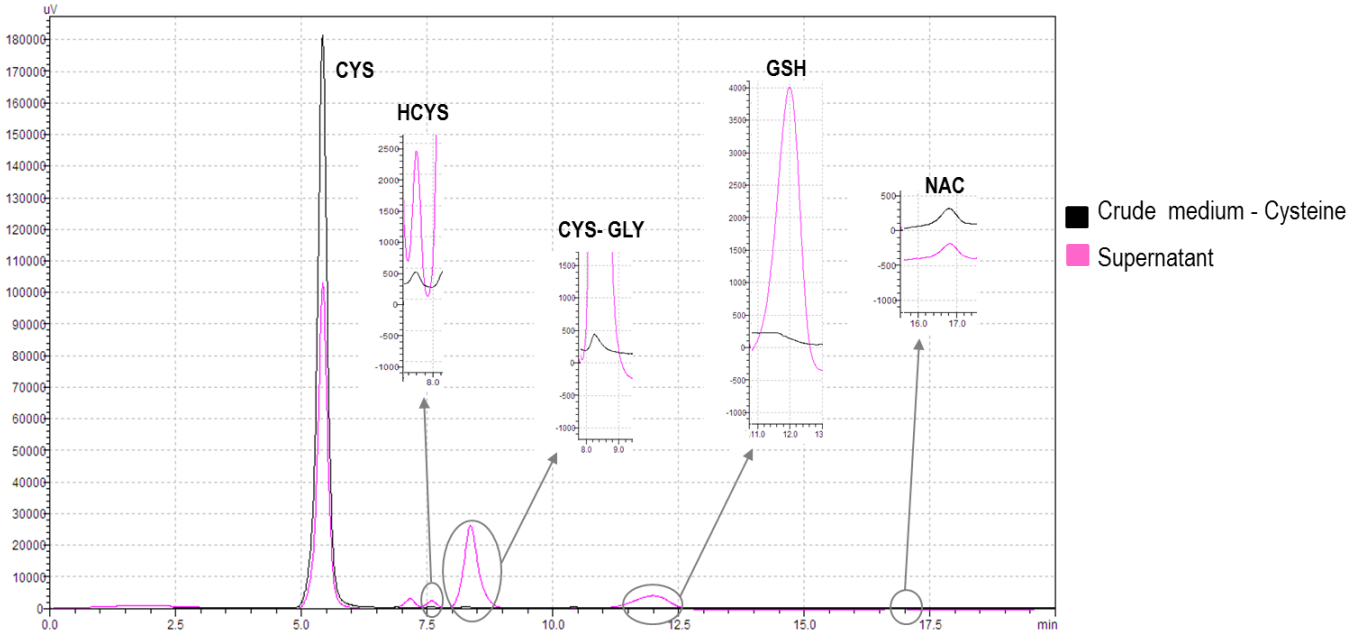

Figure A3– HPLC spectrum in cysteine crude medium and supernatant.

Cysteine is referent to glutamine plus cysteine.

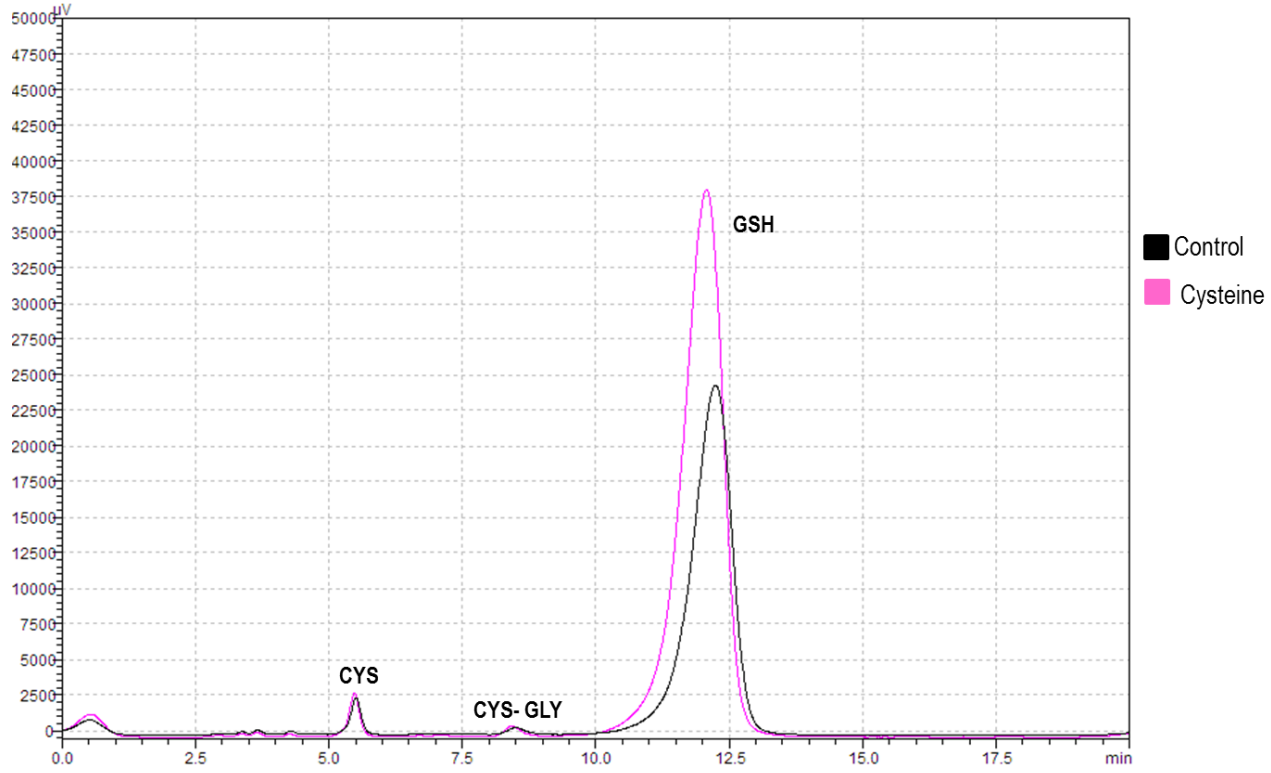

Figure A4- HPLC spectrum of intracellular contents in control and cysteine condition.

Control is referent to glutamine condition whereas cysteine is referent to glutamine plus cysteine.